



(19) **United States**

(12) **Patent Application Publication**  
**BRANAGAN et al.**

(10) **Pub. No.: US 2019/0217363 A1**  
(43) **Pub. Date: Jul. 18, 2019**

(54) **ALLOYS AND METHODS TO DEVELOP YIELD STRENGTH DISTRIBUTIONS DURING FORMATION OF METAL PARTS**

**Related U.S. Application Data**

(60) Provisional application No. 62/618,356, filed on Jan. 17, 2018.

(71) Applicant: **The NanoSteel Company, Inc.**,  
Providence, RI (US)

**Publication Classification**

(72) Inventors: **Daniel James BRANAGAN**, Idaho Falls, ID (US); **Craig S. PARSONS**, Lake Orion, MI (US); **Tad V. MACHROWICZ**, Ortonville, MI (US); **Jonathan M. CISCHKE**, Bloomfield Hills, MI (US); **Andrew E. FRERICHS**, Idaho Falls, ID (US); **Brian E. MEACHAM**, Idaho Falls, ID (US); **Grant G. JUSTICE**, Idaho Falls, ID (US); **Kurtis Clark**, Idaho Falls, ID (US); **Logan J. TEW**, Idaho Falls, ID (US); **Scott T. ANDERSON**, Idaho Falls, ID (US); **Scott LARISH**, Idaho Falls, ID (US); **Sheng CHENG**, Idaho Falls, ID (US); **Taylor L. GIDDENS**, White, GA (US); **Alla V. SERGUEEVA**, Idaho Falls, ID (US)

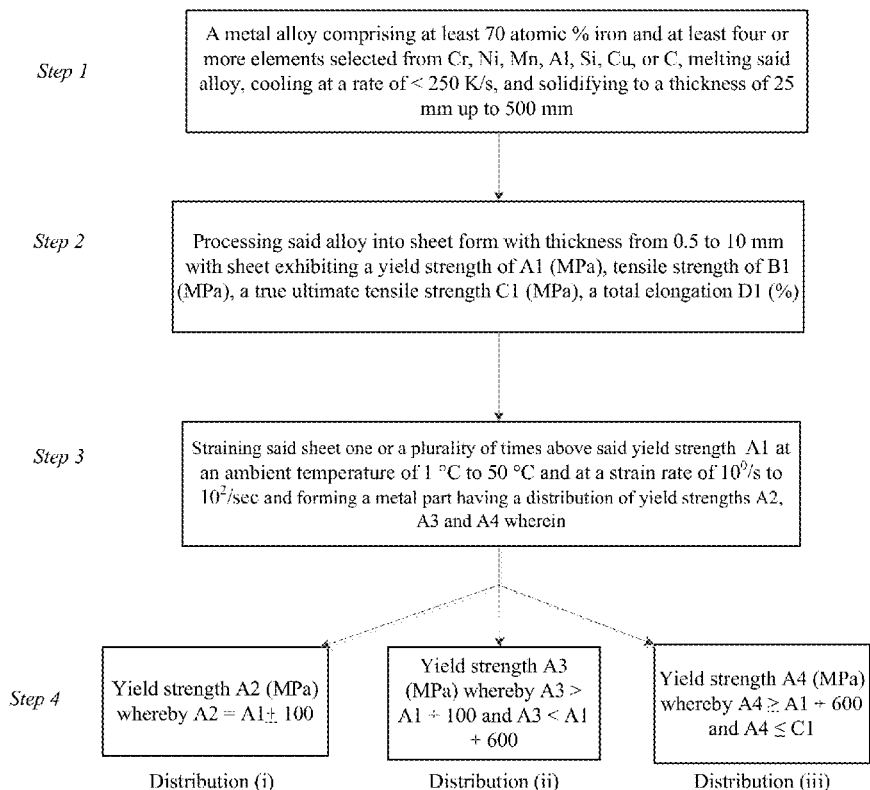
(51) **Int. Cl.**  
*B21D 22/02* (2006.01)  
*C22C 38/02* (2006.01)  
*C22C 38/04* (2006.01)  
*C22C 38/06* (2006.01)  
*C22C 38/42* (2006.01)  
*C22C 38/58* (2006.01)  
*C22C 38/34* (2006.01)  
*C21D 8/04* (2006.01)  
(52) **U.S. Cl.**  
CPC ..... *B21D 22/02* (2013.01); *C22C 38/02* (2013.01); *C22C 38/04* (2013.01); *C22C 38/06* (2013.01); *C21D 9/48* (2013.01); *C22C 38/58* (2013.01); *C22C 38/34* (2013.01); *C21D 8/0436* (2013.01); *C22C 38/42* (2013.01)

(21) Appl. No.: **16/229,584**

(57) **ABSTRACT**

(22) Filed: **Dec. 21, 2018**

This invention is related to a method to increase the strength of a metal stamping by supplying a metal blank which has the ability to strengthen in-situ during stamping to achieve sets of properties not expected and much higher based on the starting properties of the blank.



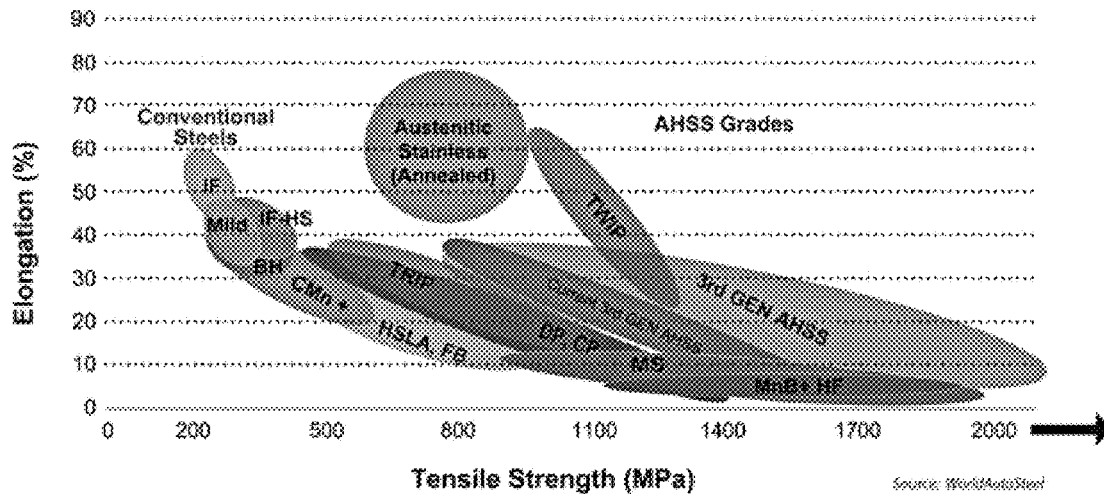


FIG. 1

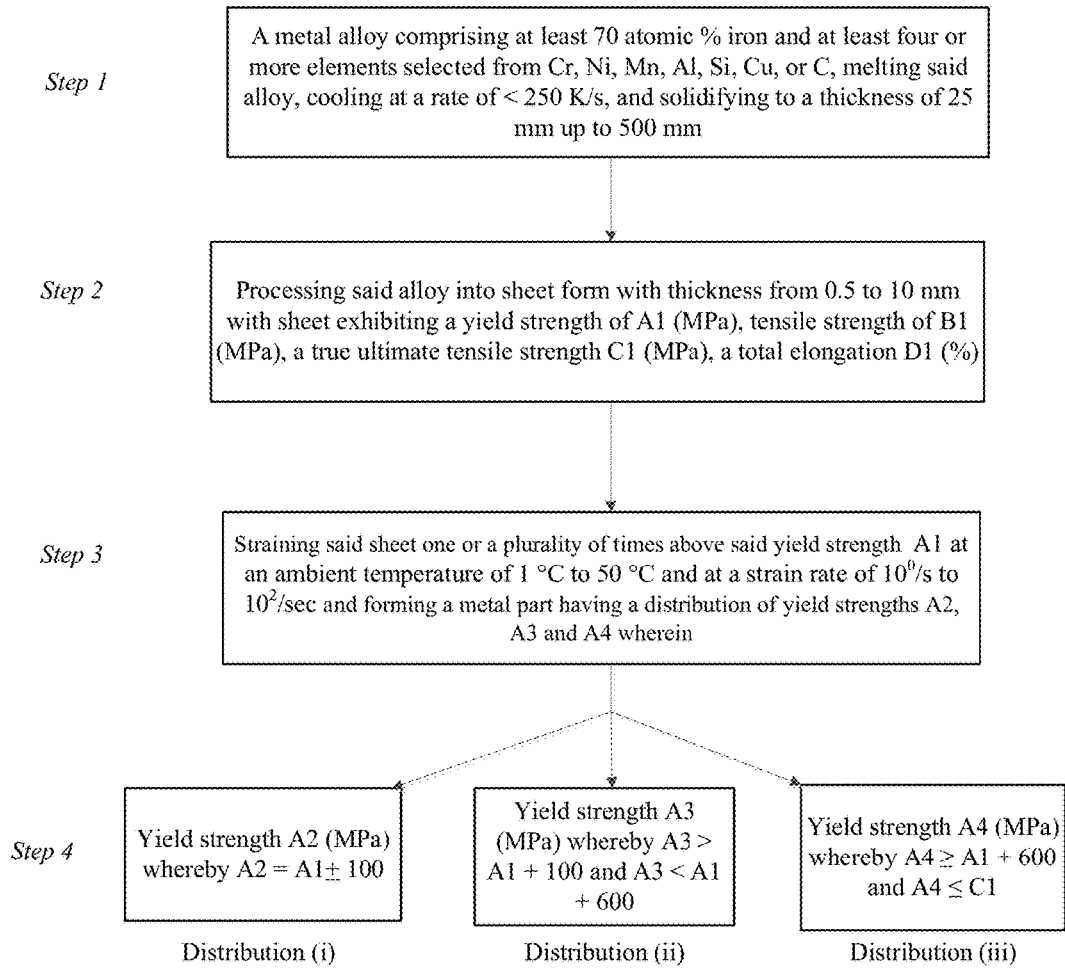


FIG. 2

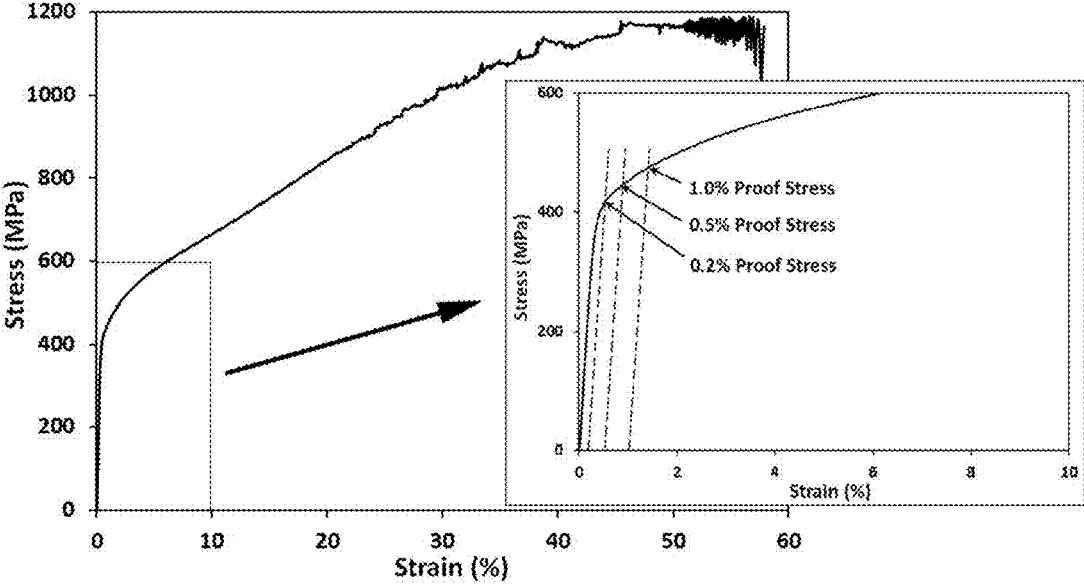


FIG. 3

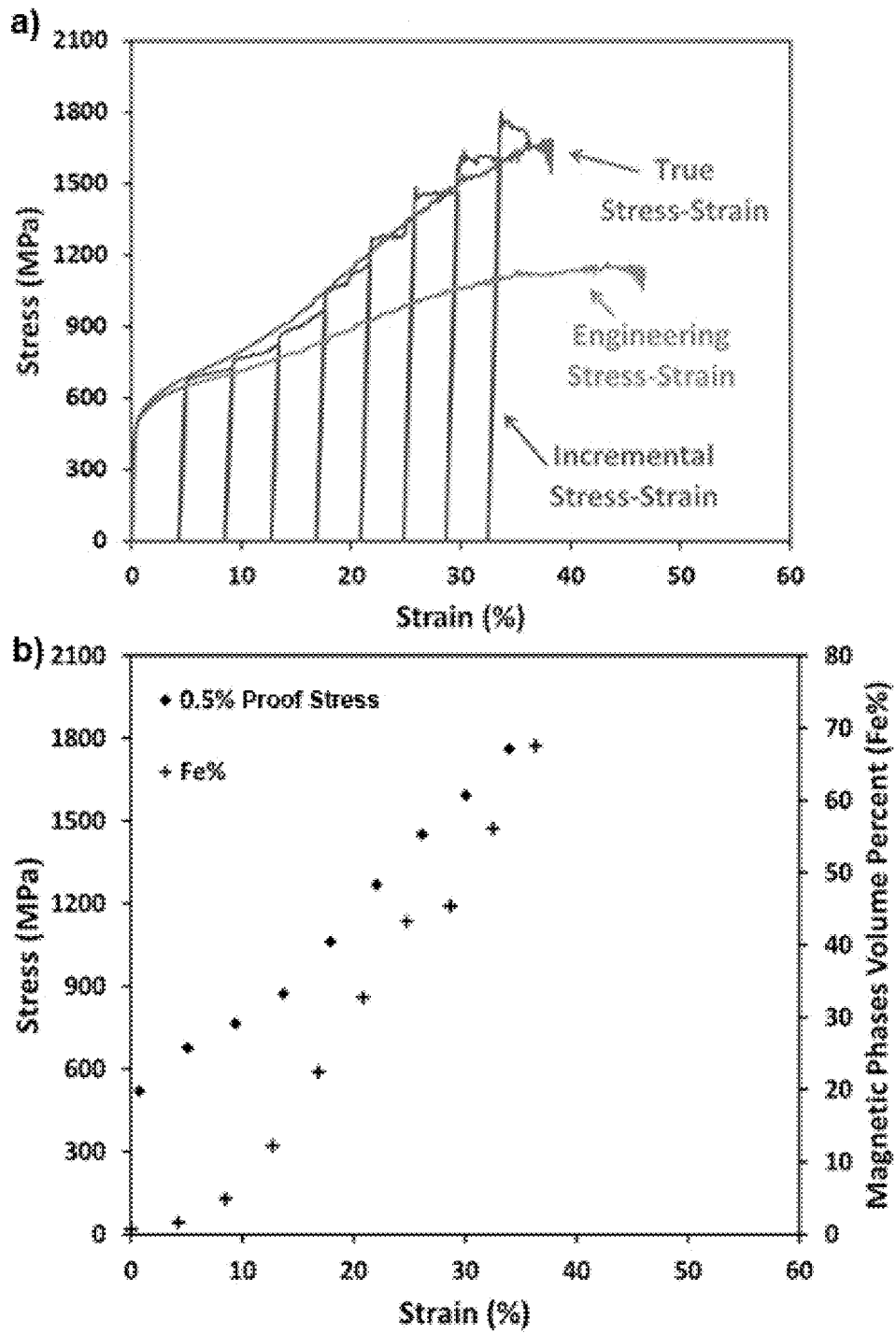


FIG. 4

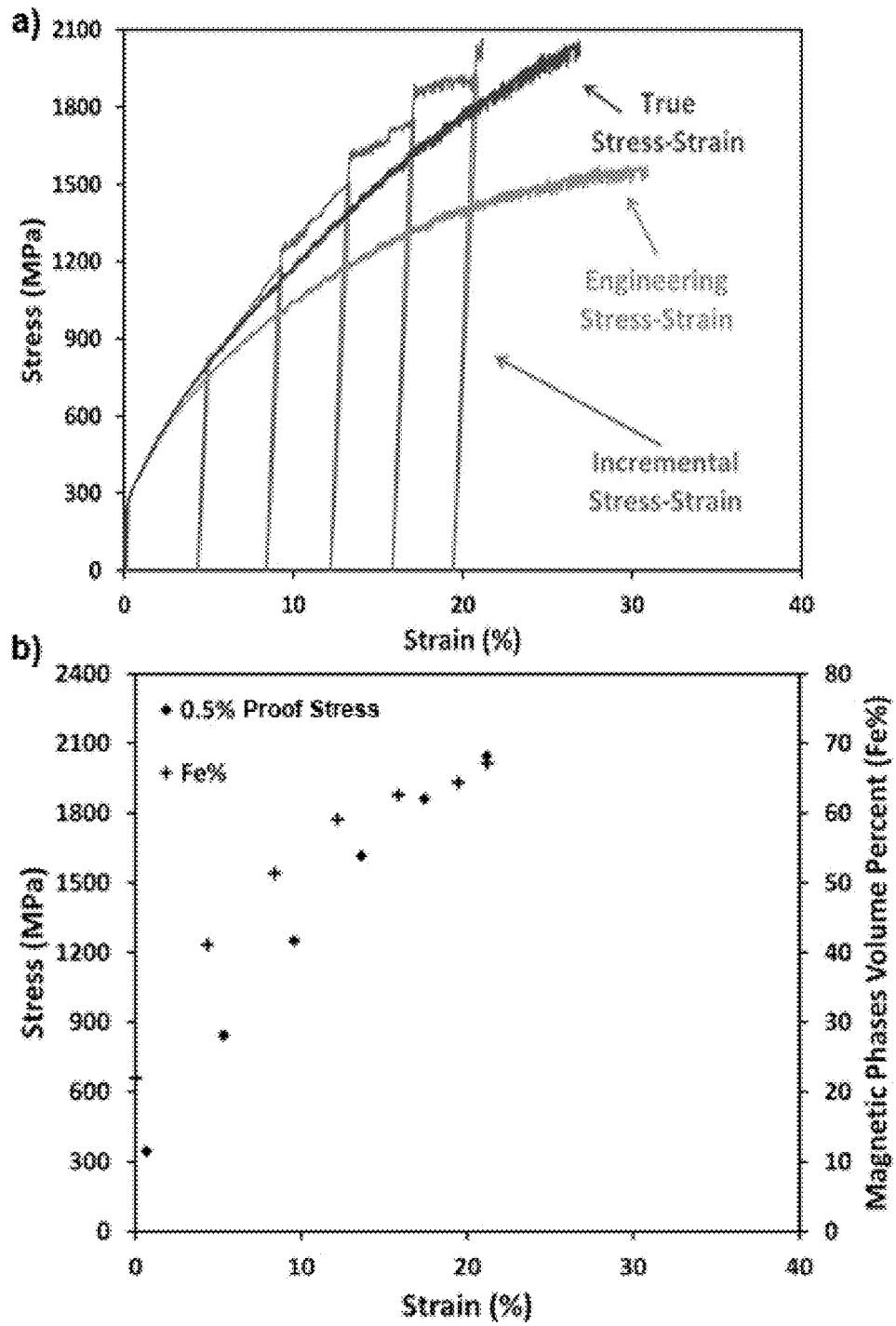


FIG. 5

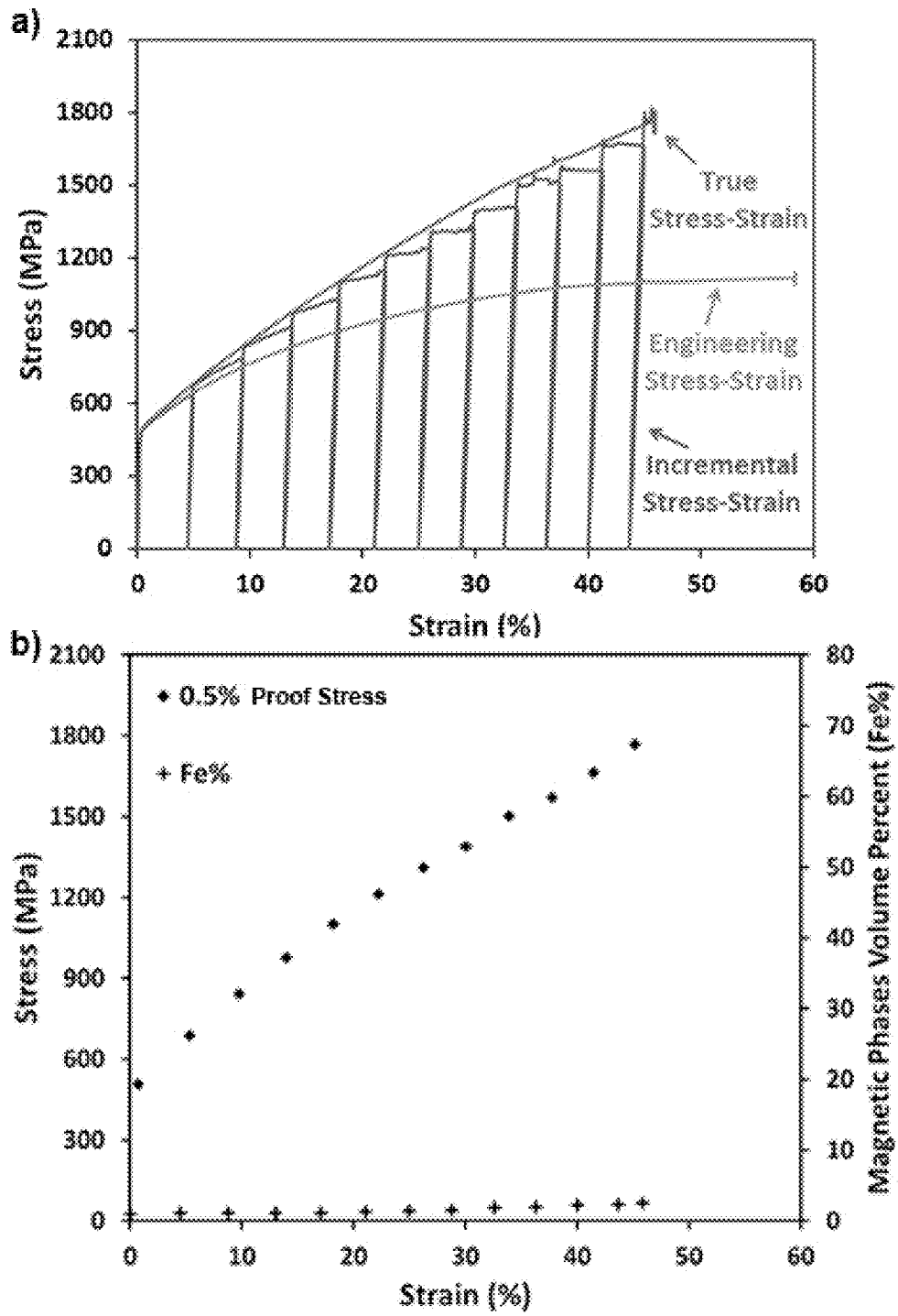


FIG. 6

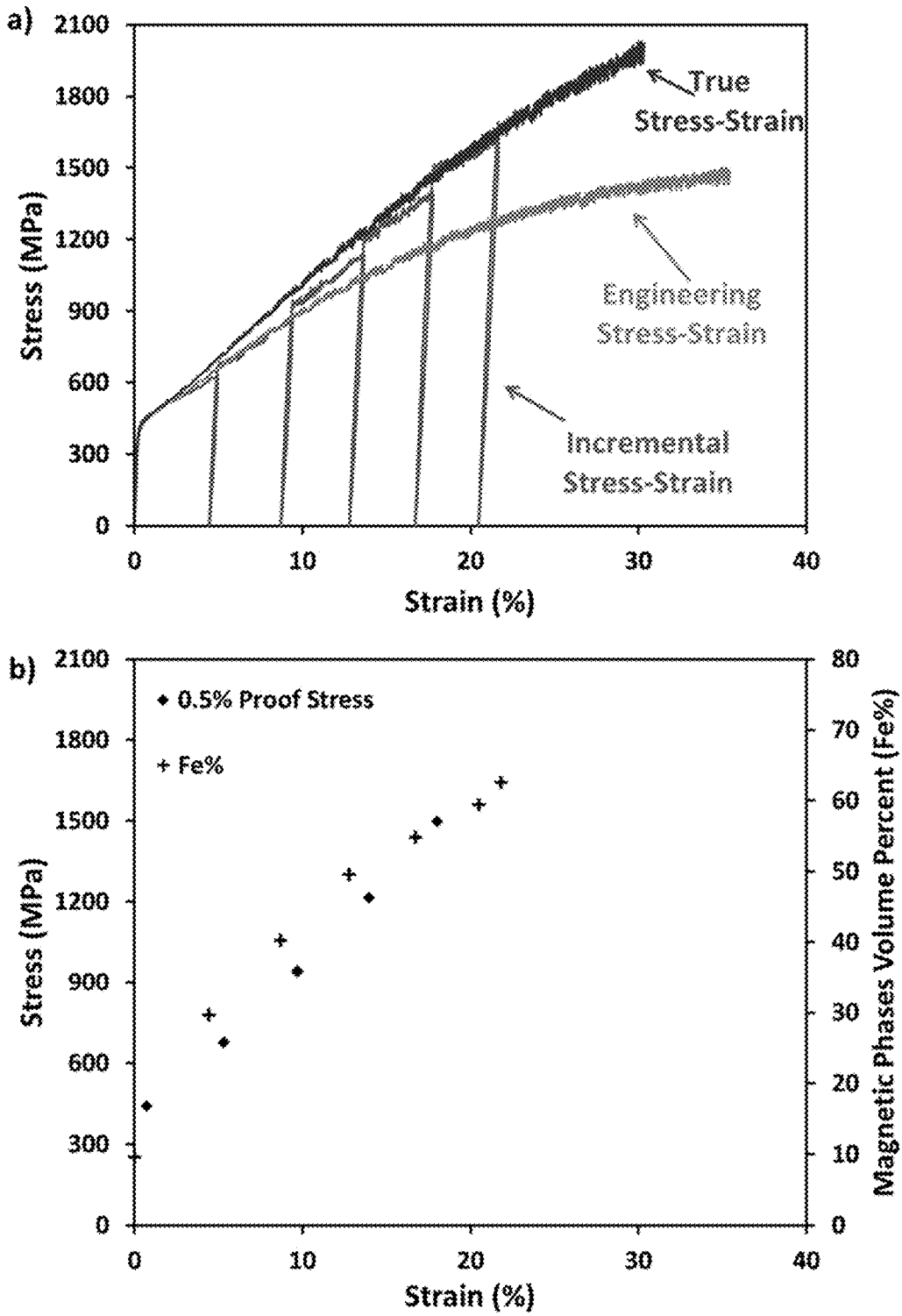


FIG. 7



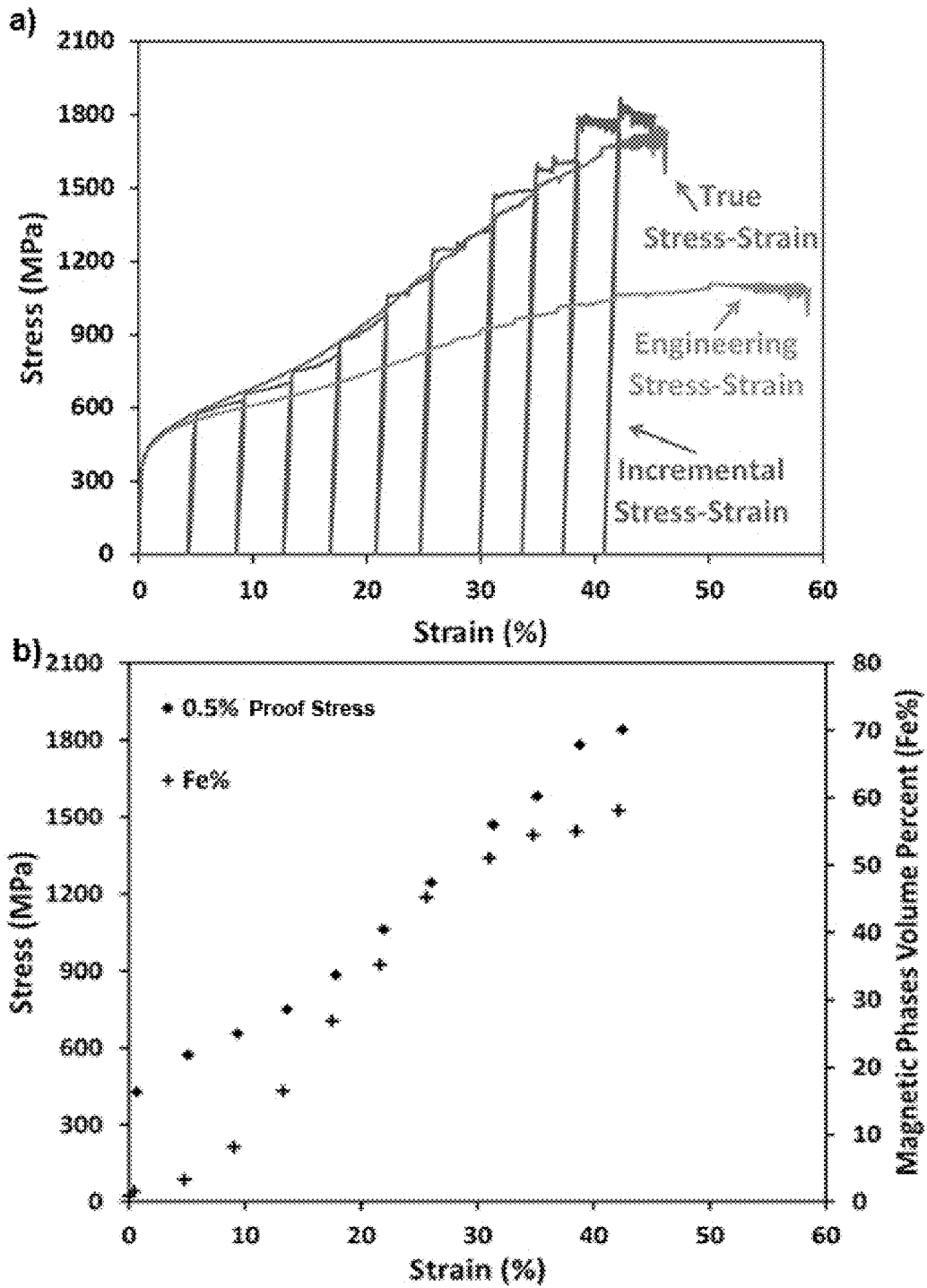


FIG. 8

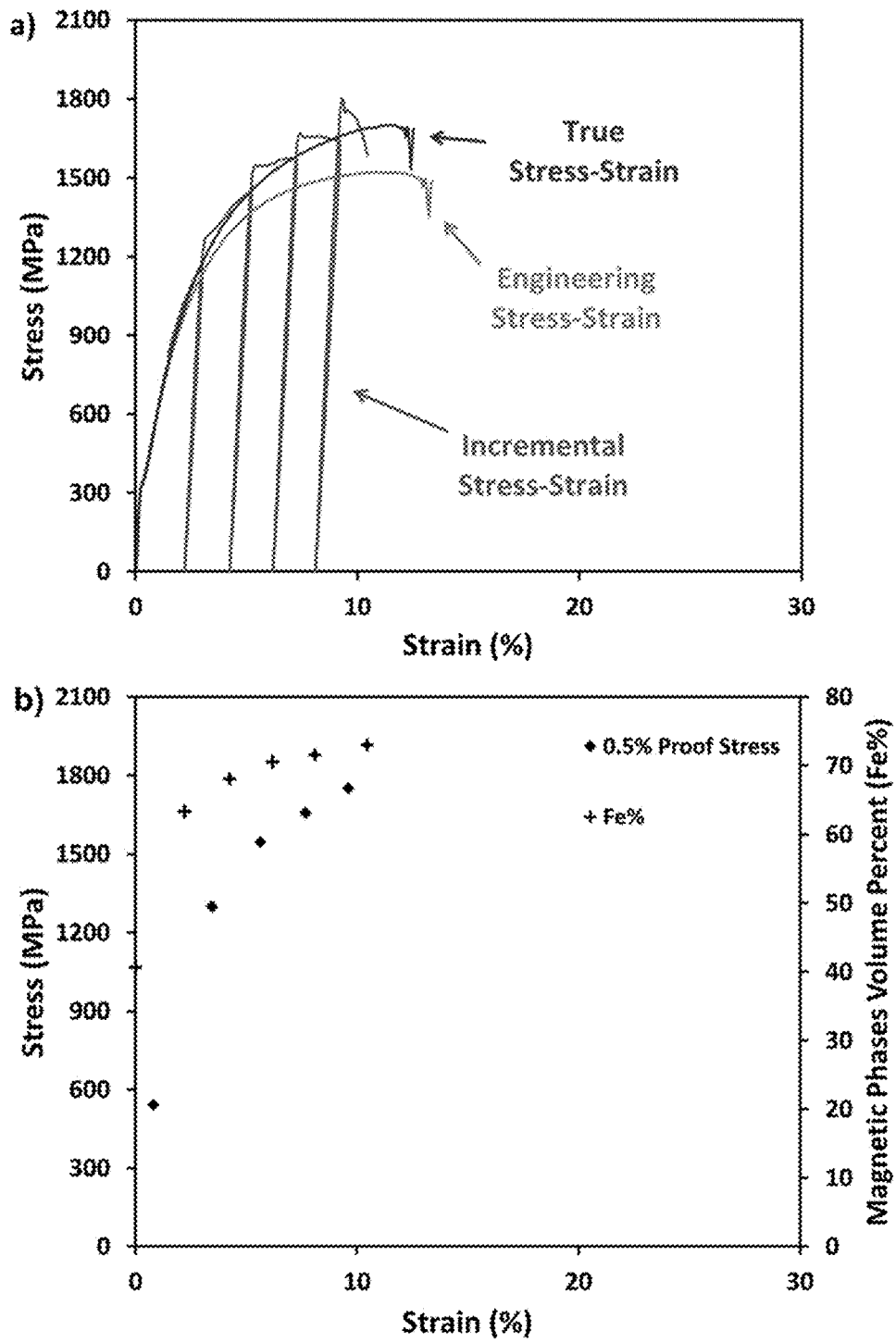


FIG. 9

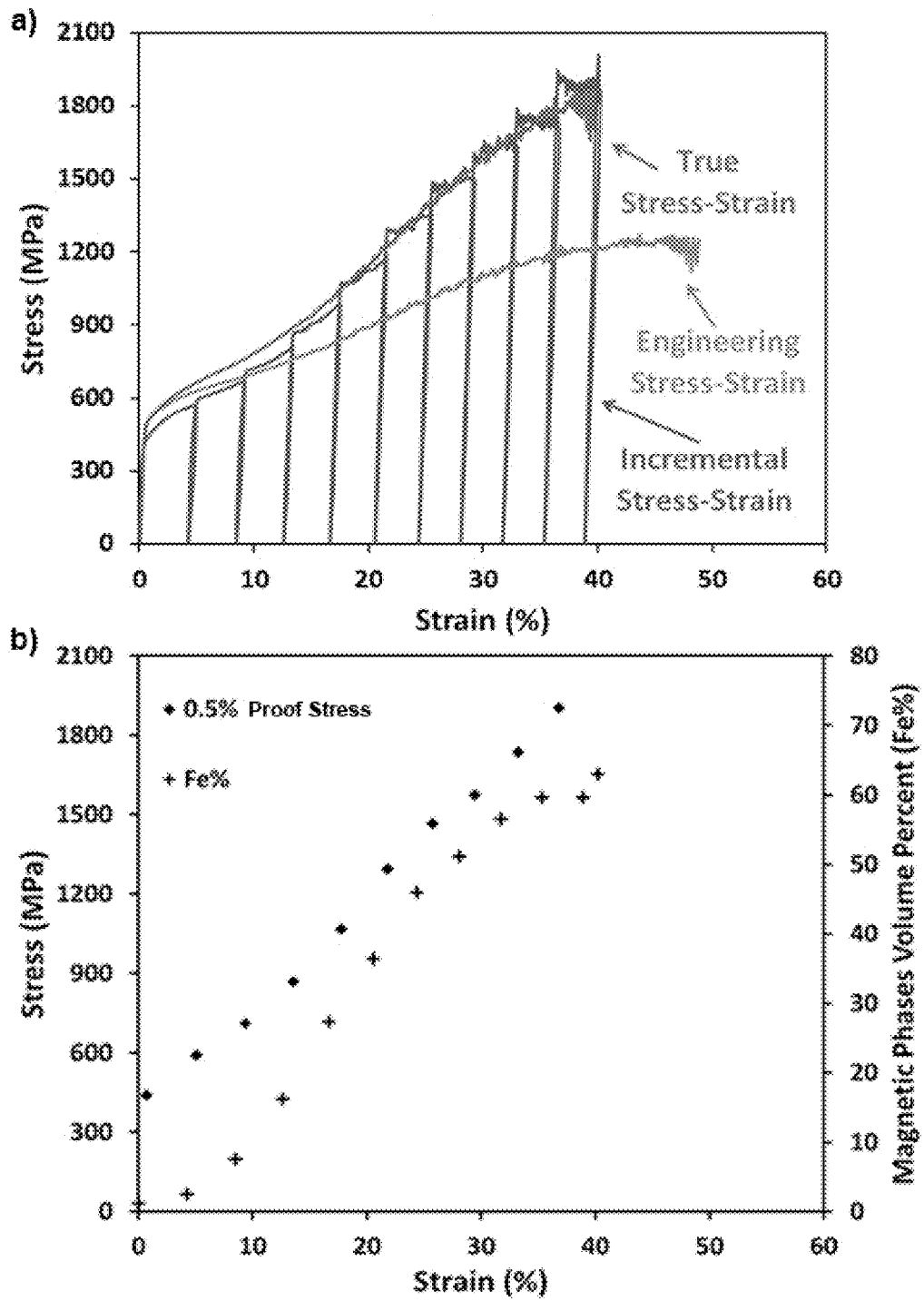


FIG. 10.

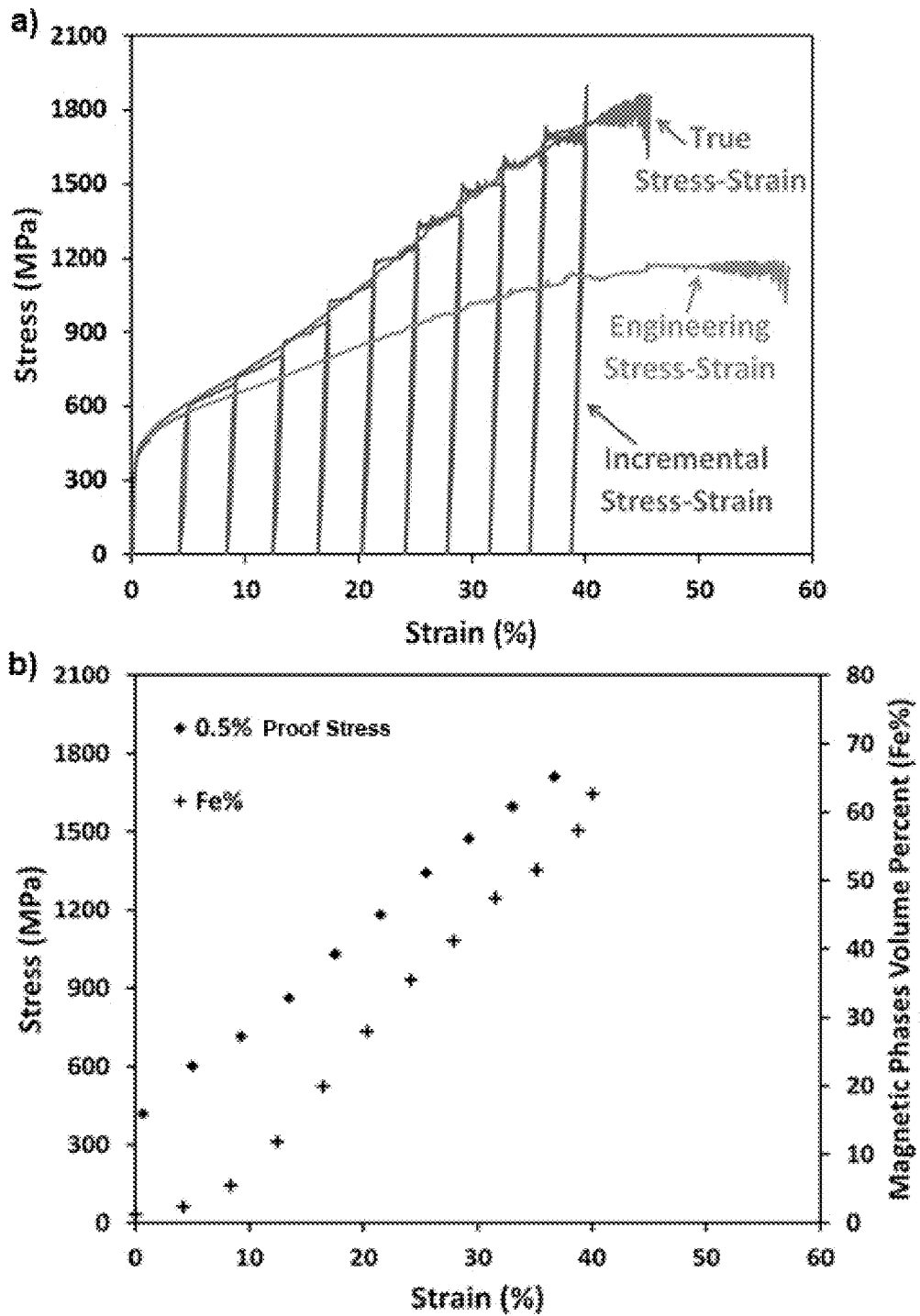


FIG. 11

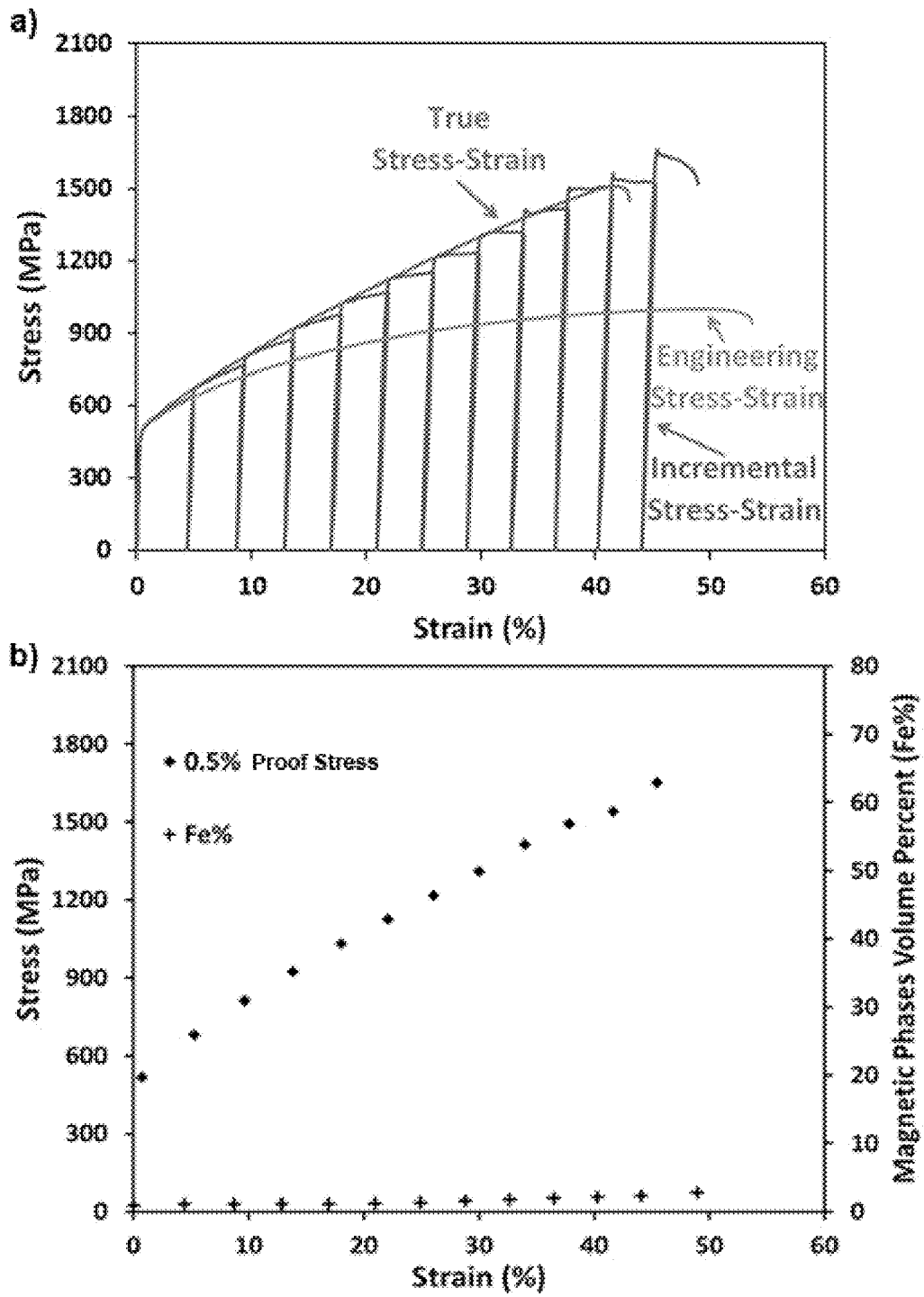


FIG. 12

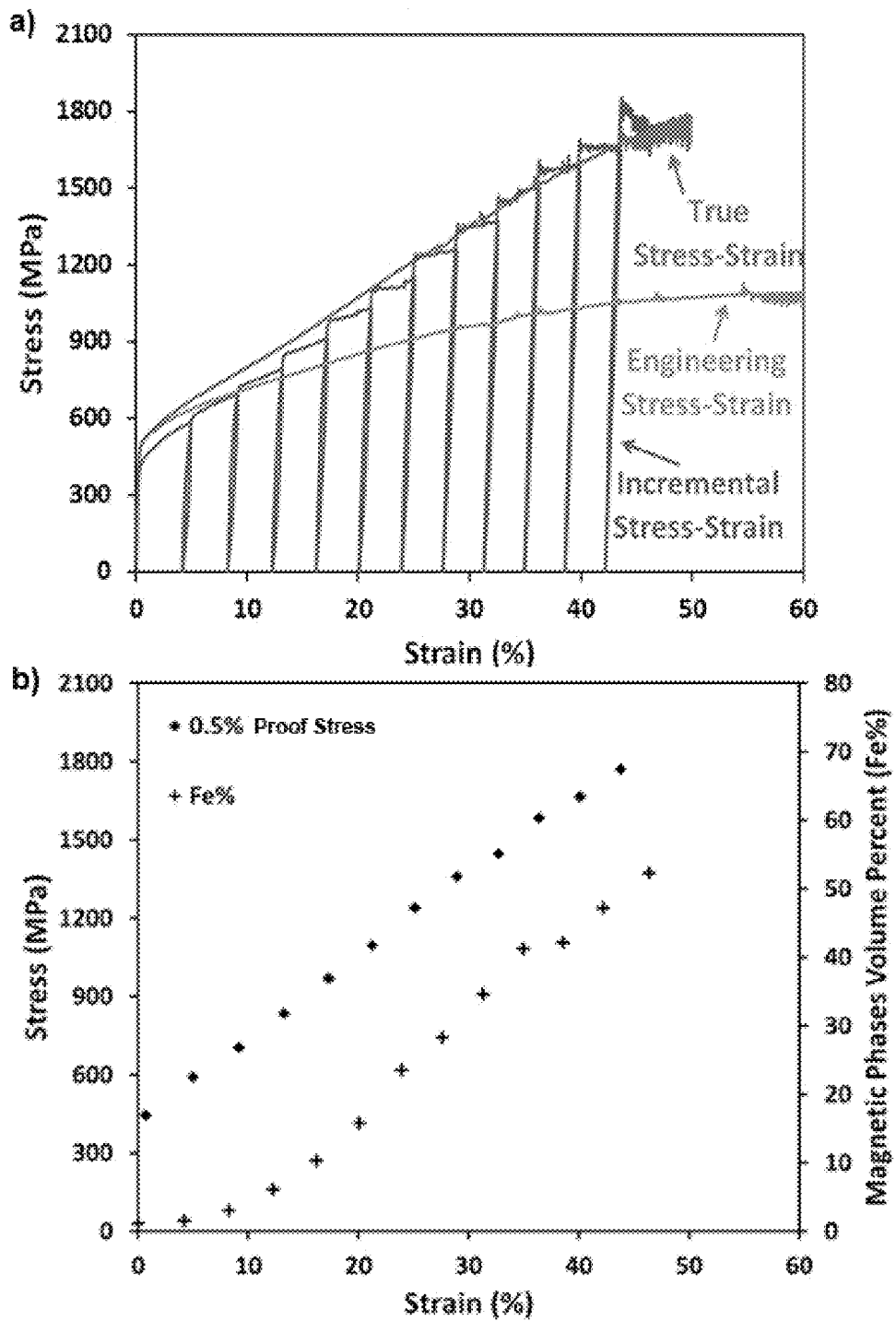


FIG. 13

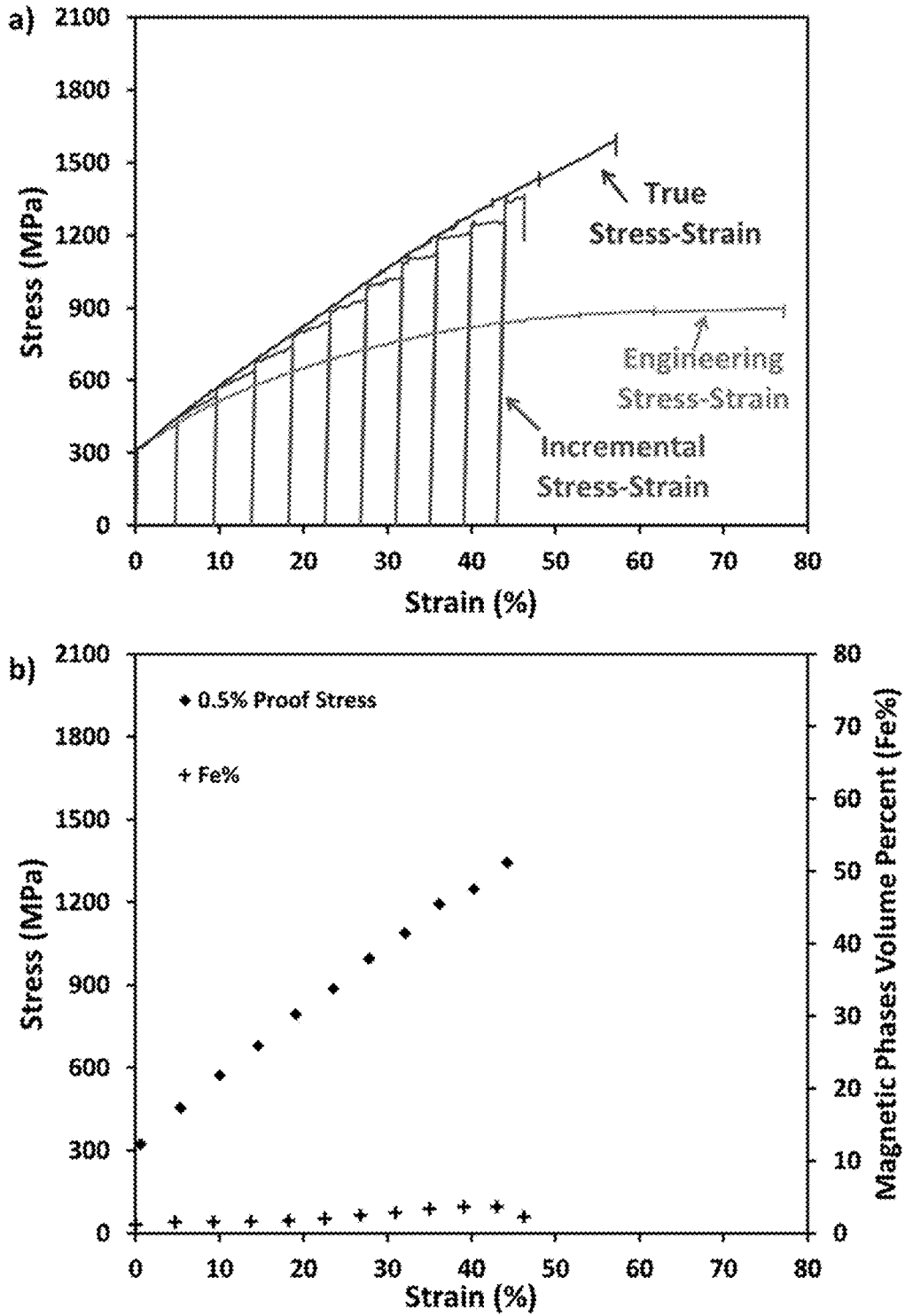


FIG. 14

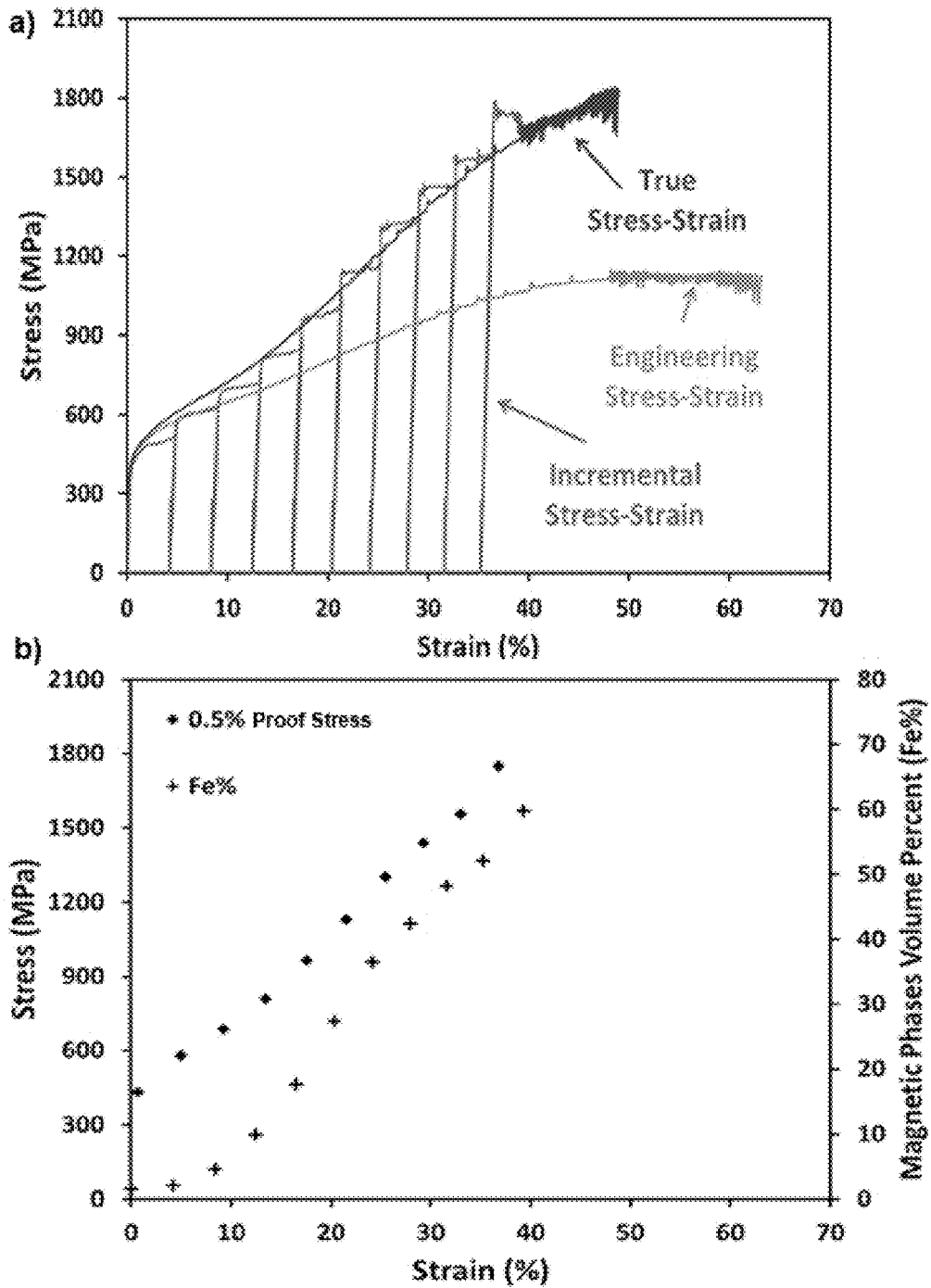


FIG. 15



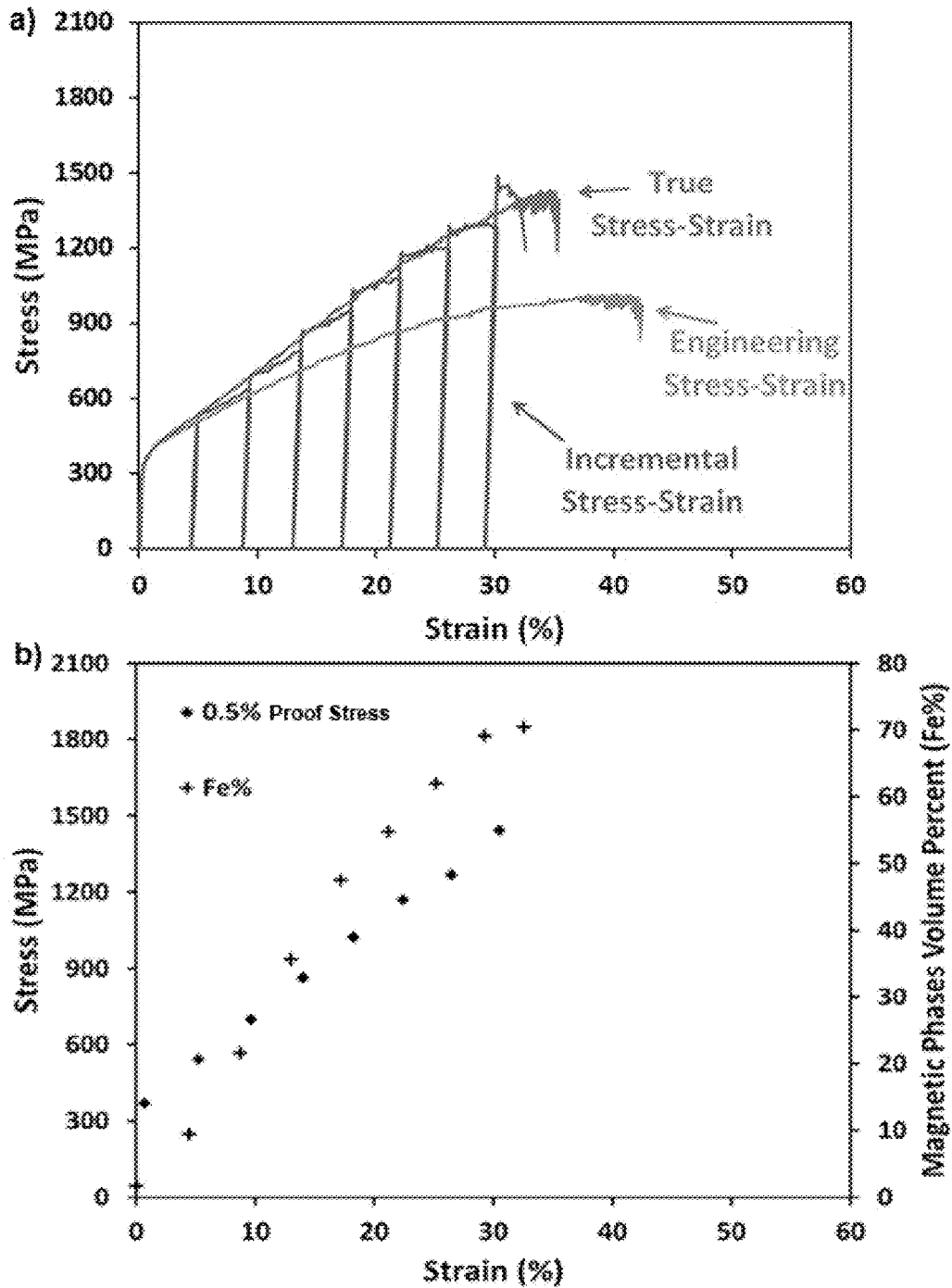


FIG. 16

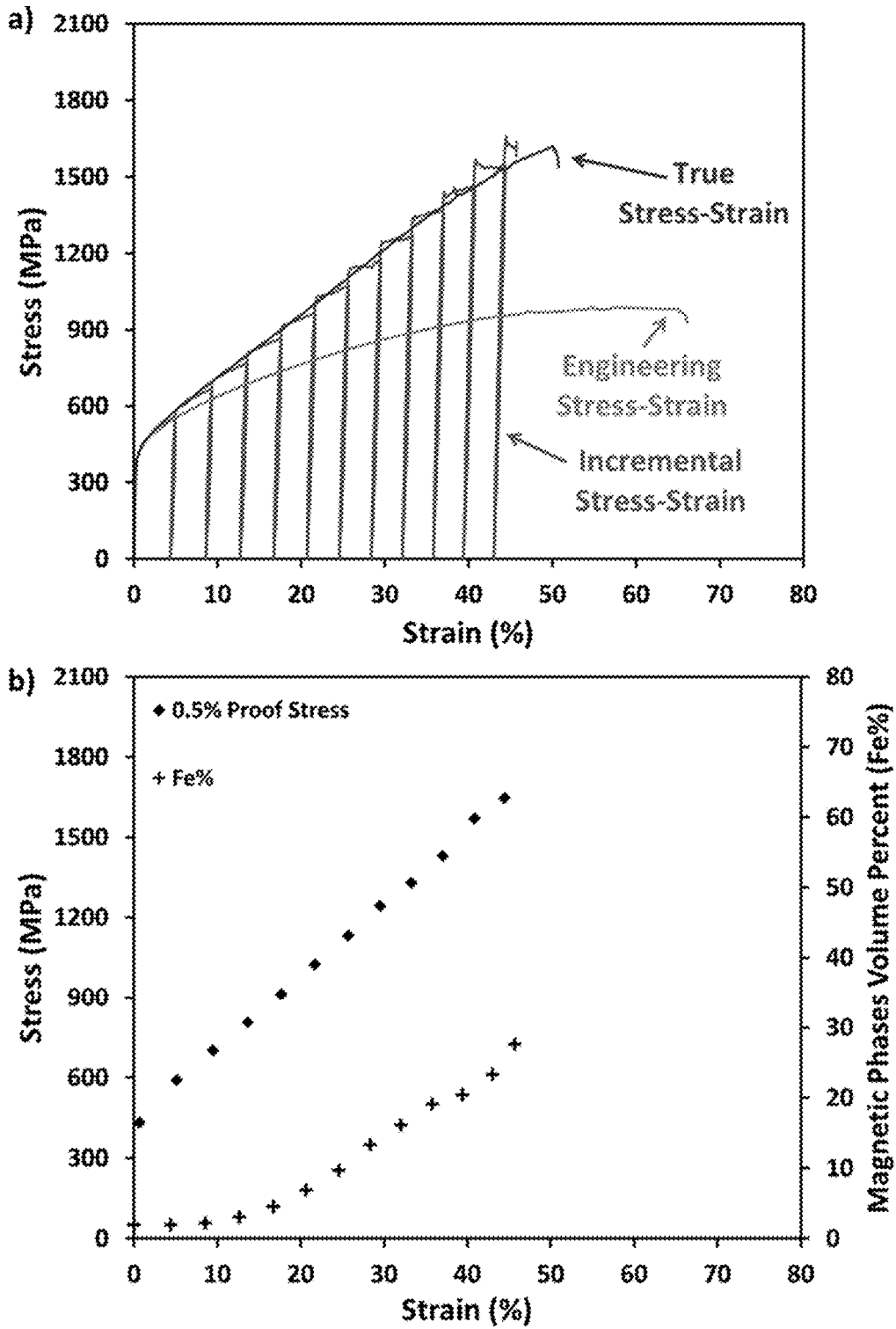


FIG. 17

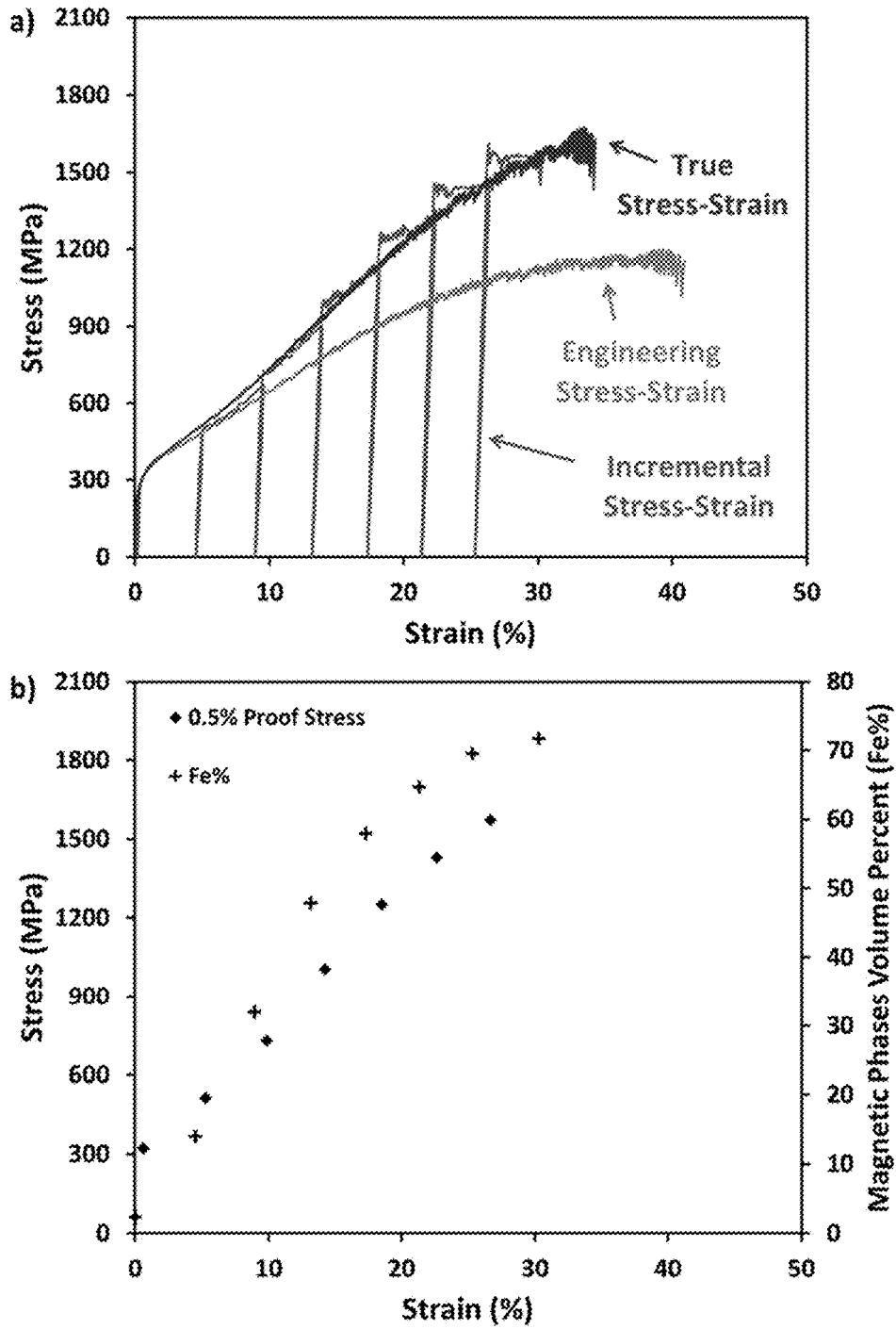


FIG. 18.

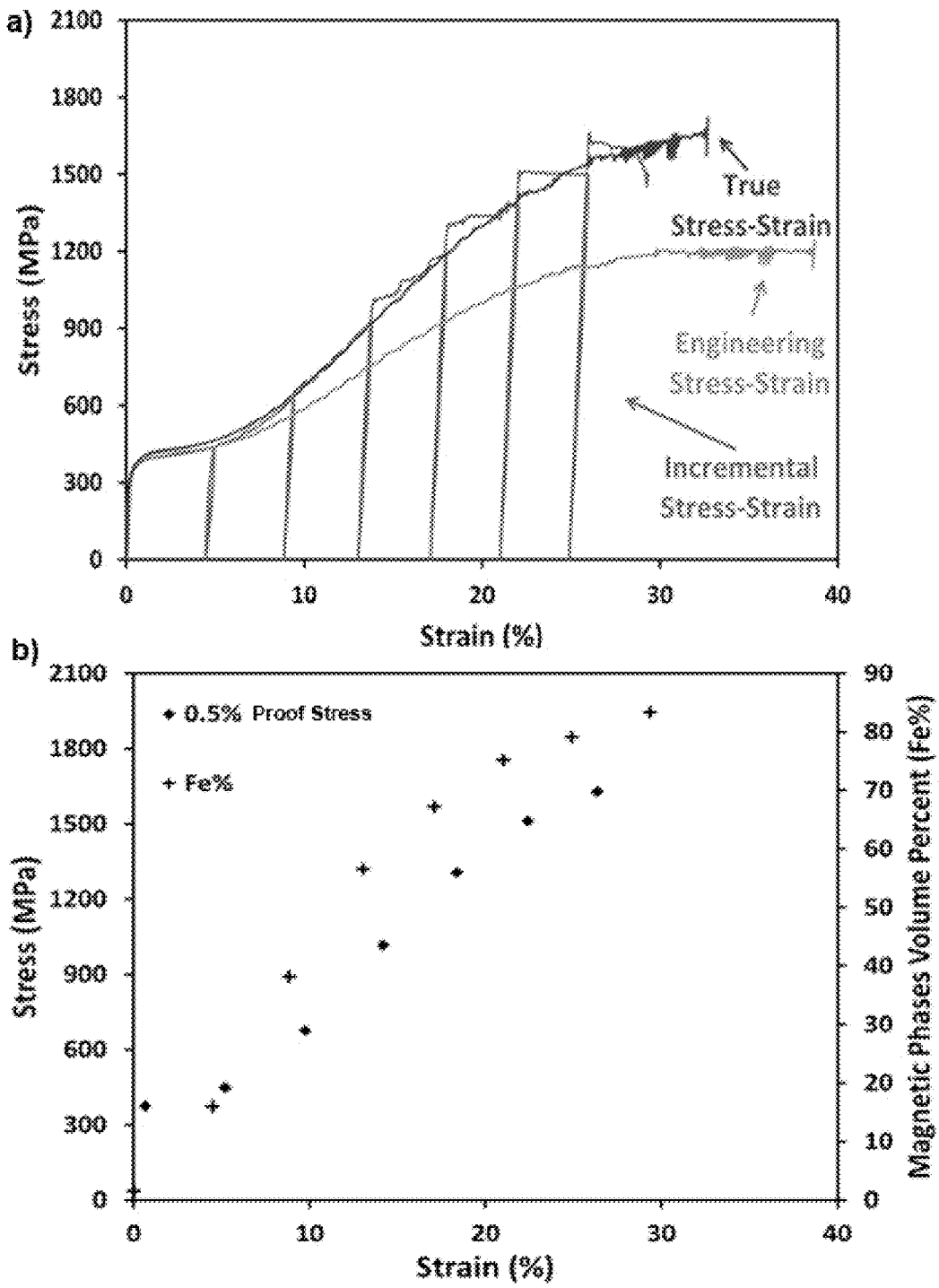


FIG. 19

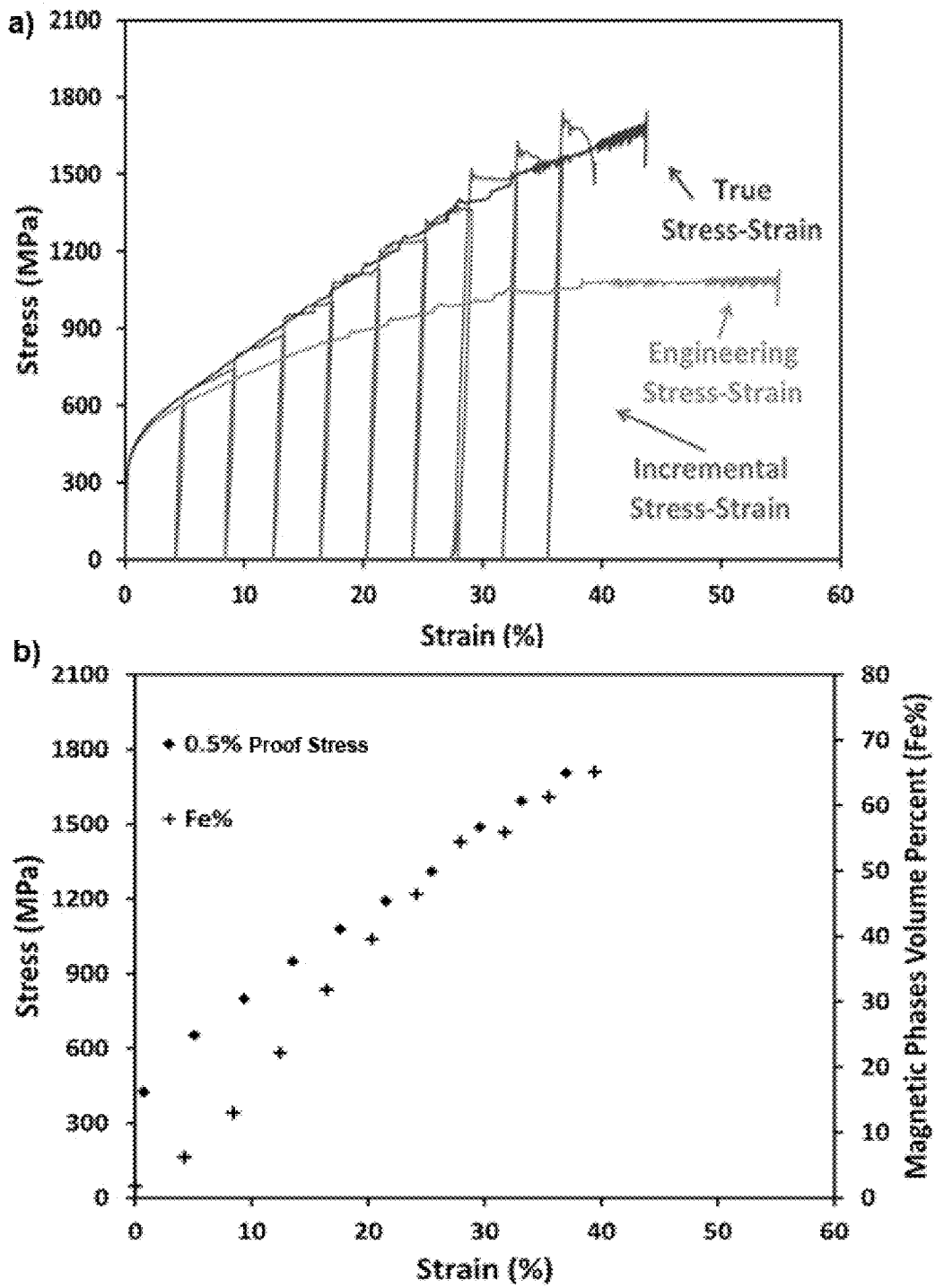


FIG. 20

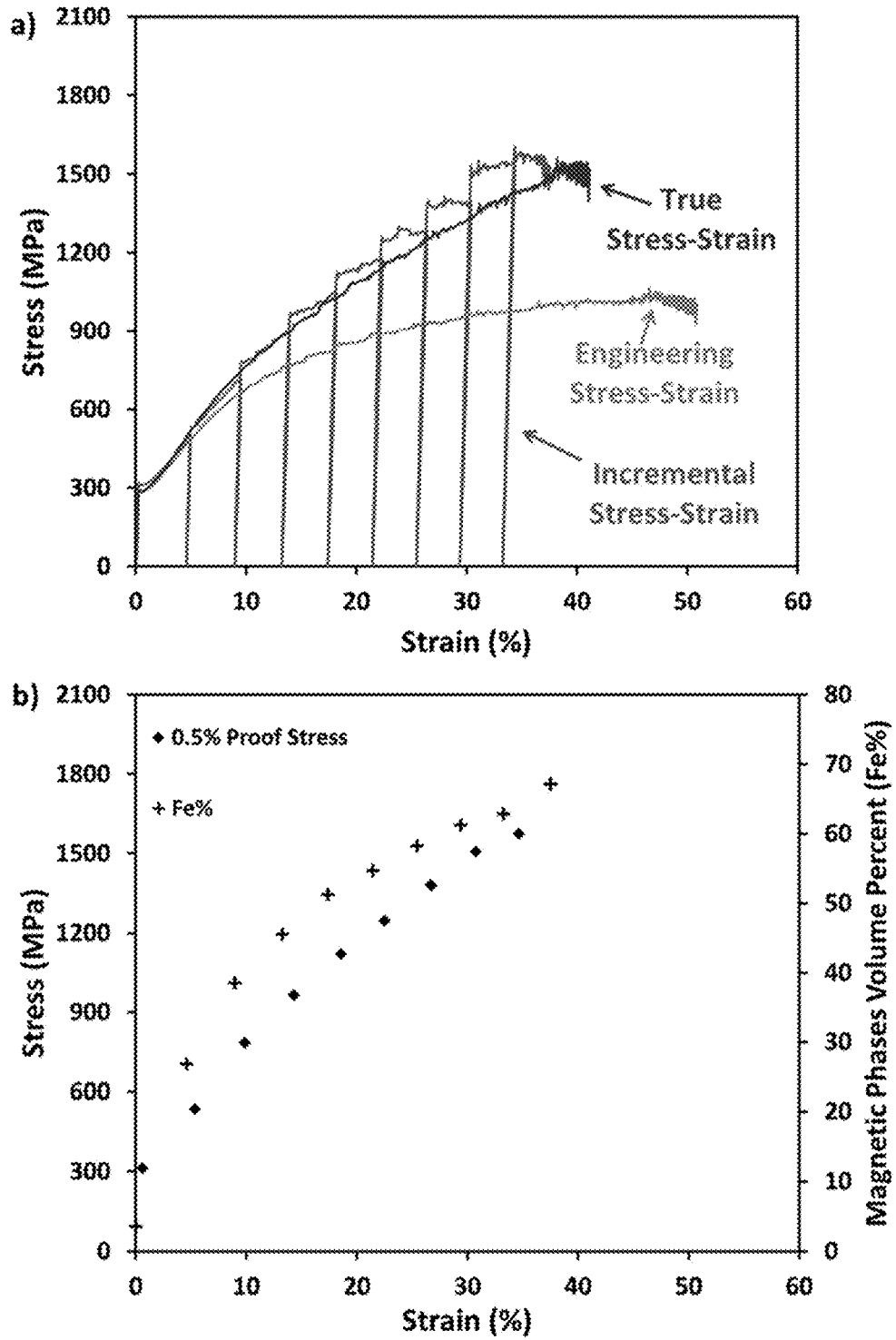


FIG. 21.

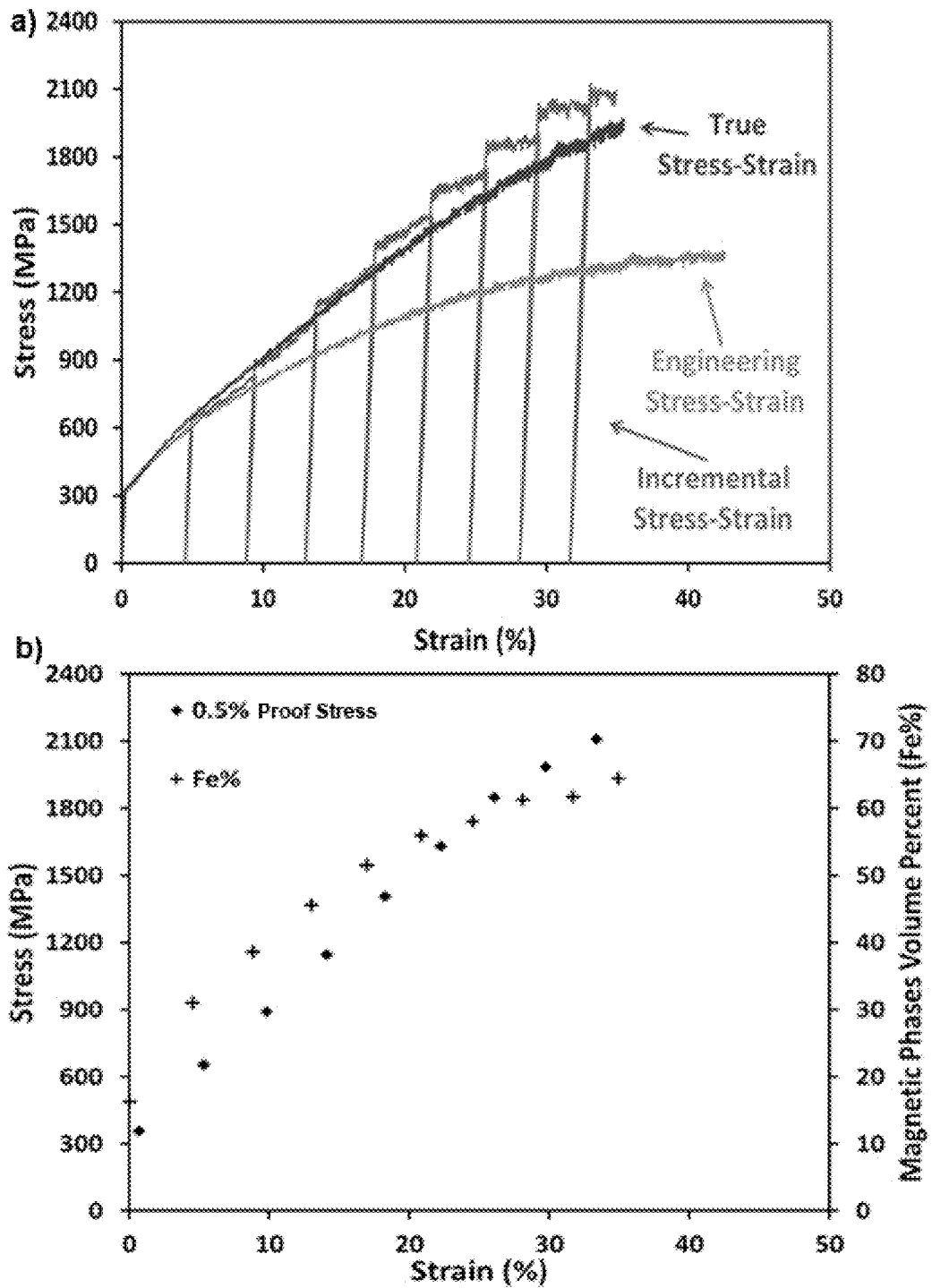


FIG. 22

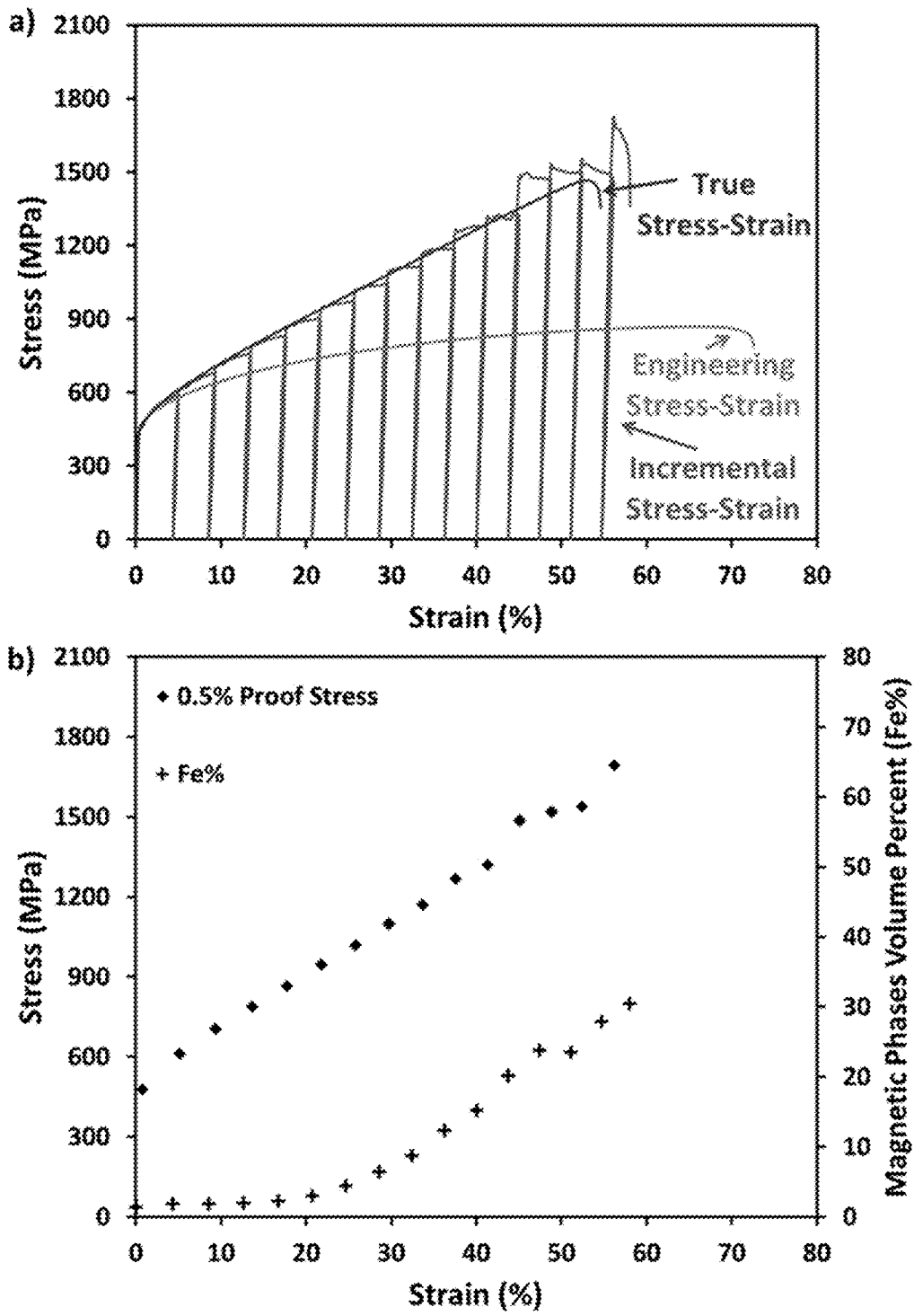


FIG. 23.



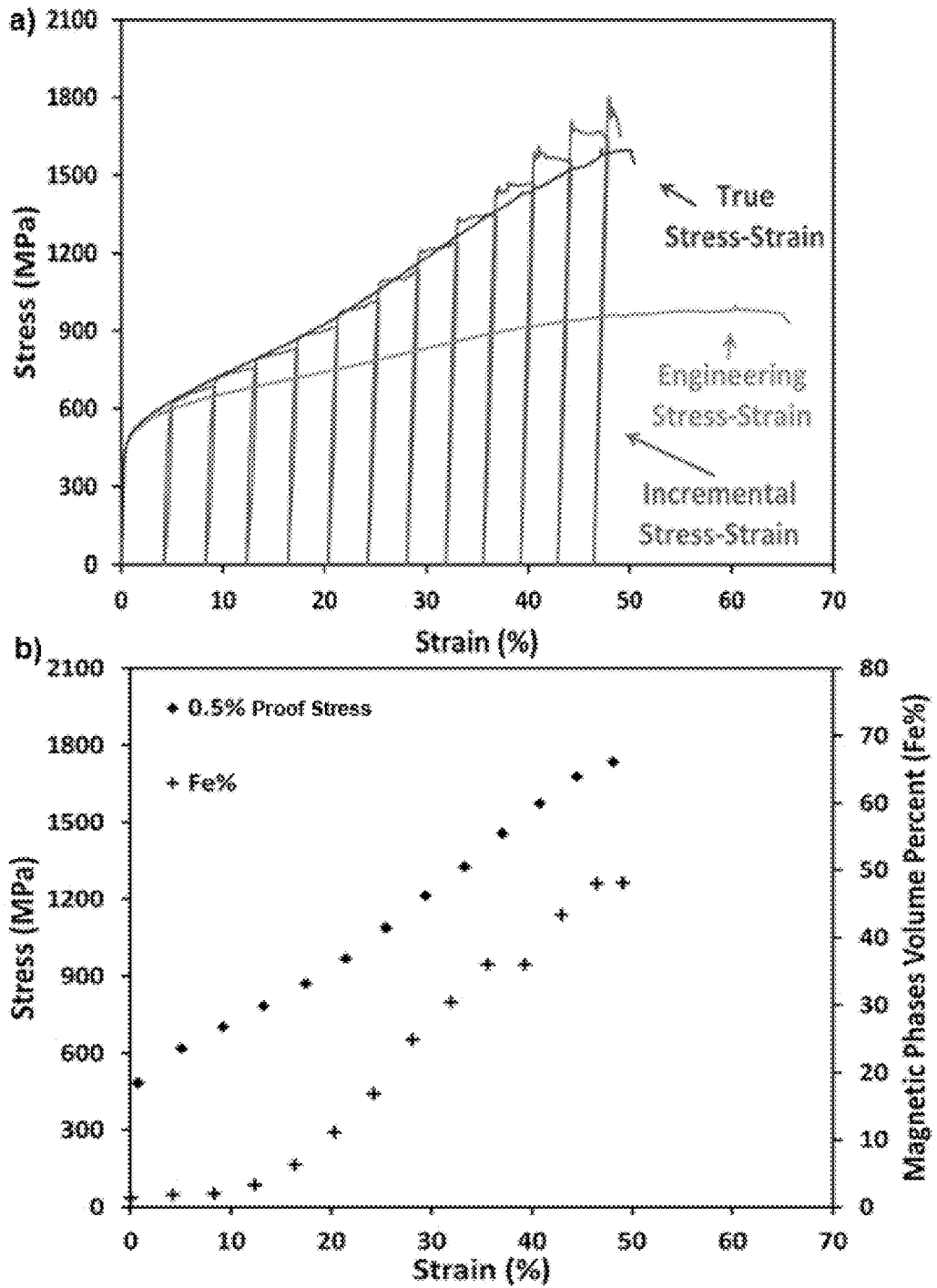


FIG. 24

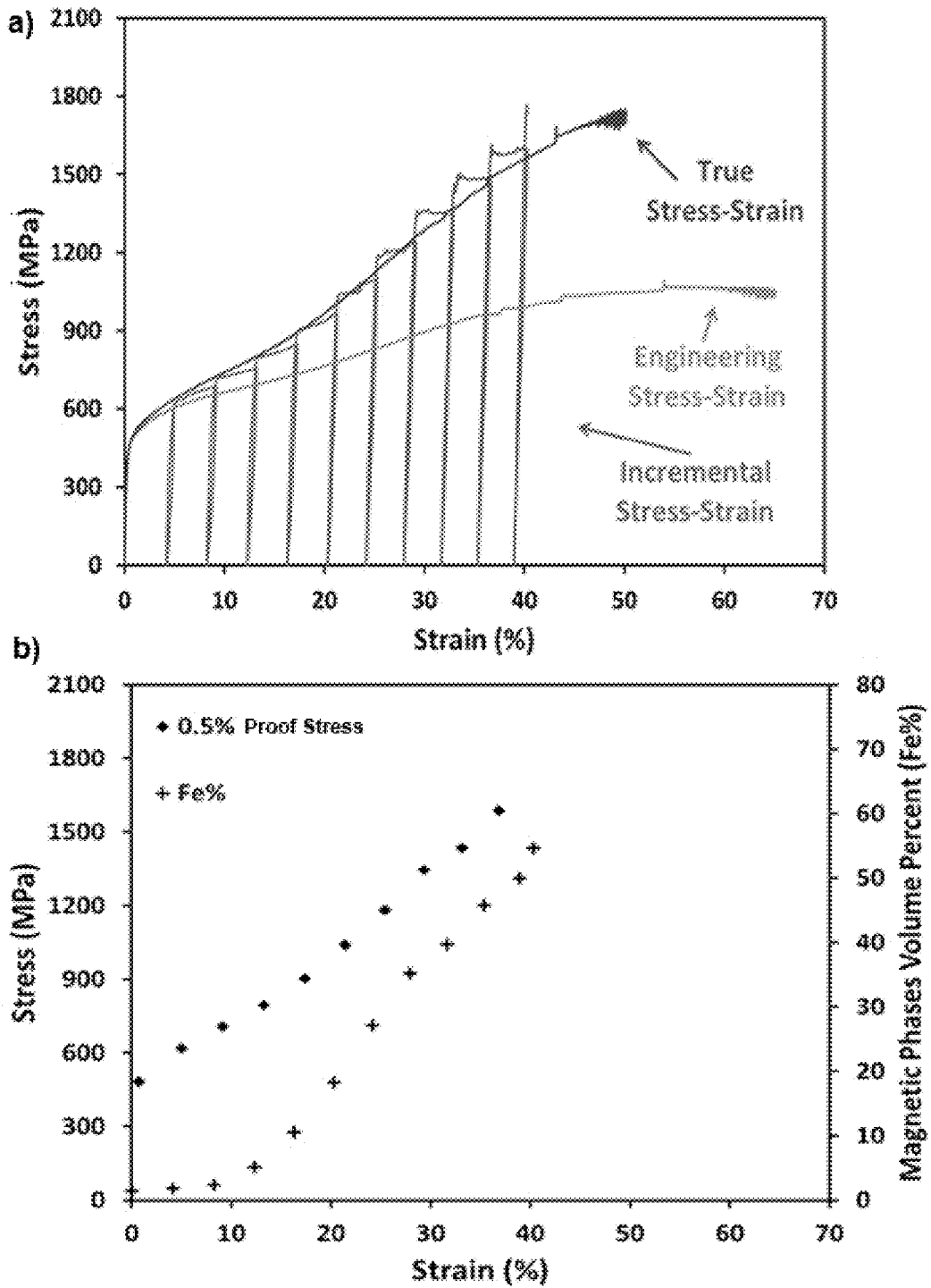


FIG. 25

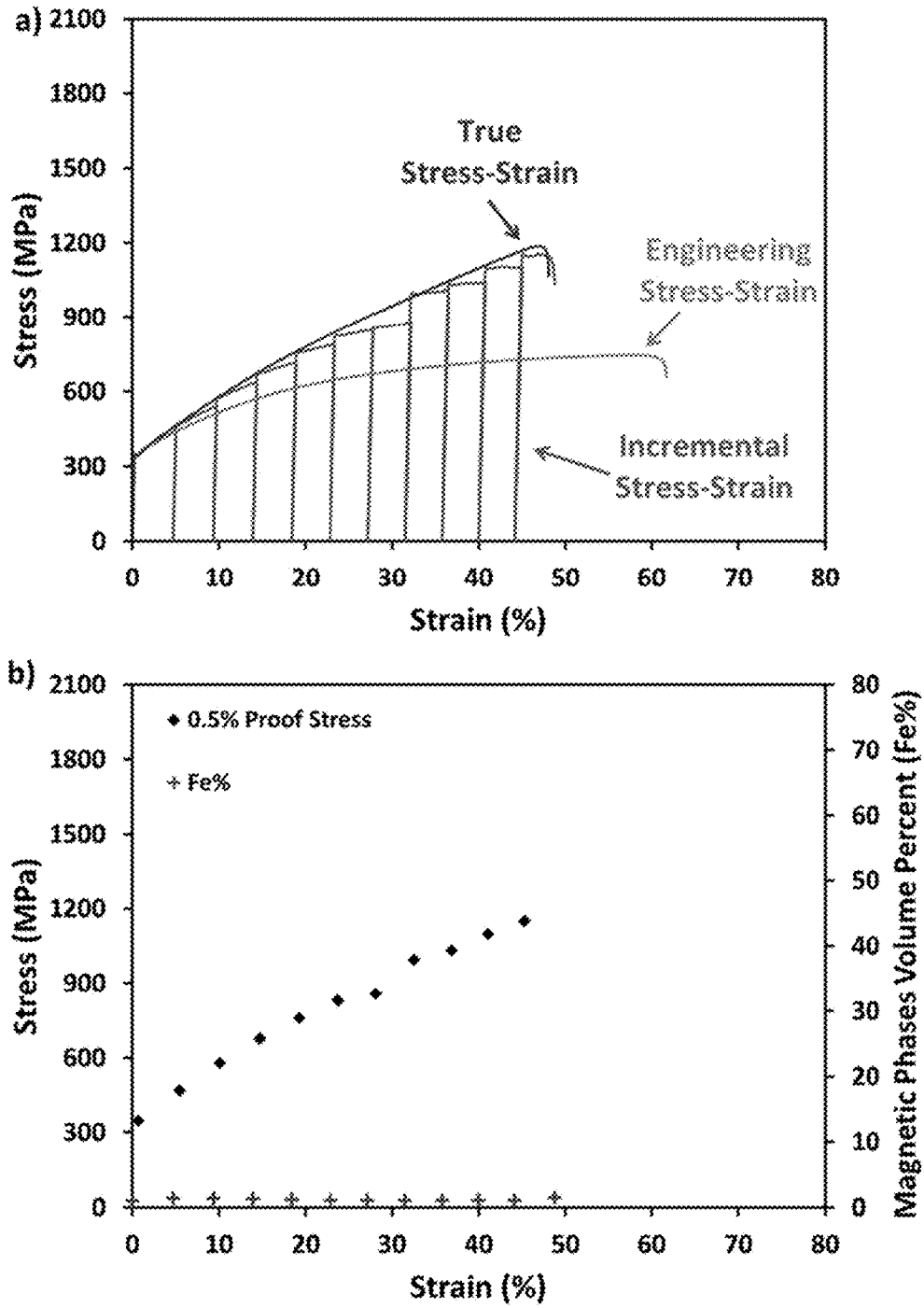


FIG. 26.

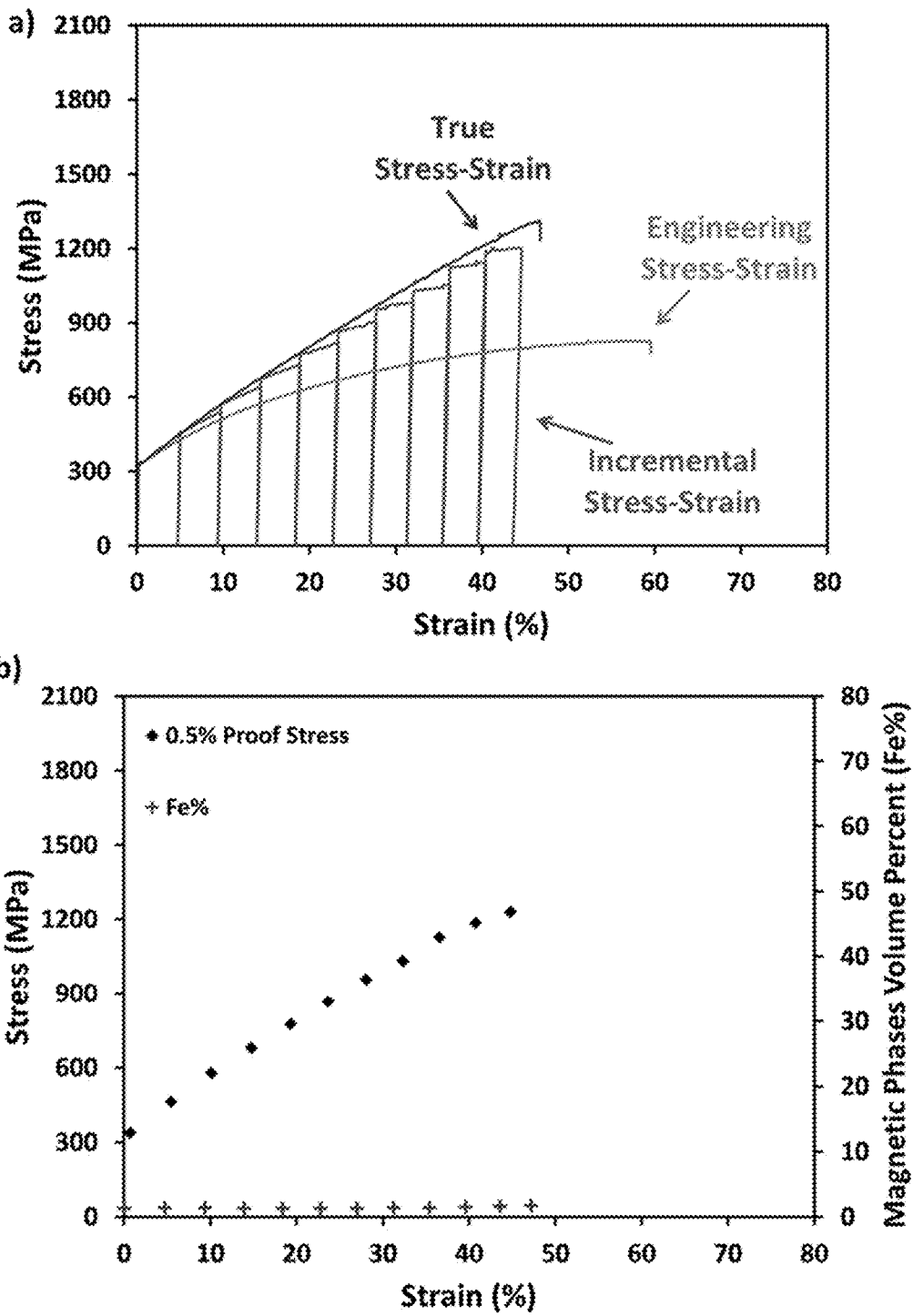


FIG. 27

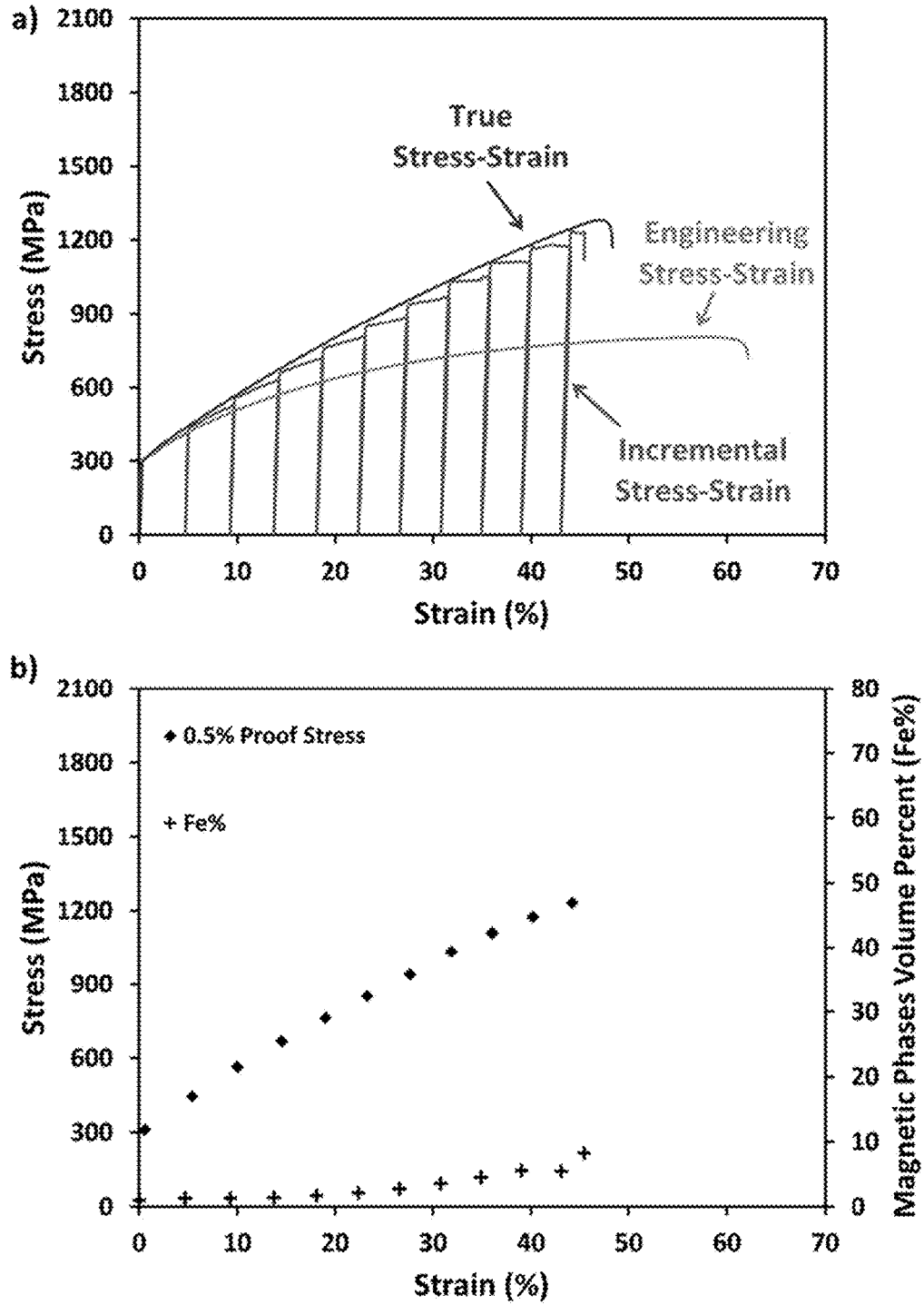


FIG. 28.

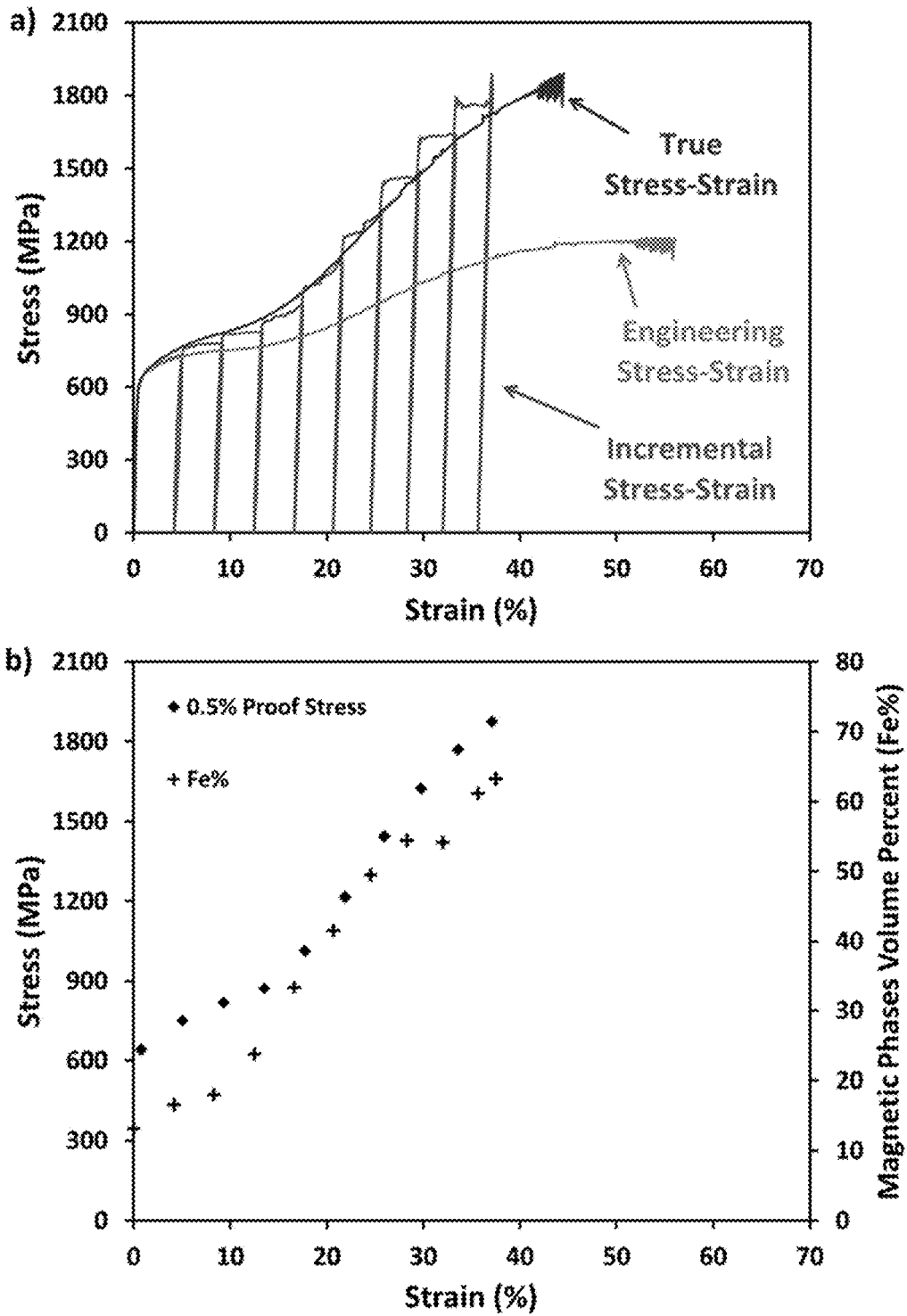


FIG. 29

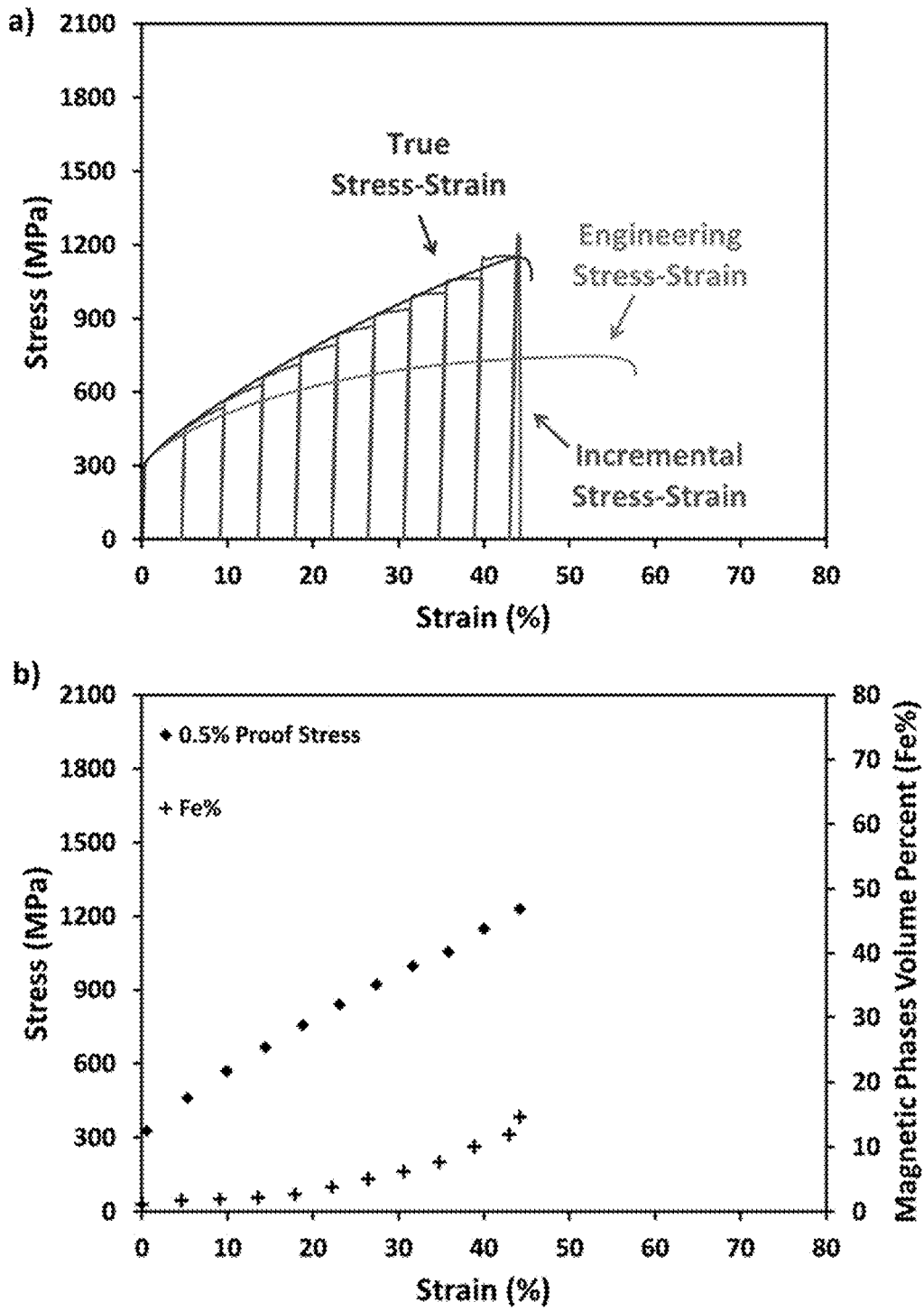


FIG. 30

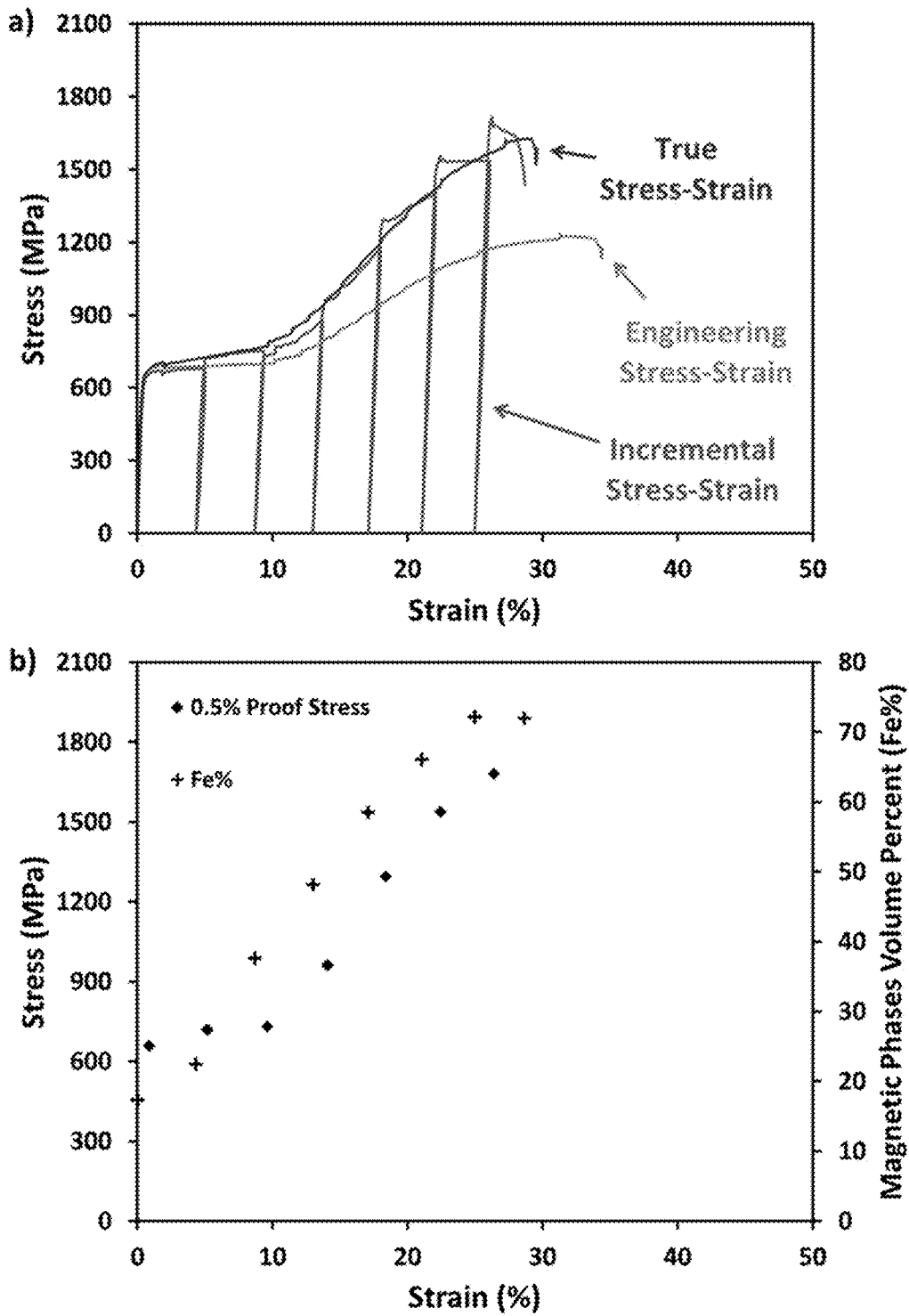


FIG. 31



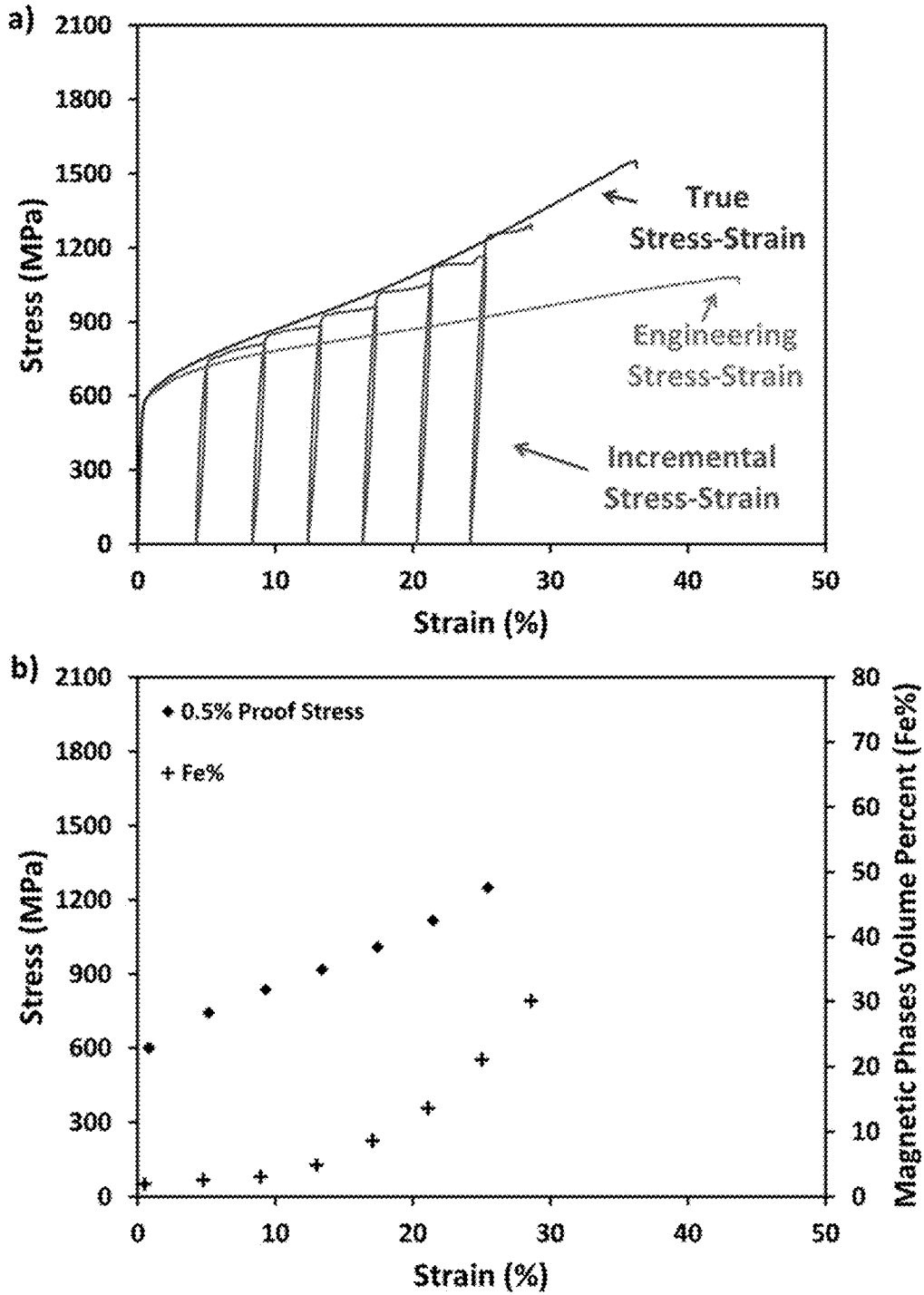


FIG. 32

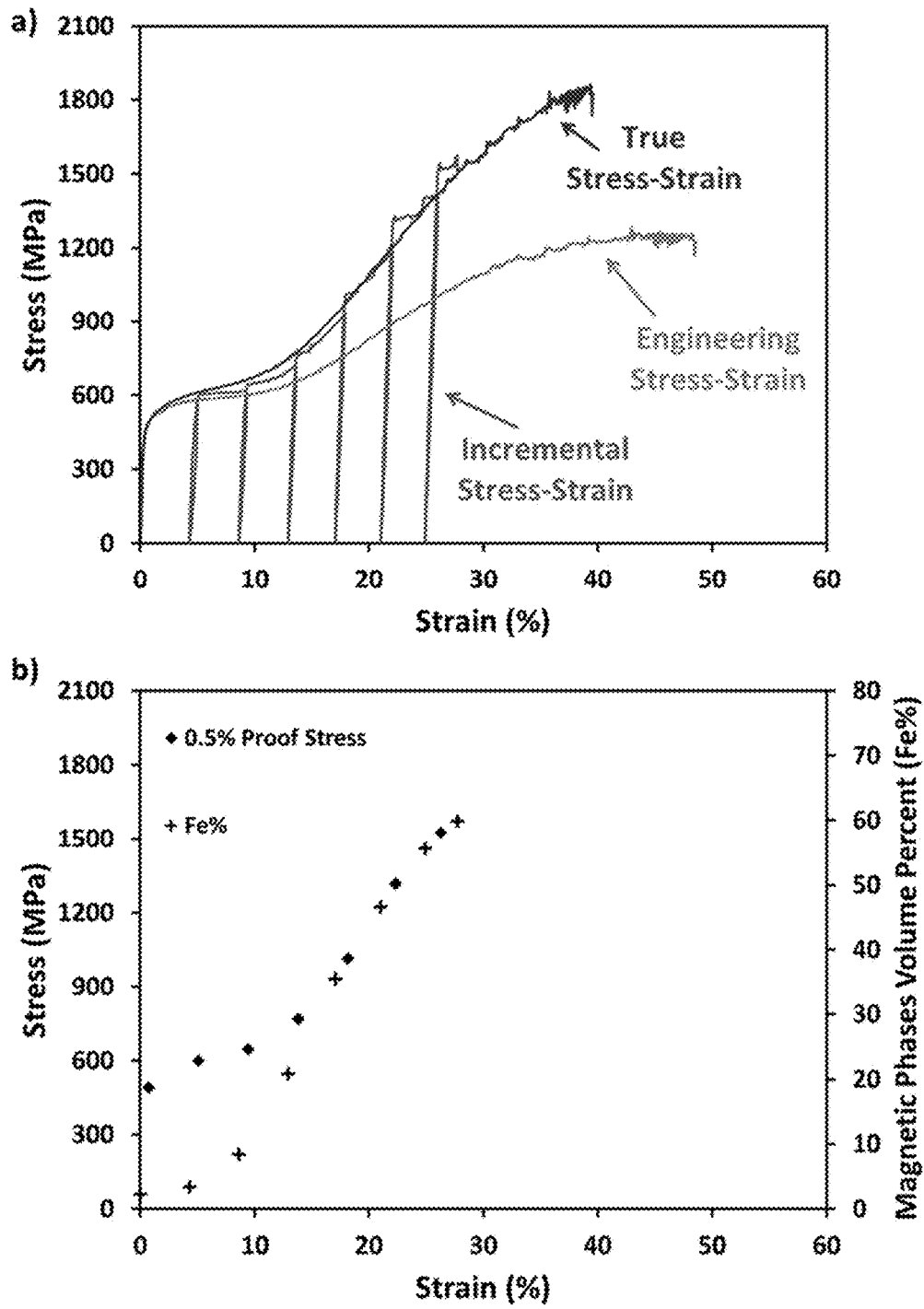


FIG. 33

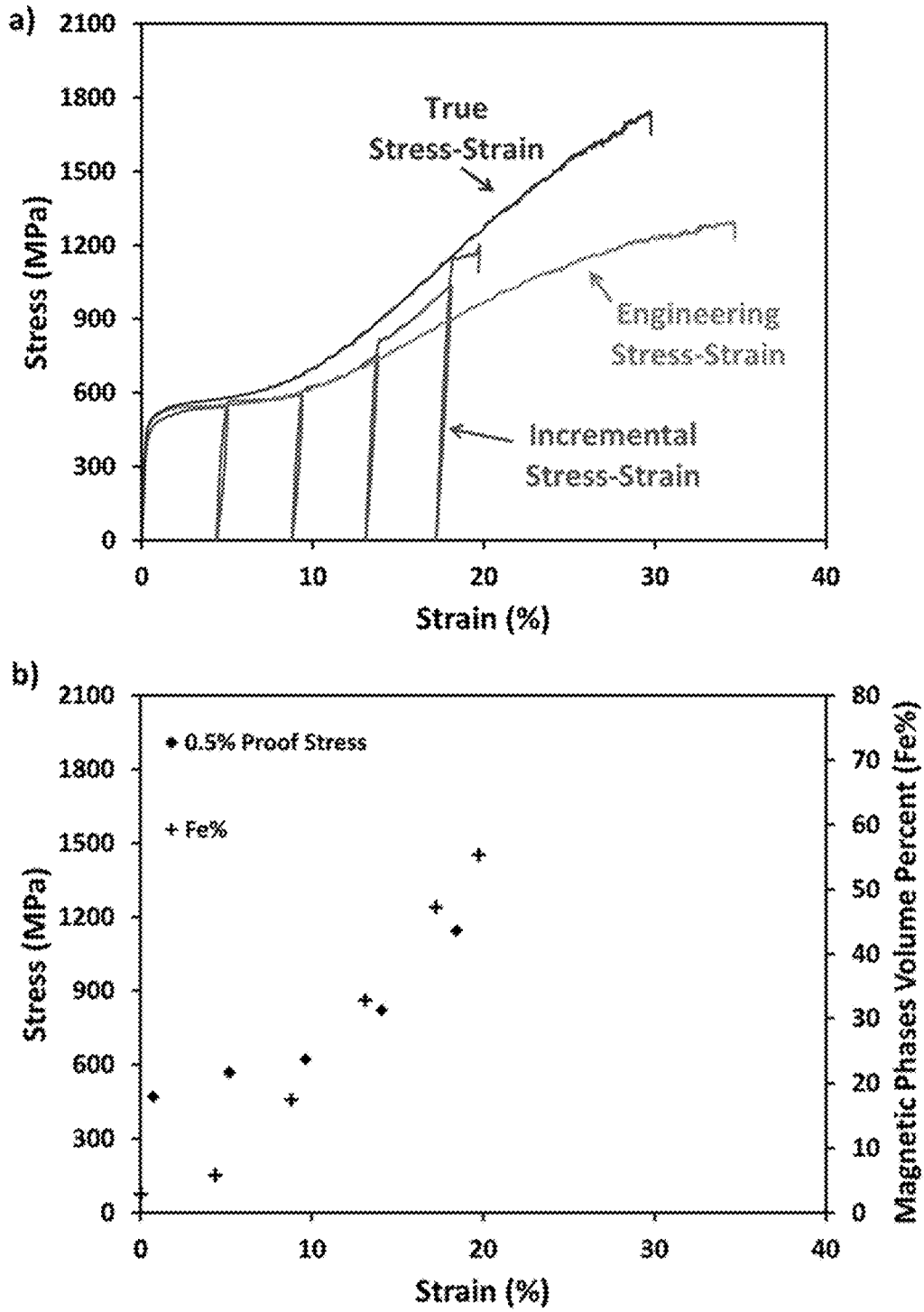


FIG. 34

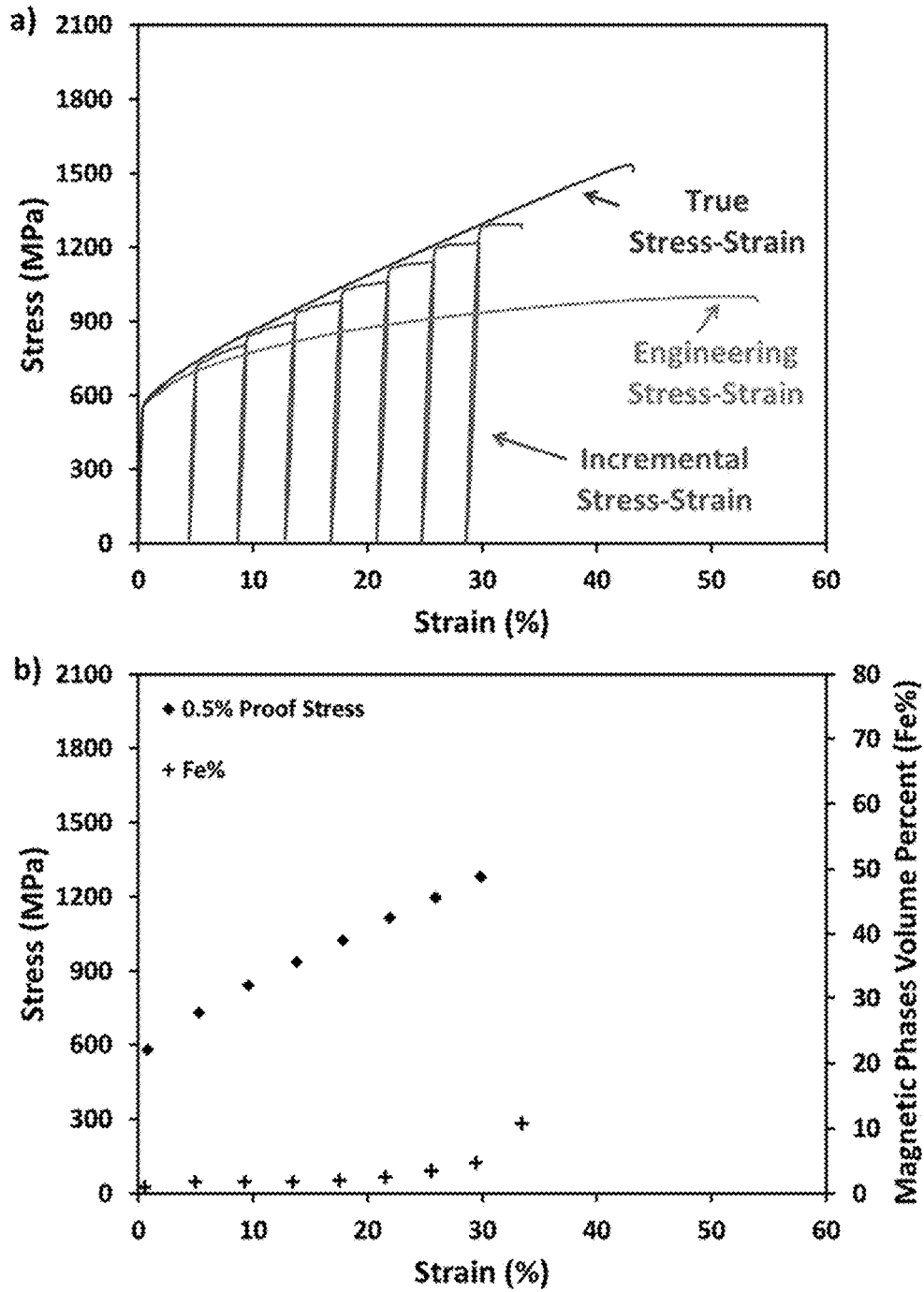


FIG. 35

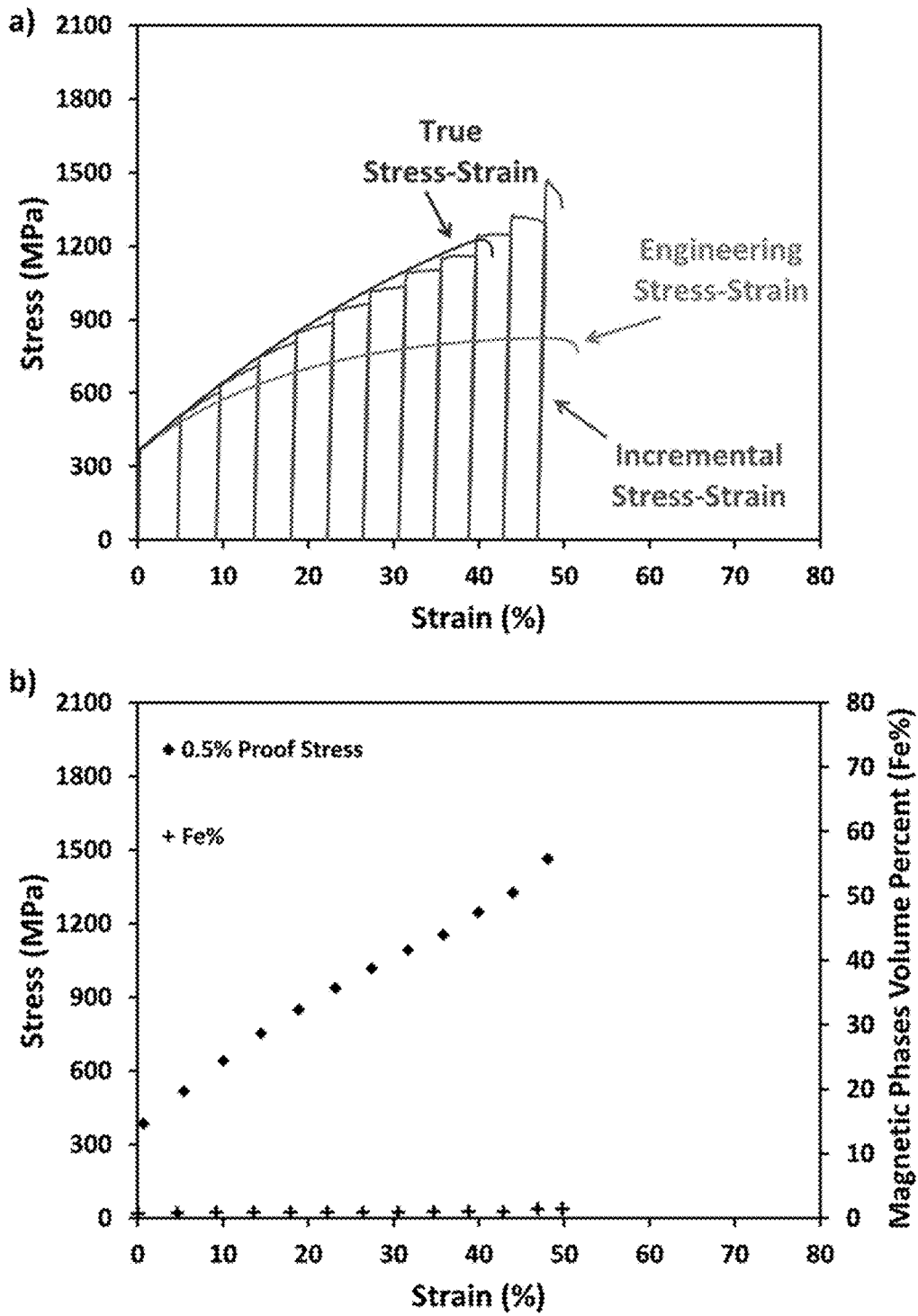


FIG. 36

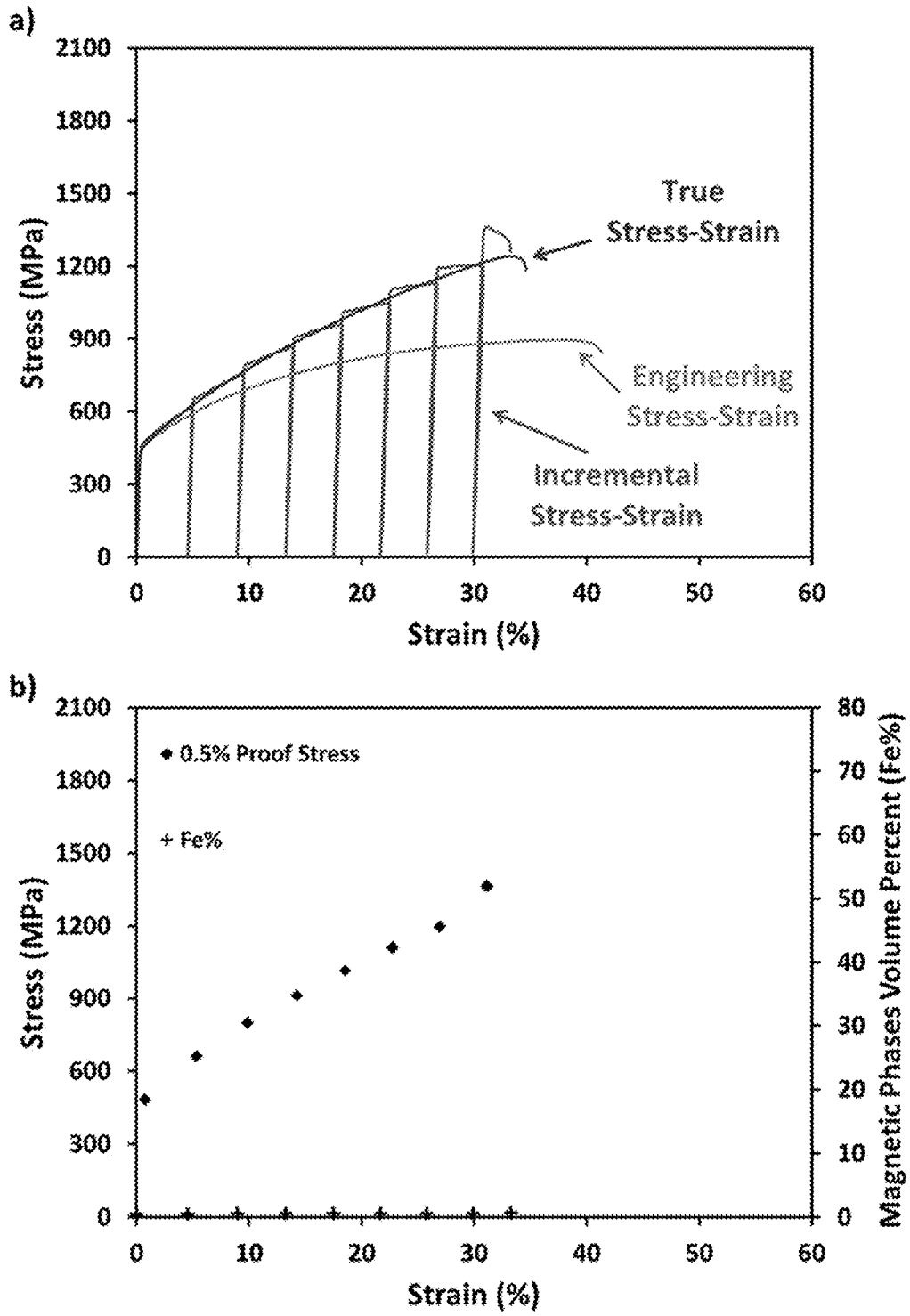


FIG. 37

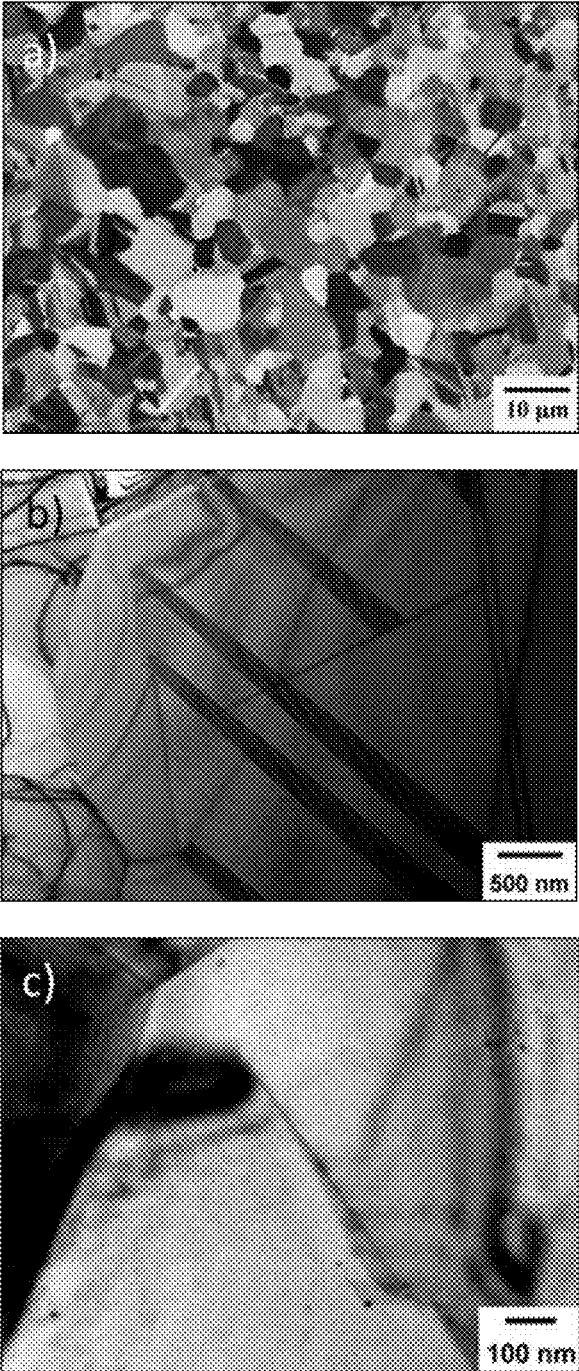


FIG. 38.

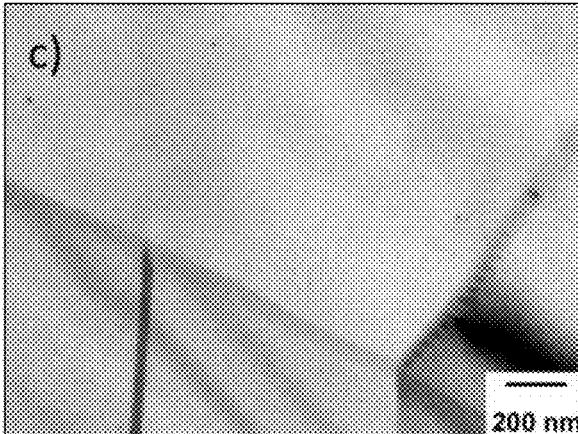
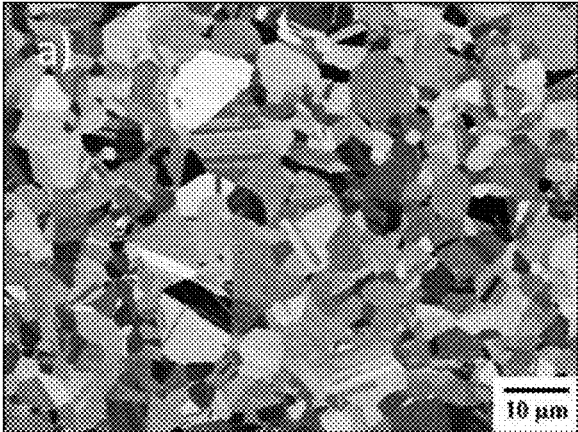


FIG. 39



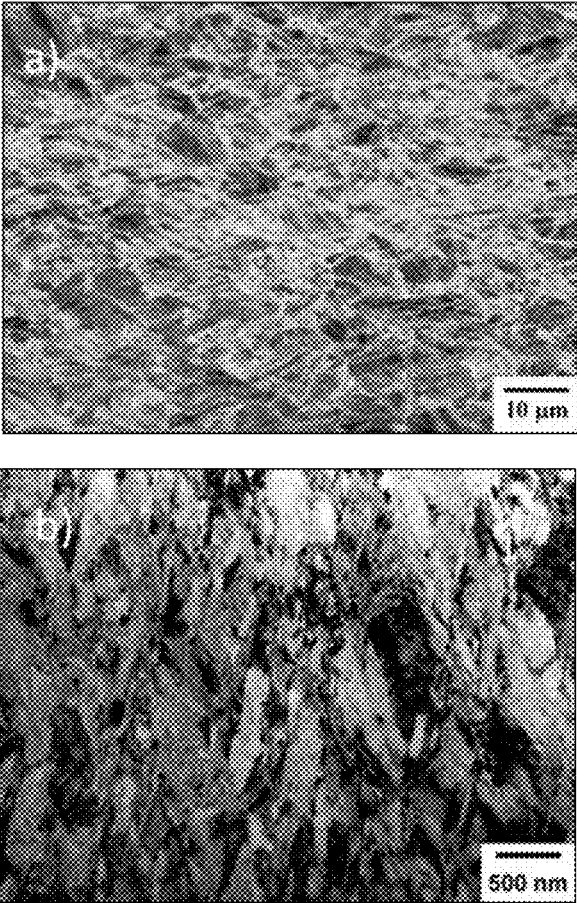


FIG. 40

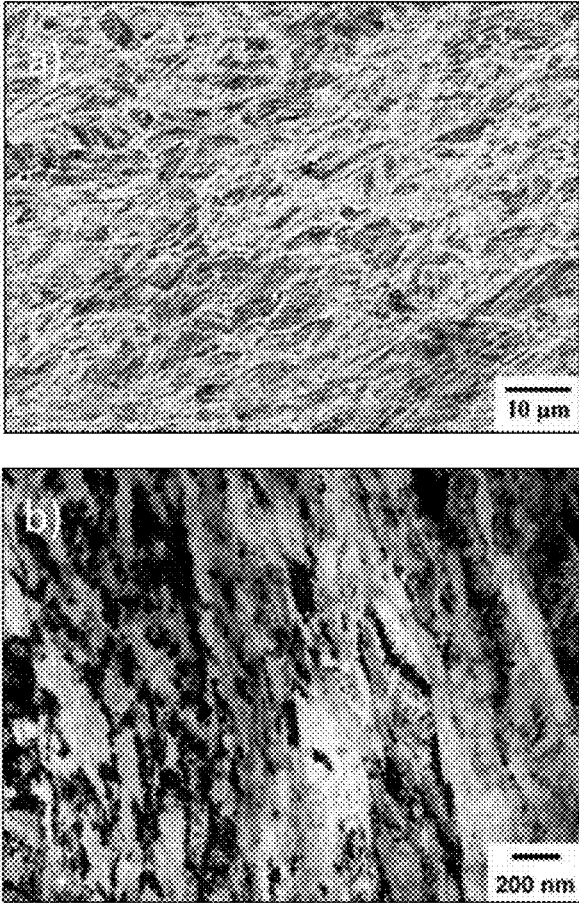


FIG. 41

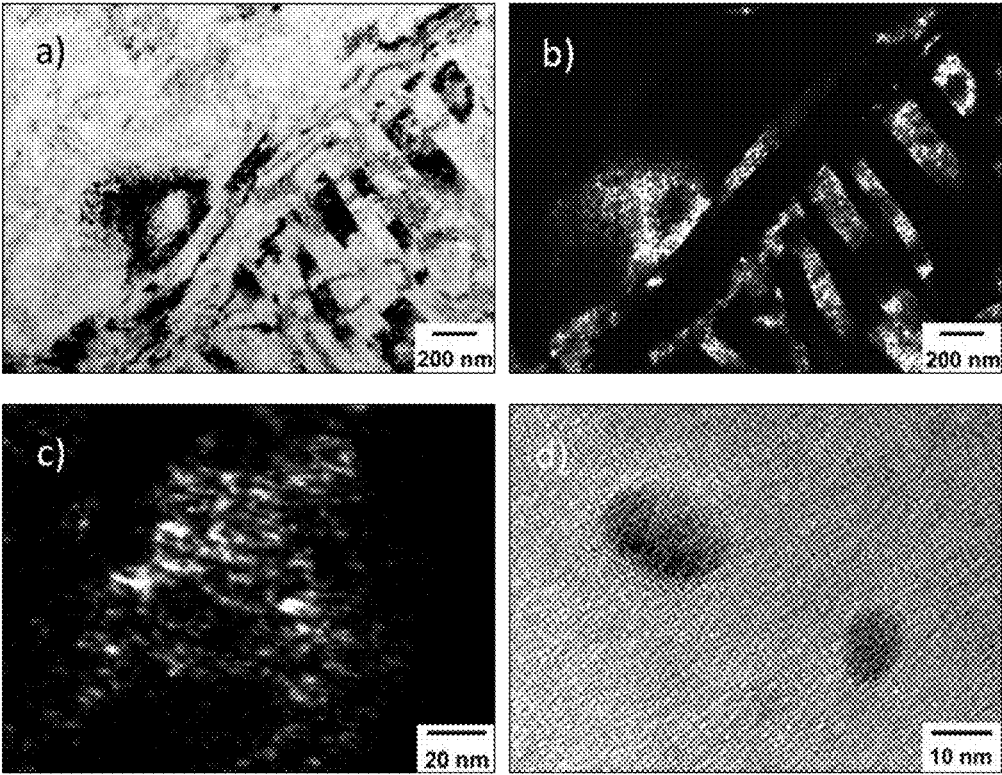


FIG. 42.

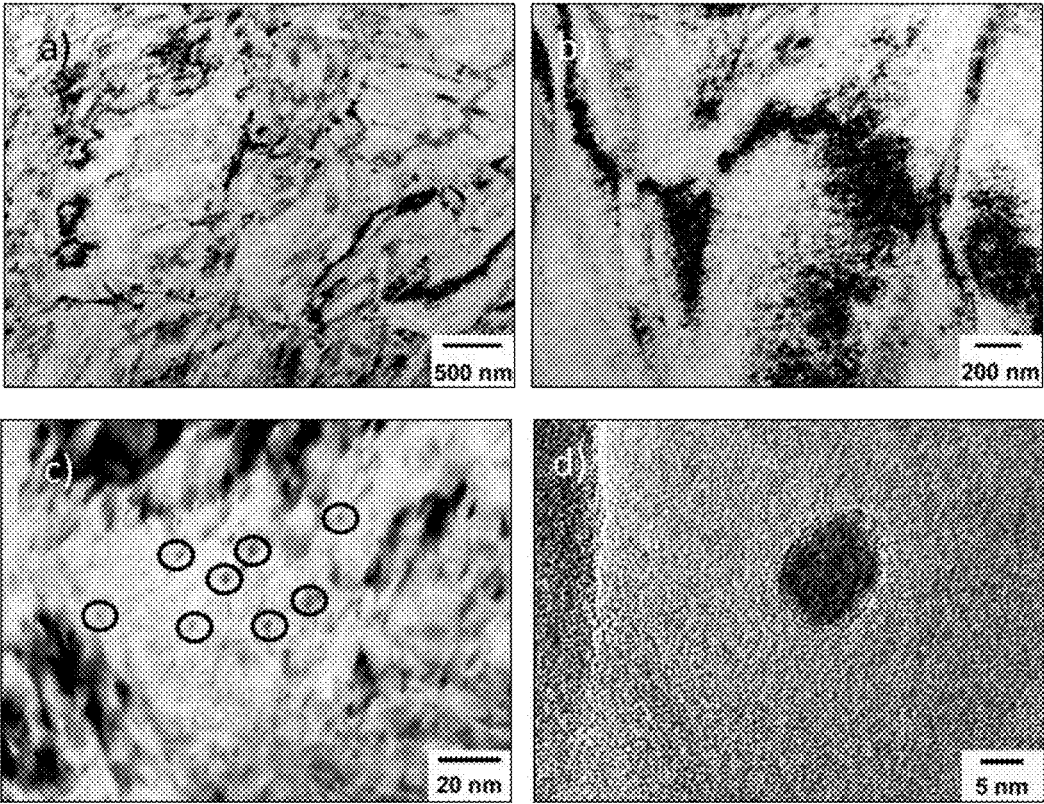


FIG. 43

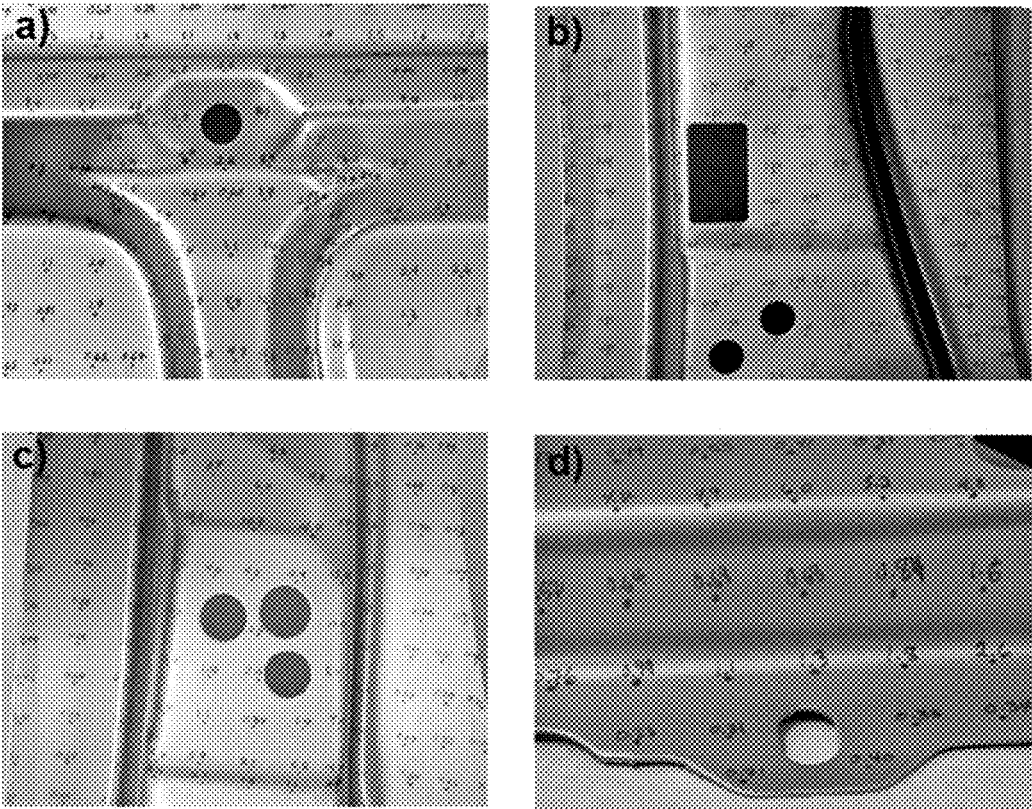


FIG. 44

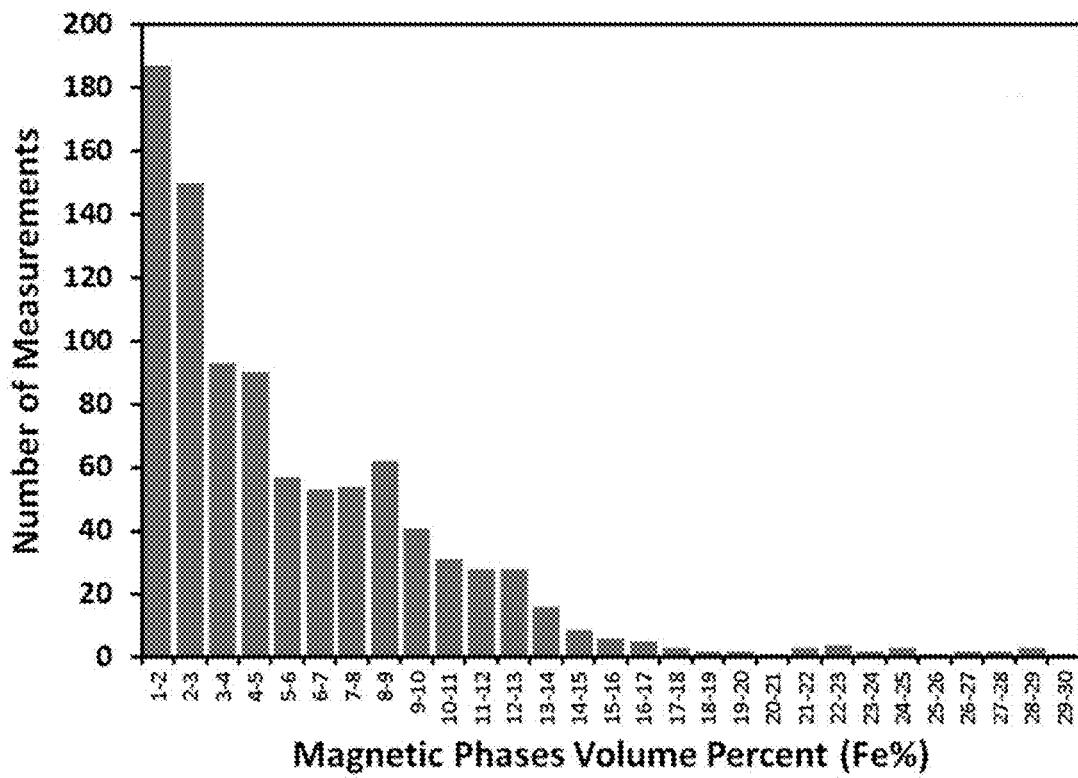


FIG. 45

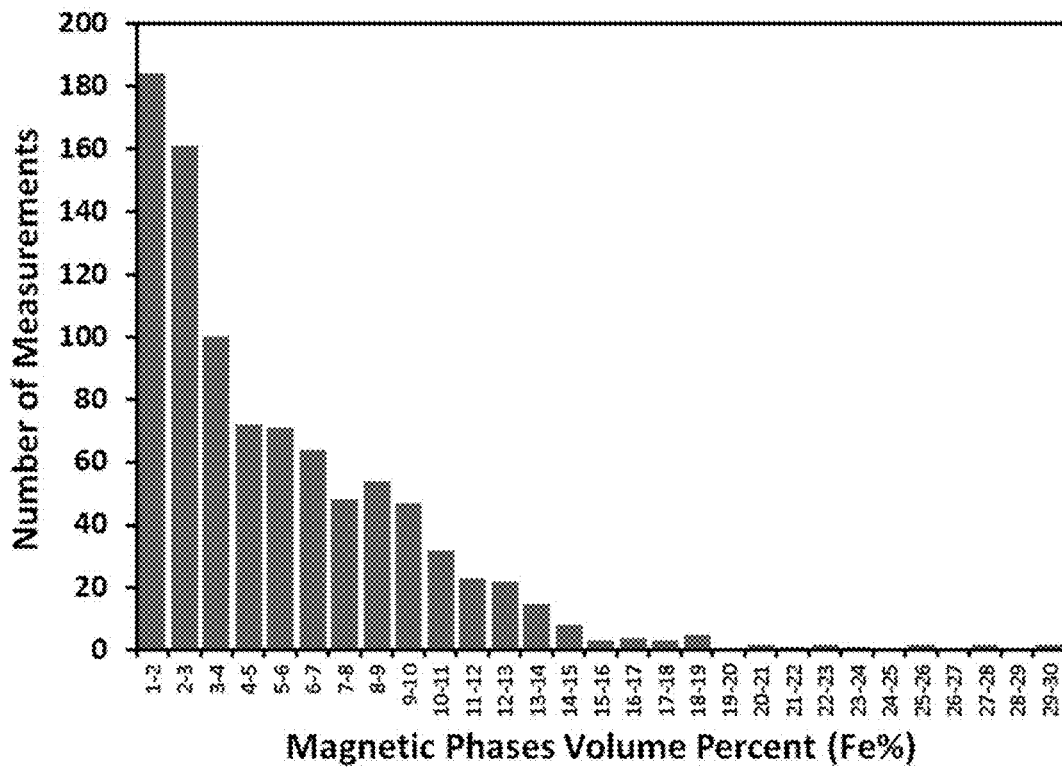


FIG. 46

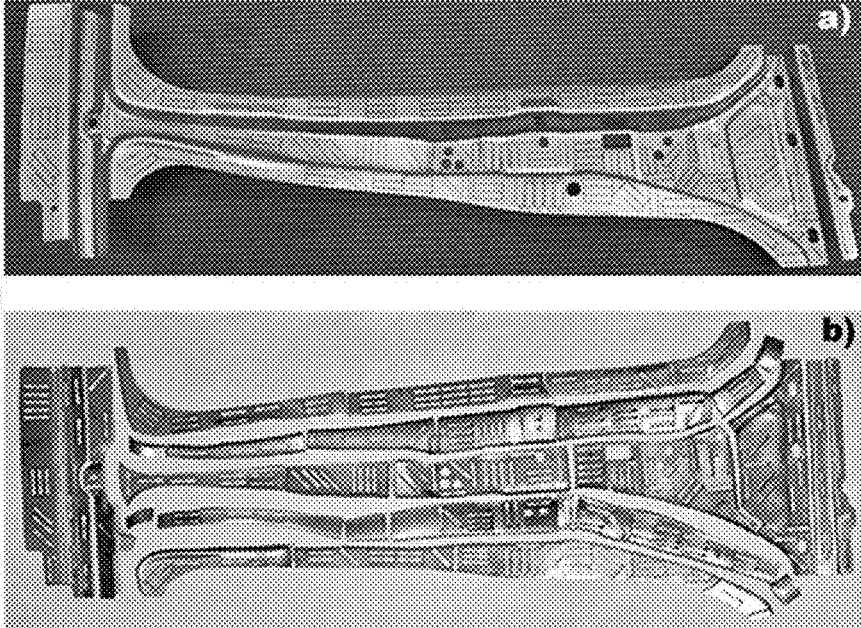


FIG. 47



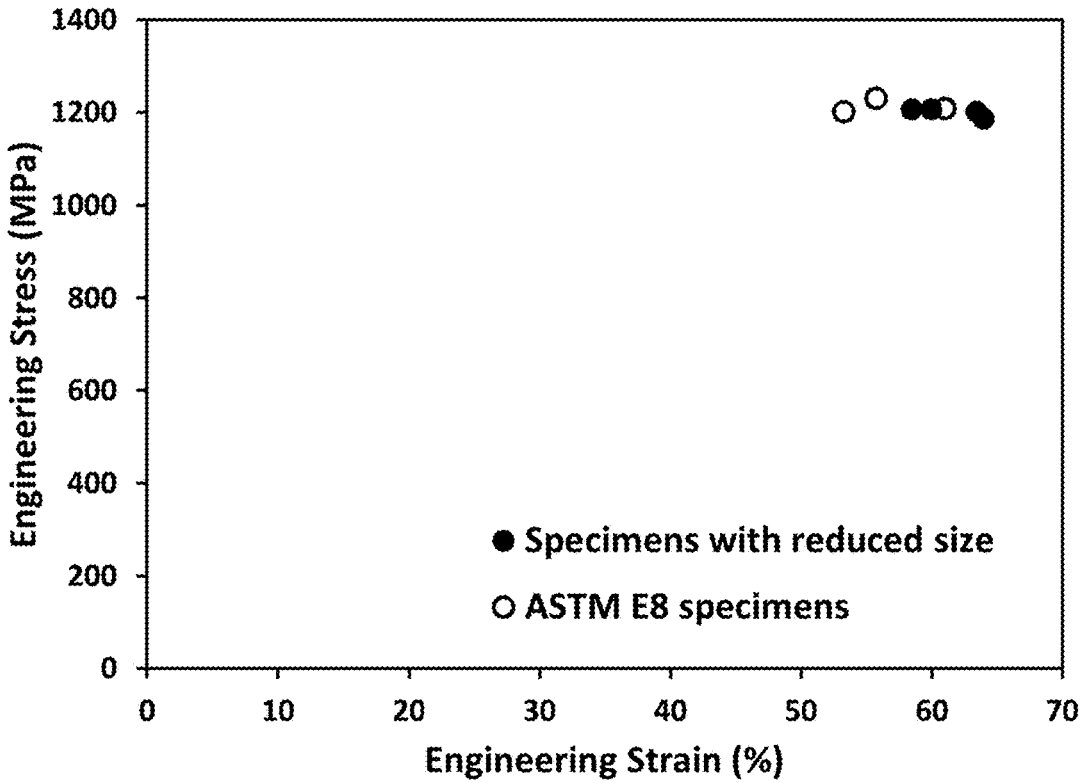


FIG. 48

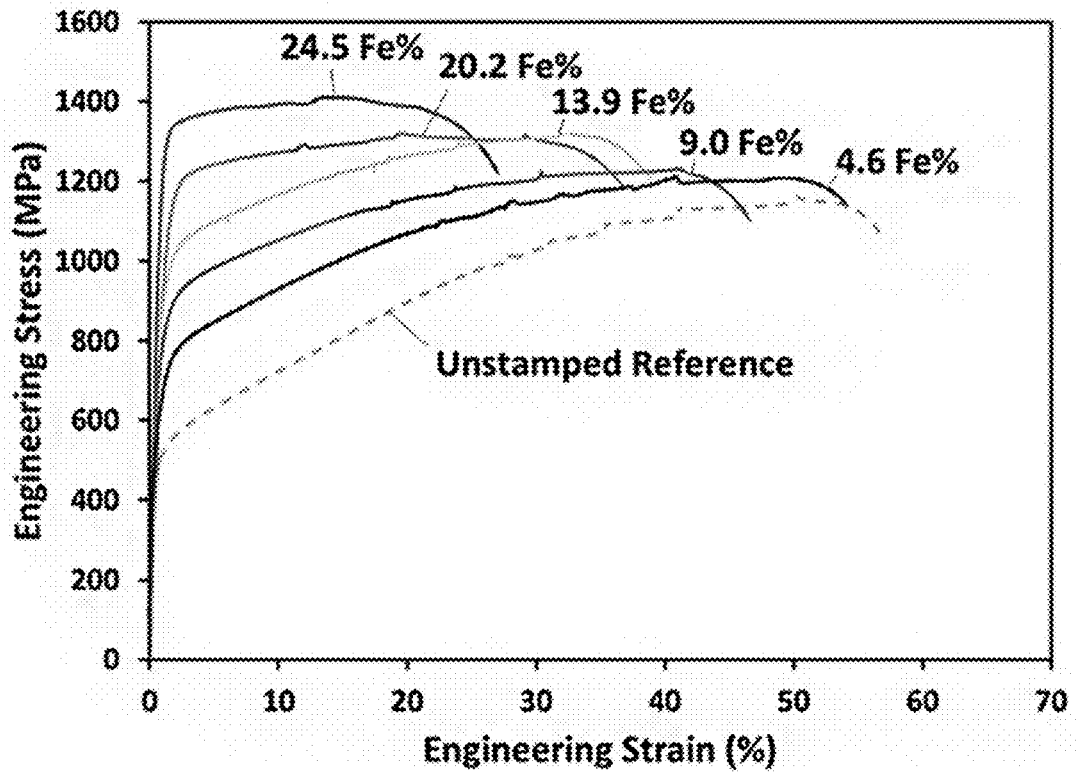


FIG. 49

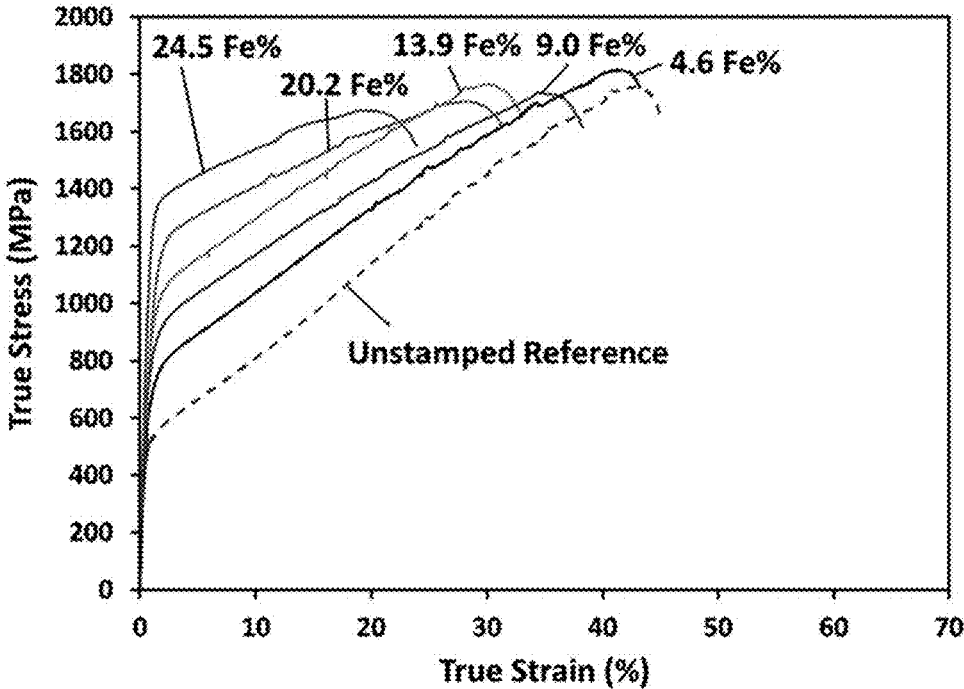


FIG. 50

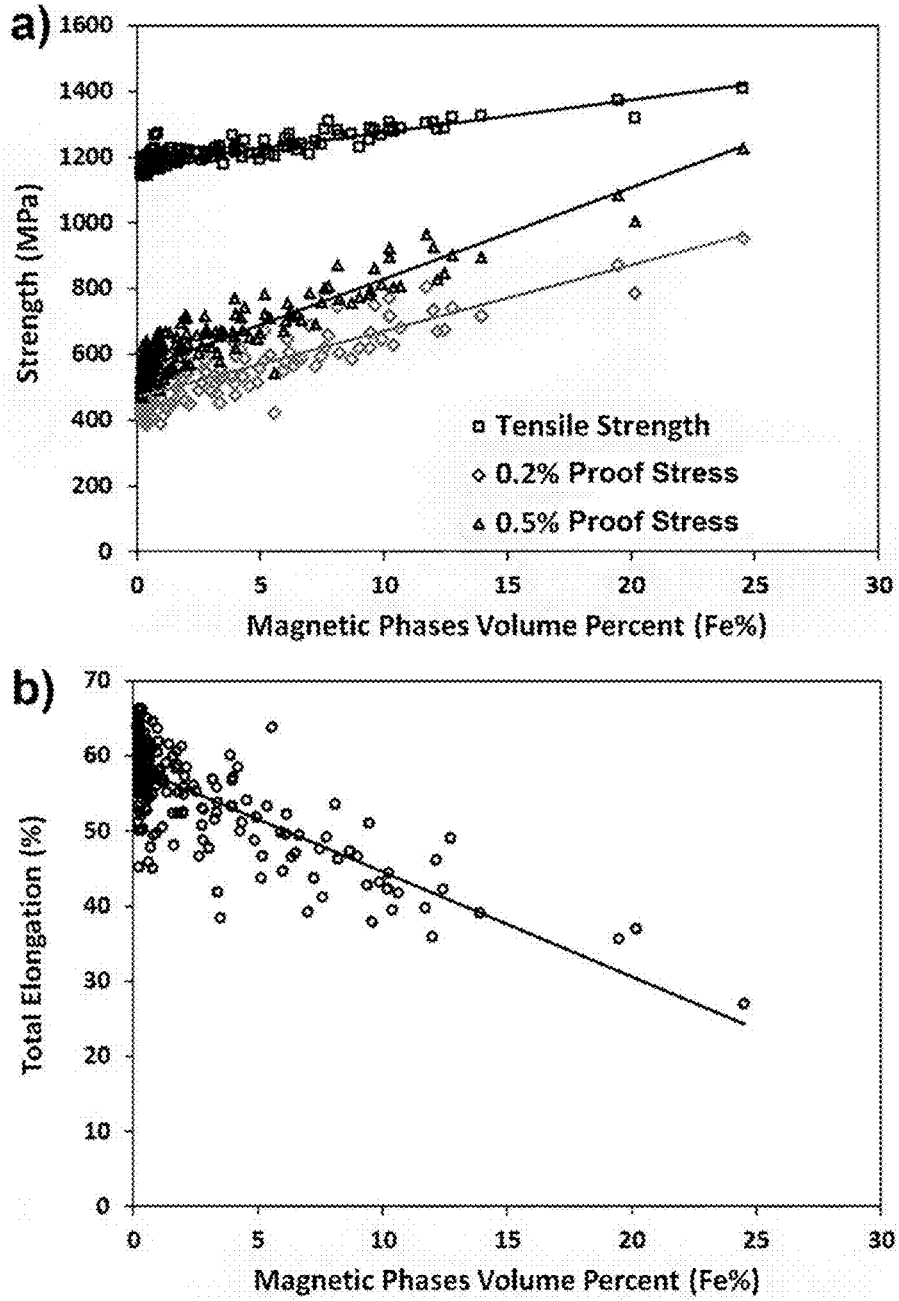


FIG. 51

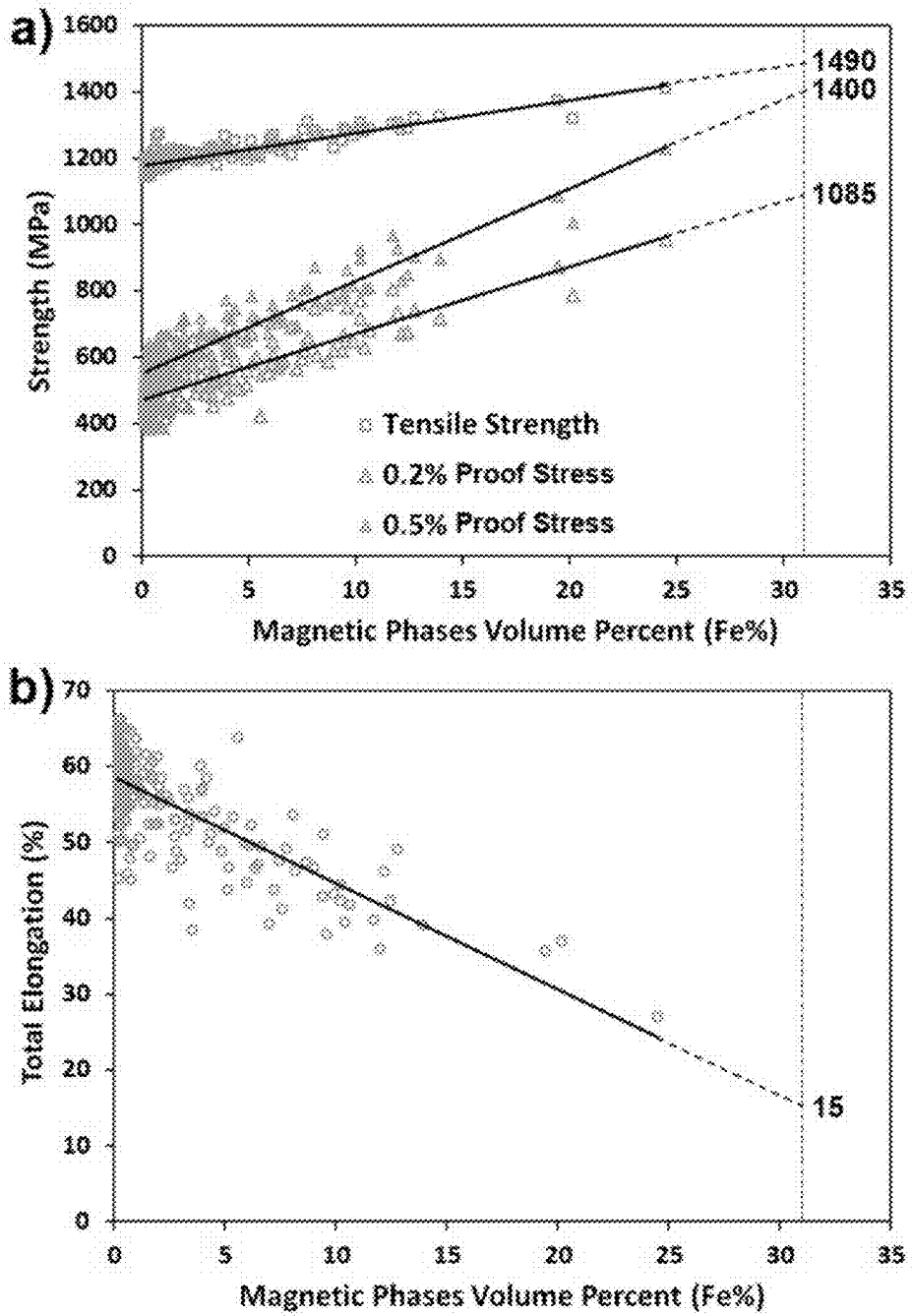


FIG. 52

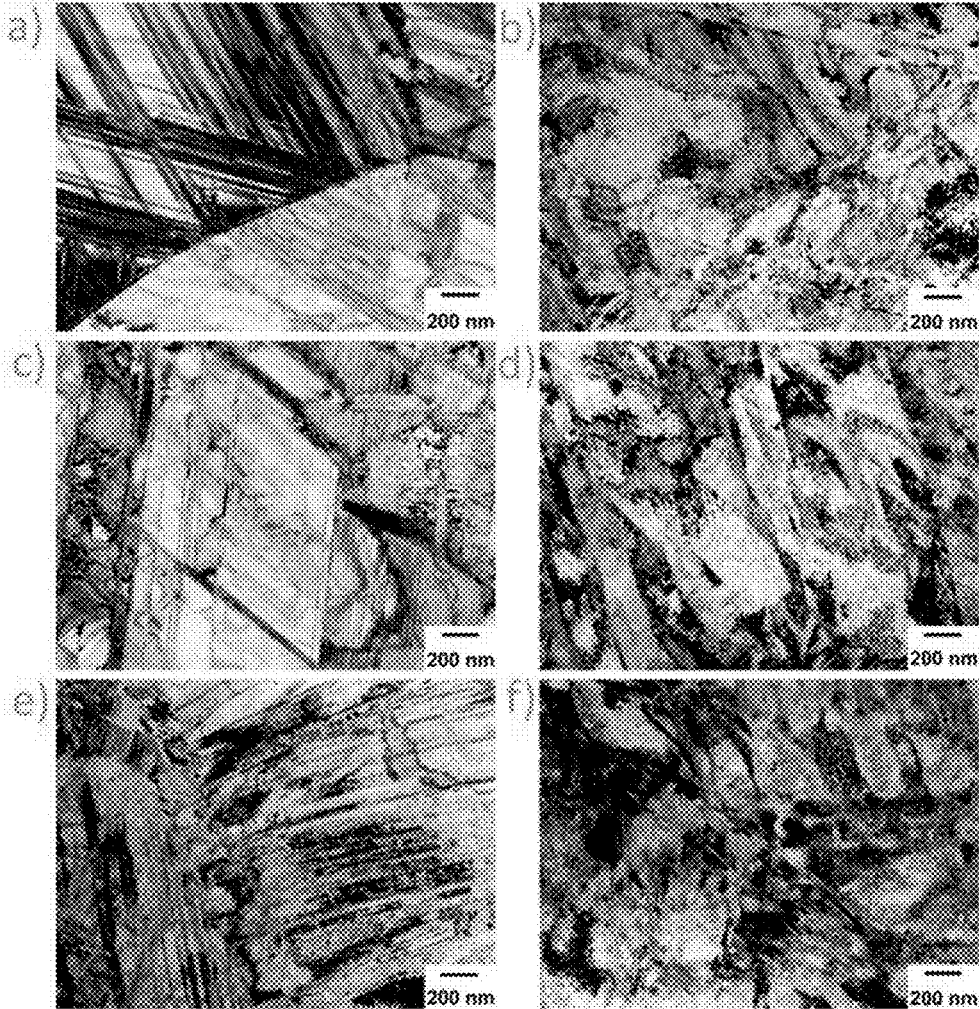


FIG. 53

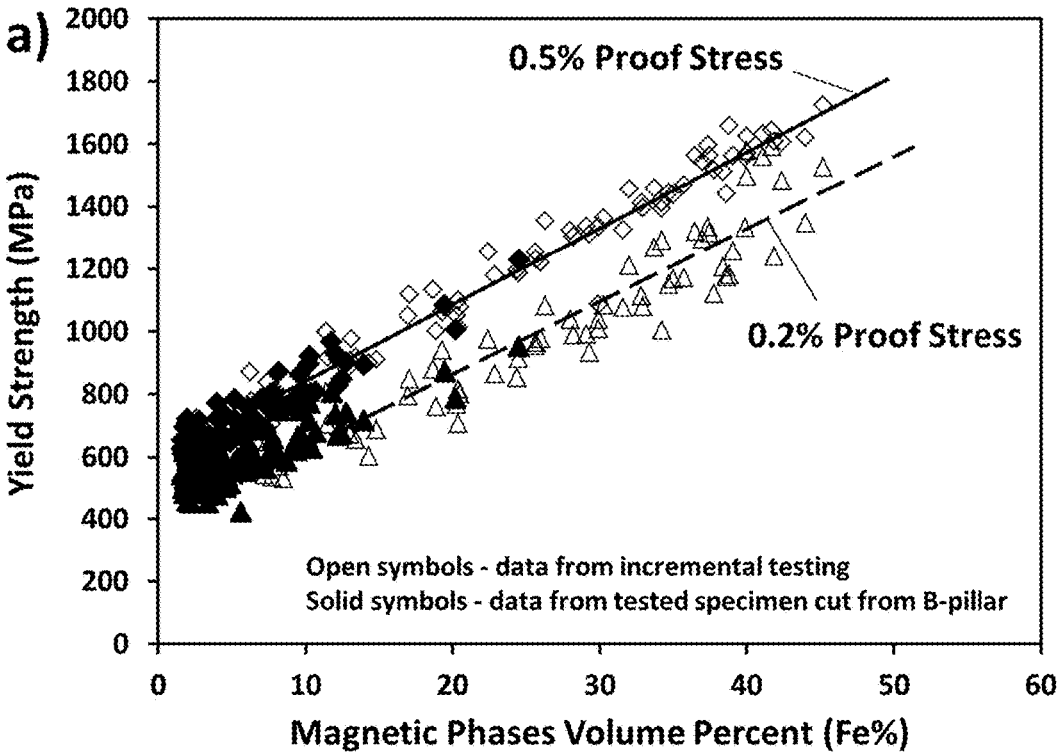


FIG. 54

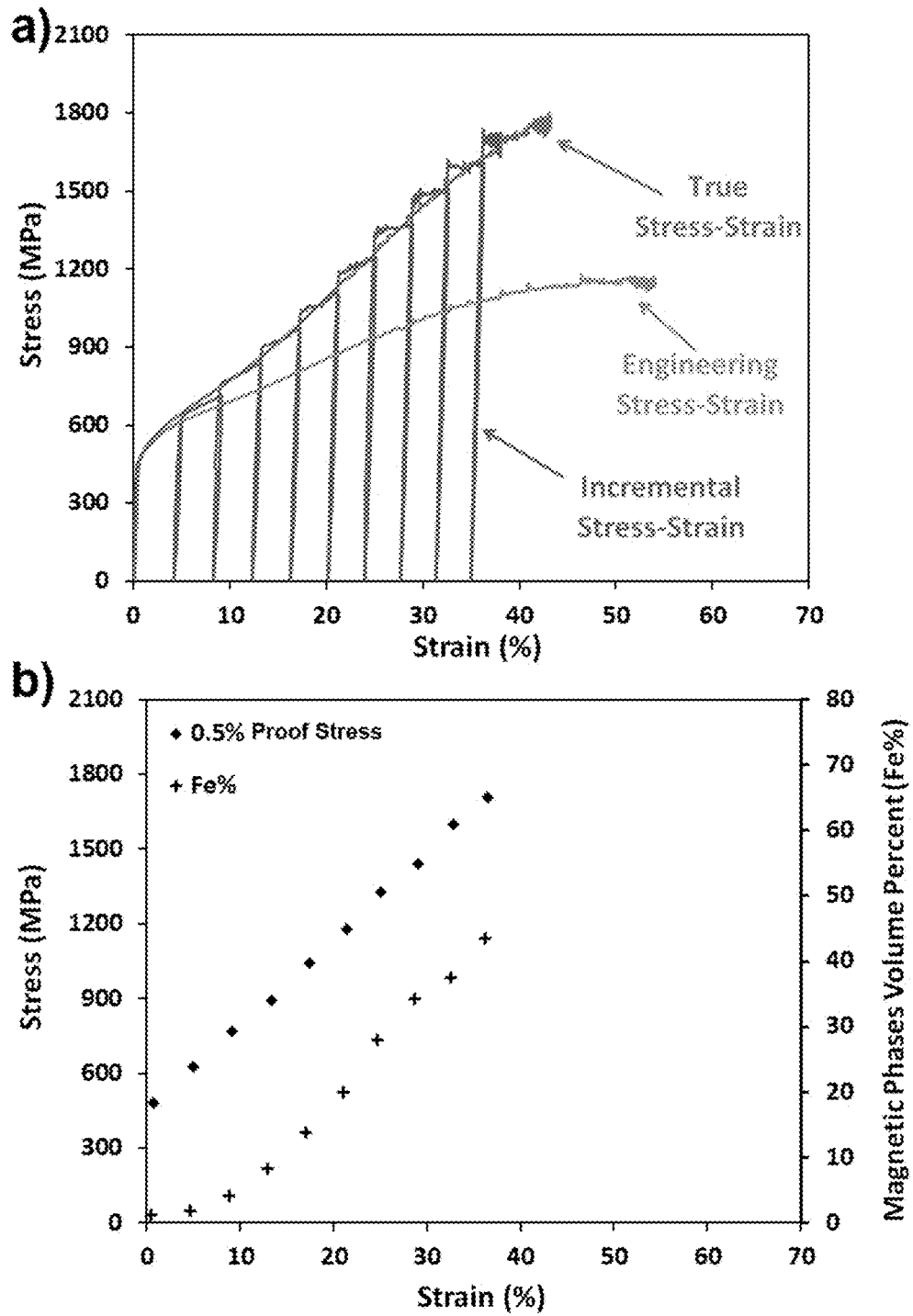


FIG. 55



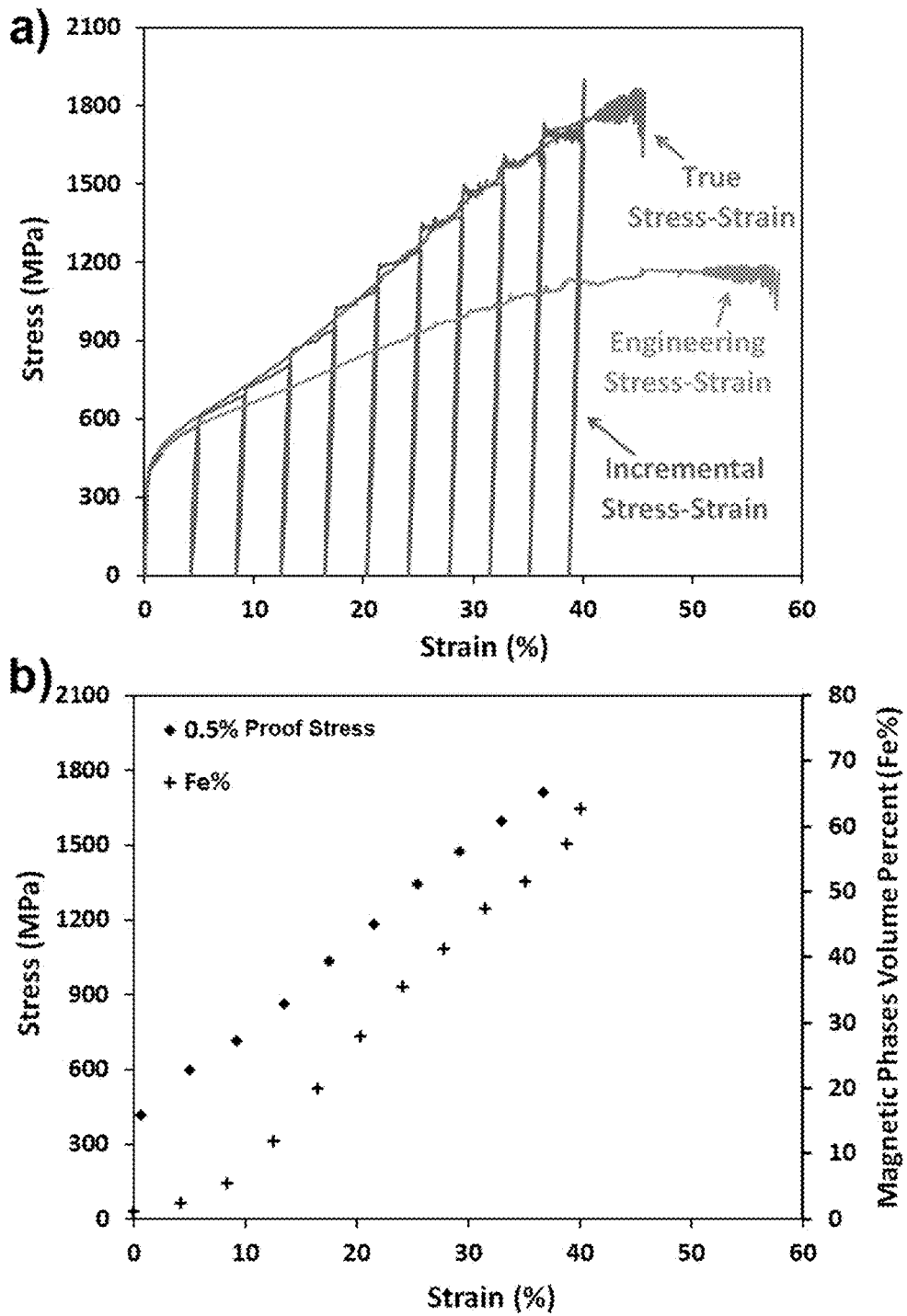


FIG. 56

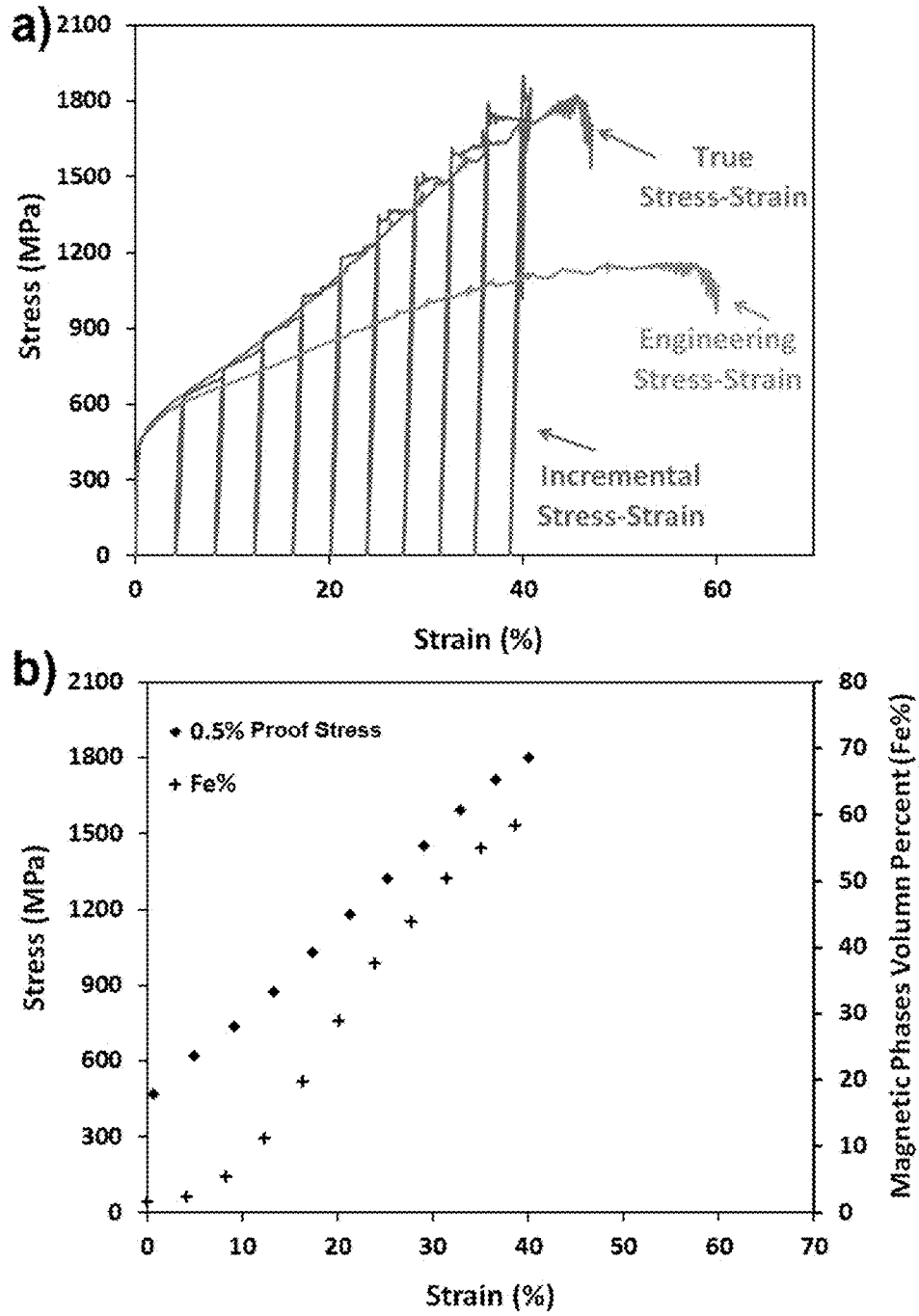


FIG. 57

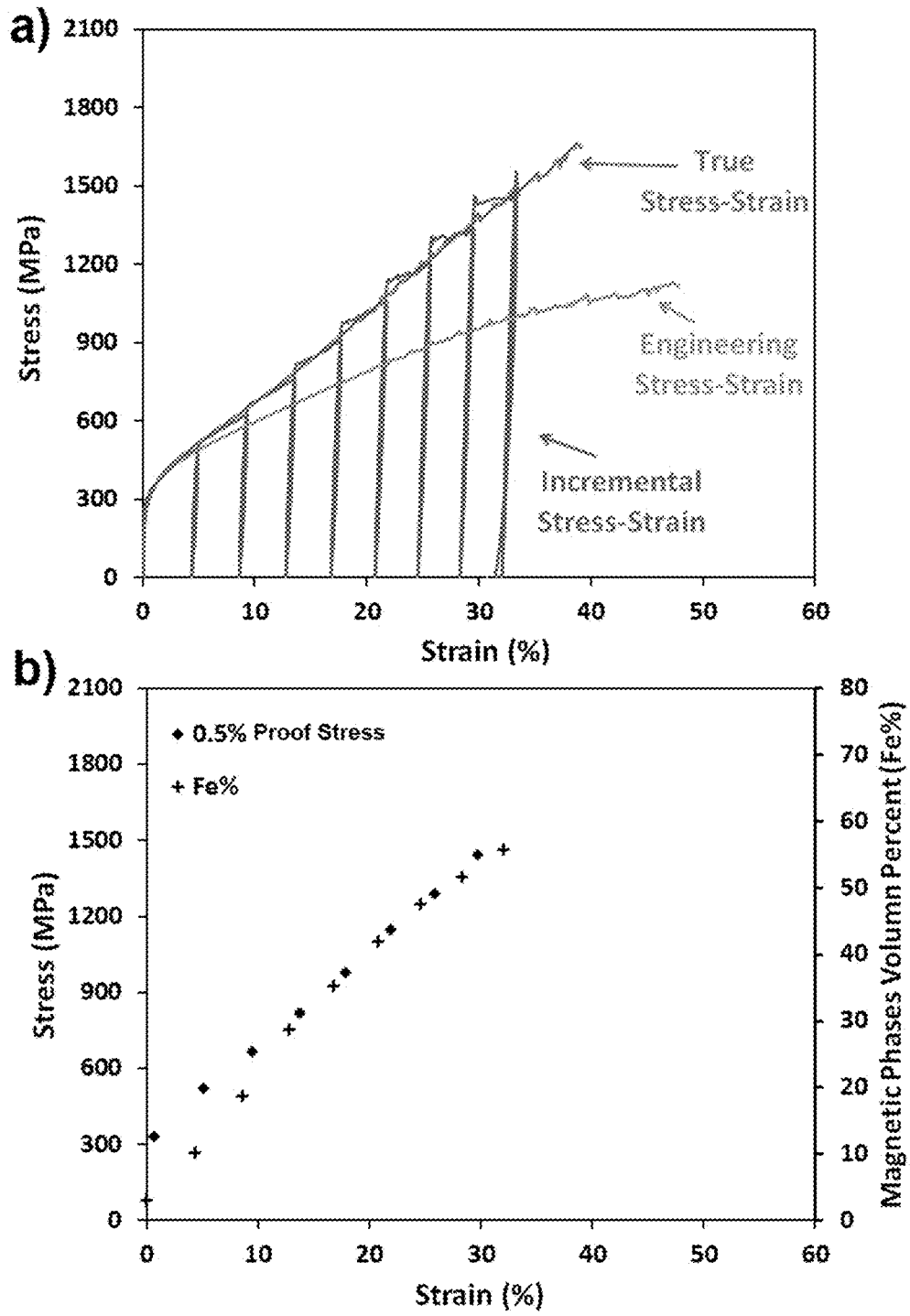


FIG. 58

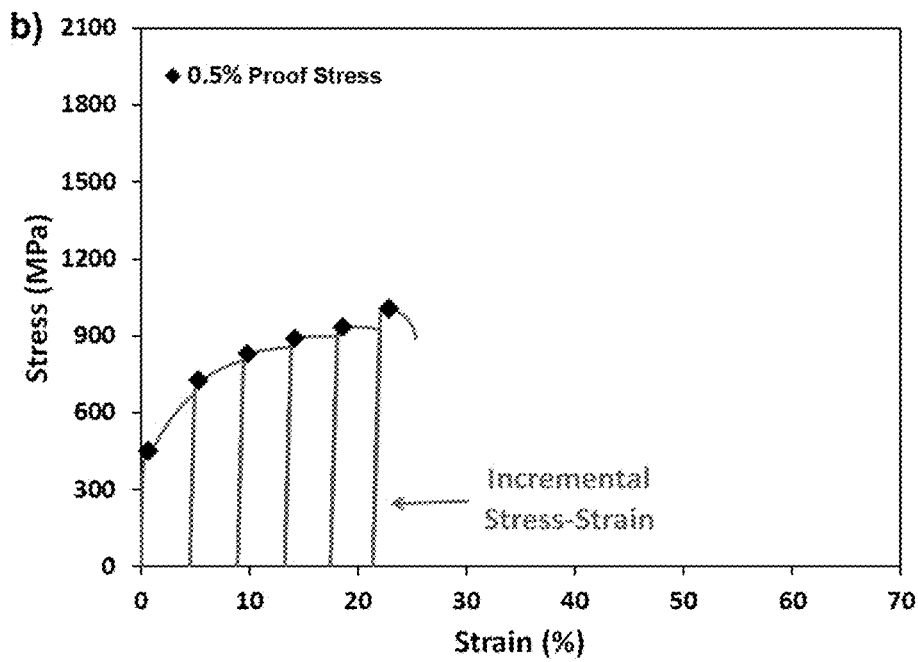
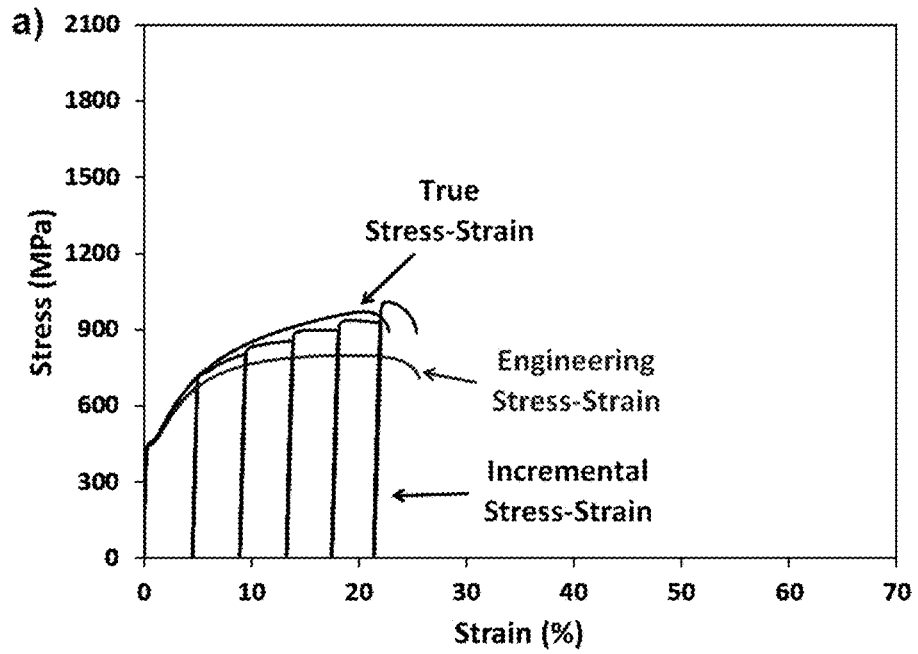


FIG. 59

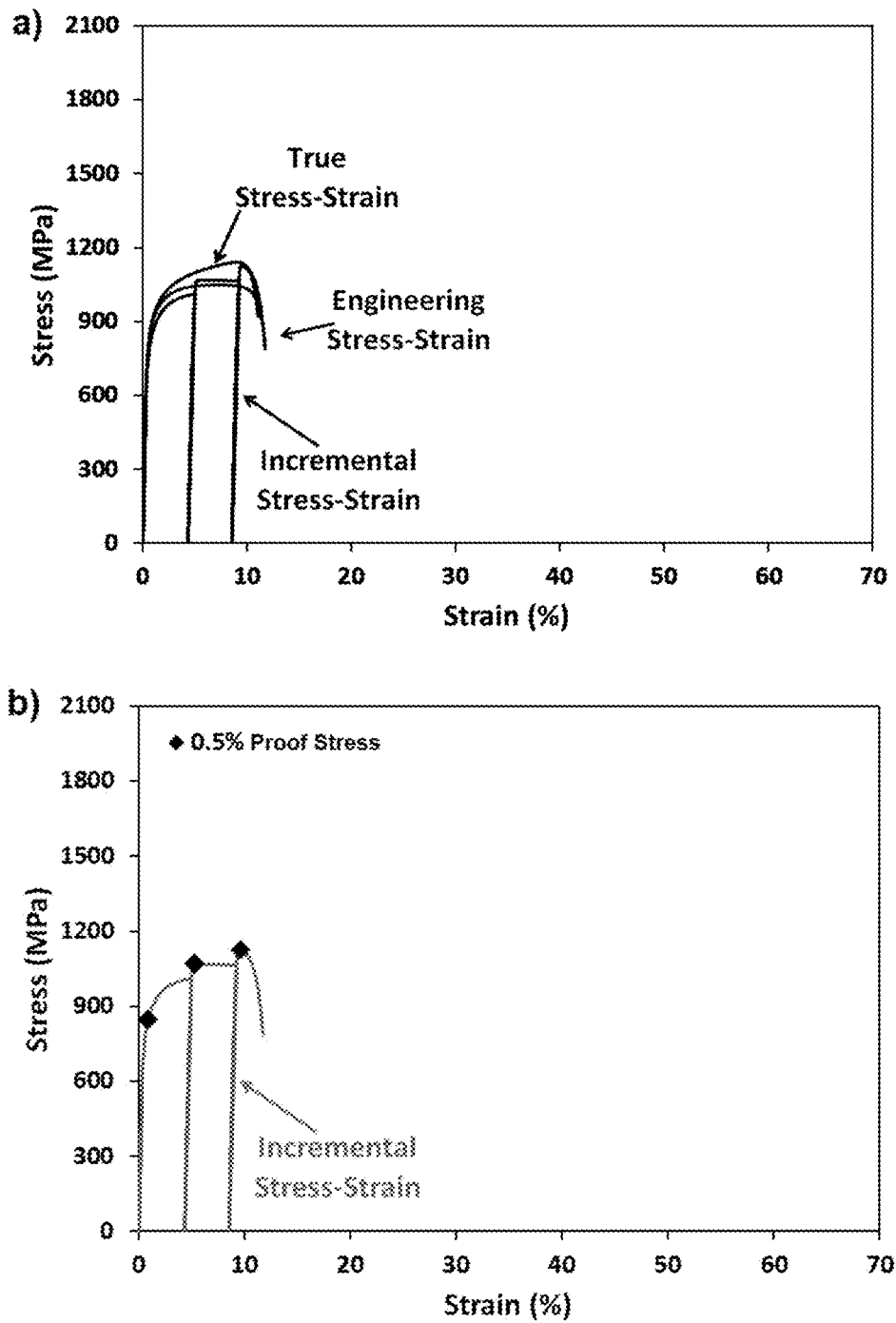


FIG. 60

**ALLOYS AND METHODS TO DEVELOP  
YIELD STRENGTH DISTRIBUTIONS  
DURING FORMATION OF METAL PARTS**

CROSS REFERENCE TO RELATED  
APPLICATION

[0001] This application claims the benefit of U.S. Provisional Application 62/618,356 filed Jan. 17, 2018 which is fully incorporated herein by reference.

FIELD OF INVENTION

[0002] This disclosure is related to alloys and methods of developing yield strength distributions during the formation of metal parts. Formation of metal parts through procedures such as stamping, especially for complex geometries, involves cold formability which requires ductility. The alloys herein provide improved yield strength distributions after formation which reduce cracking and other associated problems in metal part formation.

BACKGROUND

[0003] Metal stamping involves a number of steps including successful forming of the stamping and achieving a targeted set of properties in the stamping. Successful forming of the stamping depends on the material properties including the global and local formability under a wide variety of stress states and strain rates. Sufficient cold formability is needed to produce the targeted geometry during the stamping operation after which a very limited material ductility remains in the stamping. This makes the stamping potentially susceptible to subsequent failure through various modes since the internal plasticity is not sufficient to develop an effective plastic zone in front of the crack tip to prevent crack propagation. Additionally, due to lack of remaining ductility, the metal stamping would also have a lack of toughness.

[0004] In metal stamping, the properties of the stamping are generally not specified as long as crack free stampings are produced. Instead, the properties of the sheet material utilized for stamping are stated. For conventional steels, properties in the stamped part are similar to that in the sheet material utilized since they undergo limited strain hardening during stamping operation and limited property changes.

[0005] As the development of steels has progressed, especially for autobody applications, it has been found that the increase in strength needed for lightweighting/gauge reduction results in the reduction in ductility/formability as shown by the “Banana plot” in FIG. 1. Thus, there exists a paradox of strength and ductility and as materials have become stronger, they have become less ductile/formable.

[0006] Accordingly, a need remains for the development of alloys and methods that would provide the ability to develop improved yield strength distributions during formation of metal parts, such that failure mechanisms such as cracking are eliminated or reduced, with an overall improvement in the number of successfully formed parts produced.

SUMMARY

[0007] A method to develop yield strength distributions in a formed metal part comprising:

[0008] (a) supplying a metal alloy comprising at least 70 atomic % iron and at least four or more elements selected

from Cr, Ni, Mn, Si, Cu, Al, or C, melting said alloy, cooling at a rate of <250 K/s, and solidifying to a thickness of 25.0 mm up to 500 mm;

[0009] (b) processing said alloy into sheet form with thickness from 0.5 to 10 mm wherein said sheet exhibits a yield strength of A1 (MPa), an ultimate tensile strength of B1 (MPa), a true ultimate tensile strength C1 (MPa), a total elongation D1(%);

[0010] (c) straining said sheet one or a plurality of times above said yield strength A1 at a strain rate of  $10^0/s$  to  $10^2/sec$  at an ambient temperature of 1° C. to 50° C. and forming a metal part having a distribution of yield strengths A2, A3, and A4, wherein:

$$A2=A1\pm 100; \quad (i)$$

$$A3>A1+100 \text{ and } A3<A1+600; \text{ and} \quad (ii)$$

$$A4\geq A1+600. \quad (iii)$$

BRIEF DESCRIPTION OF THE DRAWINGS

[0011] The detailed description below may be better understood with reference to the accompanying FIGS. which are provided for illustrative purposes and are not to be considered as limiting any aspect of this invention.

[0012] FIG. 1 World Auto Steel “Banana Plot”.

[0013] FIG. 2 Summary of yield strength distributions in strained parts.

[0014] FIG. 3 Stress—strain curve example for Alloy 8 showing the definition of 0.2%, 0.5% and 1.0% proof stresses as shown in enlarged image on the right.

[0015] FIG. 4 Summary of incremental tensile testing for Alloy 1 including; a) The engineering stress-strain curve, true stress—true strain curve, and incremental engineering stress-strain curves, and b) Yield strength and Fe % as a function of strain.

[0016] FIG. 5 Summary of incremental tensile testing for Alloy 2 including; (a) the engineering stress-strain curve, true stress—true strain curve, and incremental engineering stress-strain curves, and (b) Yield strength and Fe % as a function of strain.

[0017] FIG. 6 Summary of incremental tensile testing for Alloy 3 including; a) The engineering stress-strain curve, true stress—true strain curve, and incremental engineering stress-strain curves, and b) Yield strength and Fe % as a function of strain.

[0018] FIG. 7 Summary of incremental tensile testing for Alloy 4 including; a) The engineering stress-strain curve, true stress—true strain curve, and incremental engineering stress-strain curves, and b) Yield strength and Fe % as a function of strain.

[0019] FIG. 8 Summary of incremental tensile testing for Alloy 5 including; a) The engineering stress-strain curve, true stress—true strain curve, and incremental engineering stress-strain curves, and b) Yield strength and Fe % as a function of strain.

[0020] FIG. 9 Summary of incremental tensile testing for Alloy 6 including; a) The engineering stress-strain curve, true stress—true strain curve, and incremental engineering stress-strain curves, and b) Yield strength and Fe % as a function of strain.

[0021] FIG. 10 Summary of incremental tensile testing for Alloy 7 including; a) The engineering stress-strain curve,



true stress—true strain curve, and incremental engineering stress-strain curves, and b) Yield strength and Fe % as a function of strain.

**[0047]** FIG. 36 Summary of incremental tensile testing for Alloy 33 including; a) The engineering stress-strain curve, true stress—true strain curve, and incremental engineering stress-strain curves, and b) Yield strength and Fe % as a function of strain.

**[0048]** FIG. 37 Summary of incremental tensile testing for Alloy 34 including; a) The engineering stress-strain curve, true stress—true strain curve, and incremental engineering stress-strain curves, and b) Yield strength and Fe % as a function of strain.

**[0049]** FIG. 38 Images of the microstructure in Alloy 7 sheet before deformation; a) SEM back-scattered image, b) TEM bright-field image, and c) HREM image of the nanoprecipitates.

**[0050]** FIG. 39 Images of the microstructure in Alloy 8 sheet before deformation; a) SEM back-scattered image, b) TEM bright-field image, and c) HREM image of the nanoprecipitates.

**[0051]** FIG. 40 Images of the microstructure in Alloy 7 sheet after deformation; a) SEM back-scattered image, and b) TEM bright-field image.

**[0052]** FIG. 41 Images of the microstructure in Alloy 8 sheet after deformation; a) SEM back-scattered image, and b) TEM bright-field image.

**[0053]** FIG. 42 Images of the Microconstituent 1 in the Alloy 8 sheet after deformation; a) TEM bright-field image, b) TEM dark-field image, c) TEM dark-field image of the ferrite grain at higher magnification, and d) HREM image of the nanoprecipitates.

**[0054]** FIG. 43 Images of the Microconstituent 2 in the Alloy 8 sheet after deformation; a) TEM bright-field image, b) TEM bright-field image of the deformed austenite grain at higher magnification showing dislocation cell structure, c) TEM image with highlighted nanoprecipitates by black circles, and d) HREM image of the nanoprecipitates.

**[0055]** FIG. 44 B-pillar surface with ~20 mm grid pattern; a) Top section, b) Middle section 1, c) Middle section 2, and d) Bottom section.

**[0056]** FIG. 45 A histogram of Feritscope measurements across the surface of the B-pillar after 4 stamping hits. Note that the measurements showing baseline level of Fe % (i.e. <1%) are not shown on this plot.

**[0057]** FIG. 46 A histogram of Feritscope measurements across the surface of the B-pillar after 5 stamping hits. Note that the measurements showing baseline Fe % (i.e. <1%) are not shown on this plot.

**[0058]** FIG. 47 Tensile testing of specimens cut from the stamped B-pillar; a) A view of the B-pillar with marked specimen positions, and b) A view of the B-pillar after specimen cutting.

**[0059]** FIG. 48 Tensile properties of the Alloy 8 sheet measured by using ASTM E8 standard specimens and reduced size (i.e. 12.5 mm gauge) specimens.

**[0060]** FIG. 49 Stress—strain curve examples for specimens cut from the B-pillar with various levels of magnetic phases volume percent (Fe %).

**[0061]** FIG. 50 True stress—true strain curve examples for specimens cut from the B-pillar with various levels of magnetic phases volume percent (Fe %).

**[0062]** FIG. 51 Correlations of tensile properties with Feritscope; a) Strength characteristics vs corresponding measured Fe %, and b) Total elongation vs corresponding measured Fe %.

**[0063]** FIG. 52 Extrapolated correlations of tensile properties to the maximum Feritscope measurements of 31 Fe %; a) Strength characteristics, and b) Total elongation.

**[0064]** FIG. 53 Bright-field TEM micrographs of the microstructure in specimens cut from the stamped B-pillar before tensile testing and in the gauge of the tensile specimens after tensile testing with different levels of magnetic phases volume percent (Fe %); a) 4.6 Fe % sample before tensile deformation, b) 4.6 Fe % sample after tensile deformation, c) 13.9 Fe % sample before tensile deformation, d) 13.9 Fe % sample after tensile deformation, e) 24.5 Fe % sample before tensile deformation, and f) 24.5 Fe % sample after tensile deformation.

**[0065]** FIG. 54 Correlation of yield strength with magnetic phases volume percent (Fe %) for incremental tensile tested specimens and for tensile tested specimens cut from the B-pillar during destructive analysis.

**[0066]** FIG. 55 Summary of incremental tensile testing for Alloy 8 sheet with thickness of 0.5 mm including; a) The engineering stress-strain curve, true stress—true strain curve, and incremental engineering stress-strain curves, and b) Yield strength and Fe % as a function of strain.

**[0067]** FIG. 56 Summary of incremental tensile testing for Alloy 8 sheet with thickness of 1.3 mm including; a) The engineering stress-strain curve, true stress—true strain curve, and incremental engineering stress-strain curves, and b) Yield strength and Fe % as a function of strain.

**[0068]** FIG. 57 Summary of incremental tensile testing for Alloy 8 sheet with thickness of 3.0 mm including; a) The engineering stress-strain curve, true stress—true strain curve, and incremental engineering stress-strain curves, and b) Yield strength and Fe % as a function of strain.

**[0069]** FIG. 58 Summary of incremental tensile testing for Alloy 8 sheet with thickness of 7.1 mm including; a) The engineering stress-strain curve, true stress—true strain curve, and incremental engineering stress-strain curves, and b) Yield strength and Fe % as a function of strain.

**[0070]** FIG. 59 Summary of incremental tensile testing for TRIP 780 including; a) The engineering stress-strain curve, true stress—true strain curve, and incremental engineering stress-strain curves, and b) Yield strength as a function of strain.

**[0071]** FIG. 60 Summary of incremental tensile testing for DP980 including; a) The engineering stress-strain curve, true stress—true strain curve, and incremental engineering stress-strain curves, and b) Yield strength as a function of strain.

#### DETAILED DESCRIPTION OF PREFERRED EMBODIMENTS

**[0072]** Alloys herein can be initially produced in a sheet form by different methods of continuous casting including but not limited to belt casting, thin slab casting, and thick slab casting with achievement of advanced property combinations by subsequent post-processing. After processing into a sheet form as a hot band or cold rolled sheet, which may or may not be annealed, a preferred thickness of 0.5 mm to 10.0 mm is produced.

**[0073]** In FIG. 2 the achievement in alloy strengthening during stamping is illustrated. In Step 1 in FIG. 2, the



starting condition is to supply a metal alloy. This metal alloy will comprise at least 70 atomic % iron. Preferably the level of iron is in the range of 70 atomic % iron to 85 atomic % iron. The metal alloy will contain at least four or more elements selected from Si, Mn, Cr, Ni, Cu, Al, or C. The alloy chemistry is melted, cooled at a rate of <250 K/s, and solidified to a thickness of 25 mm and up to 500 mm.

**[0074]** The casting step can preferably be done in a wide variety of processes including ingot casting, bloom casting, continuous casting, thin slab casting, thick slab casting, belt casting etc. Preferred methods would be continuous casting in sheet form by thin slab casting or thick slab casting. To produce alloys herein in a sheet form, the casting processes can vary widely depending on specific manufacturing routes and specific targeted goals. As an example, consider thick slab casting as one process route to produce sheet product. The alloy would be cast going through a water cooled mold typically in a thickness range of 150 to 350 mm in thickness and typically processed through a roughing mill hot roller into a transfer bar slab of 25 to 150 mm in thickness and through the finishing mill into a hot band with thickness of 1.5 to 10.0 mm. Another example would be to preferably process the cast material through a thin slab casting process. In this case, after casting typically forms 25 to 150 mm in thickness by going through a water cooled mold, the newly formed slab goes directly to hot rolling without cooling down and the strip is rolled into hot band coils with typical thickness from 1.5 to 5.0 mm in thickness. Note that bloom casting would be similar to the examples above but higher thickness might be cast typically from 200 to 500 mm thick and initial breaker steps would be needed to reduce initial cast thickness to allow it to go through a hot rolling roughing mill.

**[0075]** Step 2 in FIG. 2 corresponds to sheet product from alloys herein with preferred thickness from 0.5 to 10 mm. The processing of the cast material in Step 1 into sheet form can preferably be done by hot rolling, forming a hot band. Produced hot band may be further processed towards smaller gauges by cold rolling that can be applied at various reductions per pass, variable number of passes and in different mills including tandem mills, Z-mills, and reversing mills. Typically cold rolled thickness would be 0.5 to 10 mm thick. Preferably, the cold rolled material is annealed to restore the ductility lost from the cold rolling process either partially or completely.

**[0076]** Preferably, sheet material from the alloys herein have a yield strength of A1 (250 MPa to 750 MPa), a tensile strength of B1 (700 MPa to 1750 MPa), a true ultimate tensile strength of C1 (1100 MPa to 2300 MPa), and exhibits a total elongation D1 (10% to 80%). While engineering stress is determined as the applied load divided by the original cross-sectional area of the specimen gauge, true stress corresponds to the applied load divided by the actual cross-sectional area (the changing area with respect to time) of the specimen at that load. True stress is the stress determined by the instantaneous load acting on the instantaneous cross-sectional area. True ultimate tensile strength (C1) is related to ultimate tensile strength (B1) and can be calculated from the test data for each alloy herein using Eq.1. Engineering strain is determined as the change in length divided by the original length. Calculated true ultimate tensile strength values vary from 1165 to 2237 MPa:

$$\text{True Ultimate Tensile Strength(C1)} = \text{Ultimate Tensile Strength} * (1 + \text{Engineering Strain}) \quad (\text{Eq.1})$$

**[0077]** True strain at fracture corresponding to total elongation of each specimen was calculated by Eq.2. True strain at fracture was found to vary from 15.7 to 58.1%.

$$\text{True Strain at Fracture} = \ln(1 + \text{Engineering Strain}) \quad (\text{Eq.2})$$

**[0078]** Depending on alloy chemistry, the magnetic phase volume percent generally varies from 0.2 to 45.0 Fe % for hot band or cold rolled and annealed sheet. Such magnetic phase volume is then increased as discussed more fully below.

**[0079]** Straining of the alloy sheet above its yield strength, which may preferably occur via stamping of the sheet from said alloy with the indicated influence on yield strength occurring during the stamping operation, is shown by Step 3 in FIG. 2. The alloy is permanently (i.e. plastically) deformed during the stamping operation, preferably at strain rates of  $10^0/s$  to  $10^2/s$  which is reference to deformation when yield strength is exceeded. Metal stamping is the process of placing sheet metal at ambient temperature and without external heating in either blank or coil form into a stamping press where a tool and die surface forms the metal into a net shape. Ambient temperature may preferably be understood as a temperature range from 1° C. to 50° C., more preferably 1° C. to 40° C., and even more preferably 5° C. to 30° C. Note that during stamping, the blank as it is formed does experience internal heating from the stamping process which includes both frictional heating and deformation induced heating. The internal blank heat up during stamping is generally less than 150° C. and typically less than 100° C. This could be a single stage operation where every stroke of the press produces the desired form on the sheet metal part, or could occur through a series of stages, generally 2 to 7 but may occur in up to 25 stages, where each stage where the formed or partially formed metal part is deformed introduces a deformation that exceeds the yield strength of the material of previous step. Note that during each stage/press stroke, the localized deformation will vary by location so a multitude of different strains will be applied concurrently during the stamping operation and as noted, preferably at strain rates from  $10^0/s$  to  $10^2/s$ . Formability is the primary attribute of sheet metal material to undergo forming, in the plastic regime (i.e. forming at the point where yield strength is exceeded), which involves material straining during bending, stretching, and drawing etc. depending on stamping geometry.

**[0080]** The alloys herein undergoing what is illustrated in FIG. 2 may also preferably be characterized based upon the microstructure transformations when deformed above the yield strength. This is termed a Nanophase Refinement & Strengthening (NR&S) mechanism that preferably occurs with formation of new microstructure defined by two Microconstituents. Initial sheet microstructure is such that it contains areas with stable austenite meaning that it will not change into the ferrite phase during deformation and areas with relatively unstable austenite, meaning that it is available for transformation into ferrite upon plastic deformation. Upon deformation, the areas with relatively unstable austenite undergo transformation into ferrite particles with a nanoscale size from 20 nm to 750 nm (longest linear dimension) forming Microconstituent 1 along with the formation of nanoprecipitates in the range of 2 to 100 nm in size (longest linear dimension) and contributing to material strengthening due to structural refinement. As this ferrite

phase forms, it continues to deform through a dislocation mechanism contributing to sheet ductility and formability.

**[0081]** Areas of the microstructure in the initial sheet from the alloys herein with relatively stable austenite retain the austenitic nature but deform through primarily dislocation mechanisms supporting material ductility and formability during stamping and forming Microconstituent 2 in the final microstructure after deformation. Microconstituent 2 itself contains two components which are micron sized stable austenite particles, typically 1.0 to 10.0 microns in size (longest linear dimension) and nanoprecipitates typically 2 to 100 nm in size (longest linear dimension). Nanoprecipitates in either Microconstituent 1 or 2 can be directly observed through TEM microscopy and are observed to exhibit a spherical, elliptical, or rectangular shape in the size range indicated. To further identify, selected area diffraction in the TEM on the precipitates can be done to show that they have different structures (i.e. not FCC austenite or BCC Ferrite) than the matrix phases (i.e. austenite which is FCC or alpha ferrite which is BCC). Accumulation of dislocations within micron-sized austenite grains results in dislocation cell block boundaries, and dislocation cell formation leading to material strengthening. Additionally, as noted, nanoprecipitates with a size from 2 to 100 nm are present in both Microconstituents 1 and 2 also contributing to material strengthening.

**[0082]** The resulting volume fraction of Microconstituent 1 and Microconstituent 2 in the localized areas of the stamping, i.e., the final formed part, depends on alloy chemistry, the level of straining at particular location, and the level of strain hardening which occurs during the single or multistage stamping operation. Note that the microstructure and resulting properties will change in the stamped part from the starting sheet/blank depending on the local level of straining. Typically, as low as 1 volume percent and as high as 85 volume percent of the alloy structure after stamping will exist as the ferrite containing Microconstituent 1 with the remaining regions representing Microconstituent 2. Thus, Microconstituent 1 can be in all individual volume percent values from 0.5 to 85.0 in 0.1% increments (i.e. 0.5%, 0.6%, 0.7%, . . . up to 85.0%) while Microconstituent 2 can be in volume percent values from 99.5 to 15 in 0.1% increments (i.e. 99.5%, 99.4%, 99.3% . . . down to 15.0%). The volume percent of nanoprecipitates which occur in both microconstituents is anticipated to be 0.1 to 10%. While the magnetic properties of these nanoprecipitates are difficult to individually measure, it is contemplated that they are non-magnetic.

**[0083]** As ferrite is magnetic (i.e. ferromagnetic), and austenite is non-magnetic (i.e. paramagnetic), the volume fraction of the magnetic phases present provides a convenient method to evaluate the relative presence of Microconstituent 1. The magnetic phases volume percent is abbreviated herein as Fe %, which should be understood as a reference to the presence of ferrite and any other components in the alloy that identifies a magnetic response such as alpha-martensite. Note that the alpha-ferrite and alpha-martensite have similar magnetic responses and cannot be distinguished separately by the Feritscope so both will be identified as ferrite. Magnetic phase volume percent herein is conveniently measured by a Feritscope. The Feritscope uses the magnetic induction method with a probe placed directly on the sheet sample and provides a direct reading of the total magnetic phases volume percent (Fe %). After cold

deformation, the volume fraction of Microconstituent 1 is estimated using the measured Fe % value which can include alpha-ferrite and/or alpha-martensite. Microconstituent 2 which is nonmagnetic and cannot be measured by the Feritscope, would then be considered the remaining constituent.

**[0084]** While the multiple mechanistic components of the NR&S mechanism described above support deformation of the sheet during its forming into targeted shape, sheet material from alloys herein undergoes a substantial strain hardening/strengthening which results in the presence of distributions (i), (ii), and (iii) in the formed parts provided in FIG. 2. Depending on alloy chemistry, the level of straining at particular location, and local stress state during stamping operation occurring without external application of heat, results in different levels of strengthening leading to three distributions of yield strength characteristics in the formed part as show in Step 4 in FIG. 2: (i) yield strength A2 (MPa) whereby  $A2=A1\pm 100$ ; (ii) yield strength A3 (MPa) whereby  $A3>A1+100$  and  $A3<A1+600$ ; and (iii) yield strength A4 (MPa) whereby  $A4\geq A1+600$  and  $A4\leq C1$ . Distribution (iii) represents a maximum level of strengthening in the formed part with yield strength A4 in the range from 850 to 2300 MPa. In addition, it should be noted that preferably, yield strength distributions (i), (ii) and (iii) are the only yield strengths that are present in the formed part, except for reduced yield strengths that are attributed to defects in the parts that can occur due to casting and subsequent processing. Such defects therefore can include, e.g., internal cavities (voids), slag from casting, microcracks, or inclusions.

**[0085]** Forming of the alloys herein can be done by various methods including but not limited to forming in single and/or progressive dies and with one stage or multiple stages up to 25 towards targeted final form using a combination of techniques, without external heating, including but not limited to stamping, roll forming, metal drawing, and hydroforming. In connection with such procedures the deformation that exceeds the yield strength may include hole expansion, hole extrusion drawing, bending and/or stretching. Common to all of these processing techniques is the introduction of a one or a plurality of deformations (introduction of strain) such that yield strength is exceeded with the result that all of the above referenced distribution of yield strengths are achieved in the formed part. The final formed part applications include but are not limited to automotive industry (a vehicular frame, vehicular chassis, or vehicular panel), and/or railroad industry (a storage tank, freight car, or railway tank car).

## Main Body

### Alloys

**[0086]** The chemical composition of the alloys herein is shown in Table 1 which provides the preferred atomic ratios utilized.

TABLE 1

Chemical Composition Of Alloys (Atomic %)								
Alloy	Fe	Cr	Ni	Mn	Al	Si	Cu	C
Alloy 1	76.17	8.64	0.90	11.77	—	—	1.68	0.84
Alloy 2	78.17	1.85	11.42	—	—	3.94	2.68	1.94

TABLE 1-continued

Chemical Composition Of Alloys (Atomic %)								
Alloy	Fe	Cr	Ni	Mn	Al	Si	Cu	C
Alloy 3	76.55	0.78	0.72	14.43	—	3.42	0.42	3.68
Alloy 4	80.90	3.69	4.97	5.57	—	2.98	0.37	1.52
Alloy 5	75.67	2.63	3.40	11.03	—	5.13	1.35	0.79
Alloy 6	71.68	6.25	10.45	0.62	2.63	5.22	1.64	1.51
Alloy 7	75.75	2.63	1.19	13.86	—	5.13	0.65	0.79
Alloy 8	74.75	2.63	1.19	14.86	—	5.13	0.65	0.79
Alloy 9	74.59	2.61	—	15.17	—	3.59	1.86	2.18
Alloy 10	73.75	2.63	1.19	15.86	—	5.13	0.65	0.79
Alloy 11	80.93	—	2.68	12.04	—	0.79	0.89	2.67
Alloy 12	73.95	2.60	1.18	14.7	1.08	5.07	0.64	0.78
Alloy 13	80.89	0.43	0.42	14.82	—	2.03	1.41	—
Alloy 14	77.46	—	—	15.42	—	3.78	1.73	1.61
Alloy 15	81.51	2.45	3.78	11.79	—	—	—	0.47
Alloy 16	79.02	—	2.95	10.88	—	5.18	1.97	—
Alloy 17	75.55	1.67	1.63	14.92	—	6.23	—	—
Alloy 18	76.62	2.63	7.85	4.42	—	5.13	2.61	0.74
Alloy 19	77.17	1.85	12.42	—	—	3.94	2.68	1.94
Alloy 20	70.92	2.5	1.13	14.1	5.11	4.87	0.62	0.75
Alloy 21	71.96	2.53	1.15	14.31	3.72	4.94	0.63	0.76
Alloy 22	72.77	2.56	1.16	14.47	2.65	4.99	0.63	0.77
Alloy 23	77.35	—	2.56	11.51	4.42	0.76	0.85	2.55
Alloy 24	79.85	—	1.34	12.04	2.42	0.79	0.89	2.67
Alloy 25	78.86	0.29	0.78	14.41	2.68	0.87	0.96	1.15
Alloy 26	74.05	2.63	—	12.04	4.71	5.13	0.65	0.79
Alloy 27	76.83	—	3.47	13.67	0.42	2.78	2.45	0.38
Alloy 28	75.21	2.63	—	12.04	4.34	5.13	0.65	—
Alloy 29	73.63	2.63	—	12.04	4.34	5.13	0.65	1.58
Alloy 30	75.57	1.32	—	13.57	4.00	4.43	0.32	0.79
Alloy 31	77.00	—	—	13.13	4.00	4.43	0.65	0.79
Alloy 32	73.52	3.26	—	12.14	4.61	4.07	0.29	2.11
Alloy 33	75.69	4.59	0.37	14.16	3.20	—	0.48	1.51
Alloy 34	70.45	1.49	0.55	16.85	0.87	6.22	1.85	1.72

**[0087]** With regards to the above, and as can be further seen from Table 1, preferably, when Fe is present at a level of greater than 70 at. %, and one then selects the four or more elements from the indicated seven (7) elements, or selects five or more elements, or selects six or more elements or selects all seven elements to provide a formulation of elements that totals 100 atomic percent. The preferred levels of the elements, if selected, may fall in the following ranges (at. %): Cr (0.2 to 8.7), Ni (0.3 to 12.5), Mn (0.6 to 16.9), Al (0.4 to 5.2), Si (0.7 to 6.3), Cu (0.2 to 2.7), and C (0.3 to 3.7). Accordingly, it can be appreciated that if four (4) elements are selected, two of the six elements are not selected and may be excluded. If five (5) elements are selected, one of the elements of the six can be excluded. Moreover, a particularly preferred level of Fe is in the range of 70.0 to 85.0 at. %. The level of impurities of other elements is in the range of 0 to 5000 ppm. Accordingly, if there is 5000 ppm of an element other than the selected elements identified, the level of such selected elements may then in combination be present at a lower level to account for the 5000 ppm impurity, such that the total of all elements present (selected elements and impurities) is 100 atomic percent.

**[0088]** The alloys herein were processed into a laboratory sheet by processing of laboratory slabs. Laboratory alloy processing is developed to mimic closely the commercial sheet production by continuous casting and include hot rolling and cold rolling. Annealing might be applied depending on targeted properties. Produced sheet can be used in hot rolled (hot band), cold rolled, annealed, or partially annealed states.

## Laboratory Slab Casting

**[0089]** Alloys were weighed out into 3,000 to 3,400 gram charges according to the atomic ratios in Table 1 using commercially available ferroadditive powders and a base steel feedstock with known chemistry. Impurities can be present at various levels depending on the feedstock used. Impurity elements would commonly include the following elements; Co, N, P, Ti, Mo, W, Ga, Ge, Sb, Nb, Zr, O, Sn, Ca, B and S which if present would be in the range from 0 to 5000 ppm (parts per million) (0 to 0.5 wt %) at the expense of the desired elements noted above. Preferably, the level of impurities is controlled to fall in the range of 0 to 3000 ppm (0.3 wt %).

**[0090]** Charges were loaded into a zirconia coated silica crucible which was placed into an Indutherm VTC800V vacuum tilt casting machine. The machine then evacuated the casting and melting chambers and flushed with argon to atmospheric pressure twice prior to casting to prevent oxidation of the melt. The melt was heated with a 14 kHz RF induction coil until fully molten, approximately from 5 to 7 minutes depending on the alloy composition and charge mass. After the last solids were observed to melt it was allowed to heat for an additional 30 to 45 seconds to provide superheat and ensure melt homogeneity. The casting machine then evacuated the chamber and tilted the crucible and poured the melt into a water cooled copper die. The melt was allowed to cool under vacuum for 200 seconds before the chamber was filled with argon to atmospheric pressure.

## Physical Properties of Cast Alloys

**[0091]** A sample of between 50 and 150 mg from each alloy herein was taken in the as-cast condition. This sample was heated to an initial ramp temperature between 900° C. and 1300° C. depending on alloy chemistry, at a rate of 40° C./min. Temperature was then increased at 10° C./min to a max temperature between 1425° C. and 1510° C. depending on alloy chemistry. Once this maximum temperature was achieved, the sample was cooled at a rate of 10° C./min back to the initial ramp temperature before being reheated at 10° C./min to the maximum temperature. Differential Scanning Calorimetry (DSC) measurements were taken using a Netzsch Pegasus 404 DSC through all four stages of the experiment, and this data was used to determine the solidus and liquidus temperatures of each alloy, which are in a range from 1294 to 1498° C. (Table 2). Depending on the alloys chemistry, liquidus-solidus gap varies from 26 to 138° C. Thermal analysis provides information on maximum temperature for the following hot rolling processes that varies depending on alloy chemistry.

TABLE 2

Thermal Analysis Of Alloys			
Alloy	Solidus (°C.)	Liquidus (°C.)	Melting Gap (°C.)
Alloy 1	1406	1488	82
Alloy 2	1460	1489	29
Alloy 3	1294	1432	138
Alloy 4	1430	1481	51
Alloy 5	1419	1455	36
Alloy 6	1350	1441	91
Alloy 7	1390	1448	58
Alloy 8	1395	1443	48
Alloy 9	1358	1445	87

TABLE 2-continued

Thermal Analysis Of Alloys			
Alloy	Solidus (°C.)	Liquidus (°C.)	Melting Gap (°C.)
Alloy 10	1385	1443	58
Alloy 11	1456	1491	35
Alloy 12	1377	1457	80
Alloy 13	1464	1490	26
Alloy 14	1398	1452	54
Alloy 15	1471	1498	27
Alloy 16	1419	1458	39
Alloy 17	1392	1450	58
Alloy 18	1421	1461	40
Alloy 19	1416	1464	48
Alloy 20	1346	1456	110
Alloy 21	1361	1457	95
Alloy 22	1376	1448	72
Alloy 23	1423	1472	49
Alloy 24	1430	1486	56
Alloy 25	1439	1482	43
Alloy 26	1347	1466	119
Alloy 27	1426	1464	38
Alloy 28	1385	1470	85
Alloy 29	1342	1459	117
Alloy 30	1397	1474	77
Alloy 31	1389	1479	90
Alloy 32	1377	1454	77
Alloy 33	1420	1478	58
Alloy 34	1400	1452	52

[0092] The density of the alloys herein was measured on samples from hot rolled material using the Archimedes method in a specially constructed balance allowing weighing in both air and distilled water. The density of each alloy is tabulated in Table 3 and was found to be in the range from 7.48 to 8.01 g/cm<sup>3</sup>. The accuracy of this technique is ±0.01 g/cm<sup>3</sup>.

TABLE 3

Density Of Alloys	
Alloy	Density (g/cm <sup>3</sup> )
Alloy 1	7.89
Alloy 2	7.92
Alloy 3	7.77
Alloy 4	7.90
Alloy 5	7.80
Alloy 6	7.69
Alloy 7	7.78
Alloy 8	7.77
Alloy 9	7.78
Alloy 10	7.77
Alloy 11	7.93
Alloy 12	7.72
Alloy 13	7.94
Alloy 14	7.80
Alloy 15	8.01
Alloy 16	7.83
Alloy 17	7.77
Alloy 18	7.86
Alloy 19	7.93
Alloy 20	7.48
Alloy 21	7.56
Alloy 22	7.63
Alloy 23	7.69
Alloy 24	7.80
Alloy 25	7.79
Alloy 26	7.49
Alloy 27	7.90
Alloy 28	7.51
Alloy 29	7.50
Alloy 30	7.57

TABLE 3-continued

Density Of Alloys	
Alloy	Density (g/cm <sup>3</sup> )
Alloy 31	7.59
Alloy 32	7.50
Alloy 33	7.73
Alloy 34	7.82

Laboratory Processing into Sheet Through Hot Rolling, Cold Rolling, and Annealing

[0093] The alloys herein were preferably processed into a laboratory hot band by hot rolling of laboratory slabs at high temperatures. Laboratory alloy processing is developed to simulate the hot band production from slabs produced by continuous casting. Industrial hot rolling is performed by heating a slab in a tunnel furnace to a target temperature, then passing it through either a reversing mill or a multi-stand mill or a combination of both to reach the target gauge. During rolling on either mill type, the temperature of the slab is steadily decreasing due to heat loss to the air and to the work rolls so the final hot band is formed at a reduced temperature. This is simulated in the laboratory by heating in a tunnel furnace to between 1100° C. and 1250° C., then hot rolling. The laboratory mill is slower than industrial mills causing greater loss of heat during each hot rolling pass so the slab is reheated for 4 minutes between passes to reduce the drop in temperature, the final temperature at target gauge when exiting the laboratory mill commonly is in the range from 800° C. to 1000° C., depending on furnace temperature and final thickness.

[0094] Prior to hot rolling, laboratory slabs were preheated in a Lucifer EHS3GT-B18 furnace. The furnace set point varies between 1100° C. to 1250° C., depending on alloy melting point and point in the hot rolling process, with the initial temperatures set higher to facilitate higher reductions, and later temperatures set lower to minimize surface oxidation on the hot band. The slabs were allowed to soak for 40 minutes prior to hot rolling to ensure they reach the target temperature and then pushed out of the tunnel furnace into a Fenn Model 061 2 high rolling mill. The 50 mm casts were hot rolled for 5 to 10 passes though the mill before being allowed to air cool. Final thickness ranges after hot rolling are preferably from 1.8 mm to 4.0 mm with variable reduction per pass ranging from 20% to 50%.

[0095] Hot band material was media blasted prior to cold rolling to remove surface oxides which could become embedded during the rolling process. The resultant cleaned sheet material was rolled using a Fenn Model 061 2 high rolling mill down to 1.2 mm thickness. Reductions before annealing ranged from 10% to 40%.

[0096] Once the final gauge thickness of 1.2 mm was reached, tensile samples were cut from the laboratory sheet by wire-EDM. The samples were annealed under conditions intended to simulate the thermal exposure expected during an industrial continuous annealing process representing final treatment of sheet material in Step 2 in FIG. 2. Samples were wrapped in stainless steel foil to prevent oxidation and loaded into a preheated furnace at 850° C. Samples were left in the furnace for 10 minutes while the furnace purged with argon before being removed and allowed to air cool.

[0097] Tensile properties were measured on an Instron mechanical testing frame (Model 3369), utilizing Instron's Bluehill control and analysis software. All tests were run at ambient temperature in displacement control at a constant displacement rate of 0.036 mm/s. Tensile properties of 1.2 mm thick sheet from alloys herein after annealing at 850° C. for 10 minutes are listed in Table 4. The ultimate tensile strength values of the annealed sheet from alloys herein is in a range from 717 to 1683 MPa with total elongation recorded in the range from 17.1 to 78.9%. The 0.2% proof stress varies from 273 to 652 MPa, 0.5% proof stress varies from 295 to 704 MPa, and 1.0% proof stress varies from 310 to 831 MPa. True ultimate tensile strength calculated from the data for each alloy herein, which varies from 1188 to 2237 MPa with true strain at fracture from 15.7 to 58.1%.

[0098] As the exact point of yielding is difficult to determine, a range of proof tests were employed at 0.2%, 0.5%

and 1.0% proof stresses. That is, the exact point where the deformation changes from elastic to plastic is complicated by the unique deformation mechanisms of the alloys herein, resulting in a curvature of the initial portion of the stress strain curve. The 0.2%, 0.5%, and 1.0% represent offset strains whereby at these strain levels, a parallel line is drawn to the stress strain curve and the resulting points of intersection is defined at the proof stress at the identified offsets respectively. At the 0.5% proof stress, more consistent and representative values are obtained so that the yield strength herein (A1, A2, A3, and A4) will be defined at the 0.5% proof stress. In FIG. 3, a Stress—strain curve example is provided showing the definition of 0.2%, 0.5% and 1.0% proof stresses. As can be seen from Table 4 below, the 0.5% proof stress, or yield strength of the sheet (A1), ranges from 295 MPa to 704 MPa. Therefore, it is contemplated herein that the alloy sheet made from the alloys herein will have a yield strength in the range of 250 MPa to 750 MPa.

TABLE 4

Tensile Properties of Final Sheet After Annealing at 850° C. For 10 min							
Alloy	Total Elongation (%) D1	Ultimate Tensile Strength (MPa) B1	0.2% Proof Stress (MPa)	0.5% Proof Stress (MPa) A1	1.0% Proof Stress (MPa)	True Strain At Fracture (%)	True Ultimate Tensile Strength (MPa) C1
Alloy 1	50.1	1175	483	524	552	40.6	1714
	50.9	1161	472	514	544	41.1	1692
Alloy 2	50.8	1190	471	517	548	41.1	1731
	36.6	1659	292	341	405	31.2	2237
	31.0	1683	317	357	392	26.9	2202
Alloy 3	34.7	1683	292	351	439	29.7	2159
	37.3	1655	286	339	418	31.6	2194
	60.3	1134	499	516	534	47.2	1767
	58.2	1141	500	518	536	45.9	1775
	60.4	1139	500	517	535	47.3	1778
Alloy 4	64.2	1138	490	508	526	49.6	1814
	31.5	1497	416	441	466	27.4	1953
	35.6	1542	419	444	472	30.4	2042
	35.3	1504	423	447	477	30.2	2026
Alloy 5	42.3	1539	420	447	479	35.3	2182
	56.8	1165	386	422	448	45.0	1804
	67.5	1129	440	471	490	51.6	1828
	58.5	1136	396	425	449	46.1	1733
Alloy 6	62.2	1137	389	421	447	48.3	1804
	18.2	1532	474	577	793	16.6	1726
	18.7	1544	475	584	804	17.1	1742
	17.1	1539	488	603	831	15.7	1714
	19.0	1540	468	561	773	17.3	1743
Alloy 7	55.7	1267	469	495	523	44.3	1873
	52.0	1242	456	485	513	41.9	1819
	56.0	1248	470	499	525	44.5	1874
	57.7	1277	464	489	515	45.6	1887
Alloy 8	65.4	1162	491	513	537	50.3	1841
	59.4	1179	469	496	522	46.6	1812
	61.8	1193	477	502	528	48.2	1836
Alloy 9	62.6	1172	531	556	578	48.6	1806
	64.7	993	484	504	522	49.9	1574
	66.1	997	491	512	530	50.7	1592
	66.2	994	481	503	520	50.8	1593
	66.3	994	491	510	526	50.9	1587
Alloy 10	63.9	1102	463	489	514	49.4	1772
	63.5	1118	465	492	518	49.2	1792
	65.3	1127	478	503	528	50.2	1784
	70.8	1108	475	503	527	53.5	1816
Alloy 11	62.6	1112	473	498	523	48.6	1765
	66.4	892	326	337	351	50.9	1457
	61.6	876	319	323	336	48.0	1398
	64.2	889	322	335	348	49.6	1437
	67.5	886	321	327	339	51.5	1447

TABLE 4-continued

Tensile Properties of Final Sheet After Annealing at 850° C. For 10 min							
Alloy	Total Elongation (%) D1	Ultimate Tensile Strength (MPa) B1	0.2% Proof Stress (MPa)	0.5% Proof Stress (MPa) A1	1.0% Proof Stress (MPa)	True Strain At Fracture (%)	True Ultimate Tensile Strength (MPa) C1
Alloy 12	60.4	1129	423	460	489	47.2	1748
	65.3	1136	440	470	497	50.2	1807
	63.0	1144	421	458	487	48.8	1776
Alloy 13	63.8	1129	427	462	490	49.3	1785
	49.5	987	388	432	459	40.2	1403
	48.7	988	381	419	446	39.7	1392
Alloy 14	49.0	991	358	406	442	39.9	1405
	44.2	999	377	414	441	36.6	1367
	72.9	1035	413	446	473	54.7	1704
Alloy 15	70.2	1016	407	440	466	53.1	1653
	73.7	1056	429	460	485	55.2	1754
	74.3	1032	406	441	468	55.5	1729
Alloy 16	42.5	1170	273	319	354	35.3	1605
	40.5	1164	295	327	358	34.0	1551
	43.3	1164	283	321	354	35.9	1563
Alloy 17	41.9	1175	296	329	360	34.9	1574
	39.5	1196	366	394	407	33.2	1586
	39.6	1196	377	401	413	33.3	1579
Alloy 18	38.4	1213	377	405	421	32.5	1601
	39.3	1187	355	386	400	33.1	1573
	51.1	1070	402	438	478	41.3	1547
Alloy 19	51.8	1073	405	447	485	41.7	1565
	54.3	1060	381	423	466	43.3	1552
	57.9	1067	395	435	476	45.6	1593
Alloy 20	53.4	1111	320	323	329	42.7	1631
	49.7	1110	314	312	316	40.3	1607
	54.3	1102	300	301	310	43.4	1602
Alloy 21	50.7	1115	334	333	335	41.0	1591
	43.0	1471	315	328	371	35.7	2090
	48.4	1449	314	331	376	39.5	2107
Alloy 22	45.0	1505	317	331	372	37.1	2116
	41.7	1478	316	329	370	34.9	2086
	78.6	887	455	476	499	58.0	1514
Alloy 23	78.9	888	459	481	504	58.1	1513
	78.5	880	455	481	502	58.0	1500
	77.7	890	467	490	512	57.5	1512
Alloy 24	70.5	1016	465	502	528	53.3	1649
	71.2	1005	465	502	528	53.8	1650
	69.1	1001	459	494	519	52.5	1621
Alloy 25	66.3	1071	464	499	524	50.8	1713
	66.8	1072	463	498	524	51.2	1710
	64.1	1104	466	503	531	49.5	1722
Alloy 26	65.7	1093	459	497	525	50.4	1722
	76.4	762	355	359	370	56.7	1284
	73.1	756	350	352	365	54.8	1267
Alloy 27	76.4	761	356	359	371	56.7	1297
	72.0	755	352	354	367	54.2	1260
	67.4	838	339	343	353	51.5	1371
Alloy 28	65.3	825	333	338	349	50.3	1342
	62.3	830	336	342	352	48.5	1315
	62.9	815	333	335	345	48.8	1309
Alloy 29	75.4	795	287	304	319	56.1	1338
	66.3	784	292	305	319	50.9	1279
	75.8	798	293	307	321	56.3	1347
Alloy 30	56.5	1256	622	649	667	44.8	1882
	55.9	1216	652	704	724	44.4	1824
	56.9	1243	646	687	705	45.0	1885
Alloy 31	74.2	717	273	295	314	55.4	1188
	71.9	727	282	305	324	54.1	1190
	71.4	739	282	308	327	53.8	1210
Alloy 32	38.0	1251	613	638	648	32.2	1640
	37.4	1253	599	627	638	31.7	1635
	38.0	1251	610	639	651	32.2	1637

TABLE 4-continued

Tensile Properties of Final Sheet After Annealing at 850° C. For 10 min							
Alloy	Total Elongation (%)	Ultimate Tensile Strength (MPa)	0.2% Proof Stress (MPa)	0.5% Proof Stress (MPa)	1.0% Proof Stress (MPa)	True Strain At Fracture (%)	True Ultimate Tensile Strength (MPa)
	D1	B1	A1	A1	A1	C1	C1
Alloy 29	38.6	1052	581	604	626	32.6	1457
	44.7	1095	573	596	617	36.9	1580
	42.2	1085	574	603	624	35.2	1543
Alloy 30	45.1	1304	455	496	522	37.2	1840
	51.1	1287	472	512	538	41.2	1853
	46.0	1282	460	498	525	37.9	1846
Alloy 31	44.9	1326	439	478	504	37.0	1824
	43.6	1321	443	481	505	36.1	1810
	49.5	1315	442	477	502	40.2	1893
Alloy 32	67.1	1027	551	574	592	51.3	1707
	73.2	1048	571	587	603	54.9	1802
	66.6	1051	574	590	605	51.0	1744
Alloy 33	67.1	1027	551	371	381	52.3	1319
	73.2	1048	571	376	385	52.0	1322
	66.6	1051	574	380	388	52.4	1342
Alloy 34	50.3	918	478	504	525	40.8	1332
	53.4	918	477	507	529	42.8	1353
	53.1	899	449	472	491	42.5	1324

Incremental Tensile Testing

[0099] Incremental tensile testing was done on an Instron mechanical testing frame (Model 5984), utilizing Instron's Bluehill control and analysis software. All tests were run at ambient temperature in displacement control. Samples were tested at a displacement rate of 0.025 mm/s during initial loading to 2% strain and 0.125 mm/s for the remaining duration of the test. Due to the variation in sample length during testing effective strain rates generally ranged from  $\sim 10^4/s$  to  $10^{-3}/s$  for the initial loading and after initial loading strain rates ranged from  $\sim 10^{-3}/s$  to  $\sim 10^{-2}/s$ . It should be noted that while the incremental tensile testing was done at these indicated strain rates, such incremental tensile testing is considered to support the yield strength distributions (i.e. values of A2, A3 and A4) and increase in magnetic phase volume for the alloys herein at the recited at strain rates ( $10^0/sec$  to  $10^2/sec$ ). See, e.g., Case Example #3 (stamping) and Table 13 (incremental tensile testing).

[0100] A control specimen from the same area of the sheet was tested up to failure from each alloy to evaluate initial sheet properties of the specific sample set used for incremental testing and the results are listed in Table 5 for each alloy herein. The ultimate tensile strength values are in a range from 745 to 1573 MPa with total elongation recorded in the range from 13.3 to 77.1%. The 0.5% proof stress or yield strength (A1) varies from 287 to 668 MPa and true ultimate tensile strength is in a range from 1175 to 2059 MPa. After each control specimen was tested, a new duplicate sample of each alloy was then strained approximately 5%, and then unloaded. The specimen dimensions were measured as well as the magnetic phases volume percent (Fe %) prior to the next increment of testing. Magnetic phases volume percent (Fe %) was measured by Fisher Feritscope.

TABLE 5

Tensile Properties of Alloys From Incremental Testing					
Alloy	Total Elongation (%)	0.5% Proof Stress (MPa)	Ultimate Tensile Strength (MPa)	True Ultimate Tensile Strength (MPa)	Difference Between True and Engineering Ultimate Tensile Strength (MPa)
	D1	A1	B1	C1	
Alloy 1	46.7	523	1166	1688	522
Alloy 2	30.9	350	1573	2059	486
Alloy 3	58.3	509	1140	1805	665
Alloy 4	35.4	450	1501	2029	528
Alloy 5	58.9	424	1112	1751	639
Alloy 6	13.3	503	1522	1701	179
Alloy 7	52.8	420	1223	1814	591
Alloy 8	57.9	440	1190	1863	673
Alloy 9	53.7	512	1001	1509	508
Alloy 10	62.5	449	1126	1781	655
Alloy 11	77.1	324	914	1618	704
Alloy 12	63.1	444	1150	1876	726
Alloy 13	42.5	360	1014	1428	414
Alloy 14	66.1	424	993	1649	656
Alloy 15	40.9	314	1199	1689	490
Alloy 16	38.7	378	1240	1720	480
Alloy 17	54.9	428	1126	1744	618
Alloy 18	50.9	287	1064	1606	542
Alloy 19	42.5	346	1386	1975	589
Alloy 20	72.6	465	869	1500	631
Alloy 21	65.7	483	999	1655	656
Alloy 22	65.2	485	1094	1807	713
Alloy 23	61.7	345	746	1206	460
Alloy 24	59.6	334	826	1318	492
Alloy 25	62.1	314	804	1303	499
Alloy 26	56.0	634	1214	1894	680
Alloy 27	57.7	325	745	1175	430
Alloy 28	34.4	668	1236	1661	425
Alloy 29	43.7	600	1080	1552	472
Alloy 30	48.6	490	1282	1905	623
Alloy 31	34.7	499	1295	1743	448
Alloy 32	54.0	579	1003	1545	542
Alloy 33	51.5	377	824	1248	424
Alloy 34	41.3	461	895	1265	370

[0101] Incremental test data for each alloy herein is listed in Table 6 through Table 39 and illustrated in FIG. 4 through FIG. 37. Sheet materials from alloys herein before testing have magnetic phases volume percent ranging from 0.2 to 40.7 Fe %. An increase in magnetic phases volume percent was observed in each alloy herein during incremental testing with difference between initial state and after the last cycle from 0.7 up to 83.3 Fe % depending on alloy chemistry. Incremental testing results also demonstrate a significant strengthening of the materials with increase in yield strength (0.5% proof stress). In all of the alloys herein from first cycle to the last one, more than 600 MPa increase in yield strength is found. Maximum difference in yield strength of 1750 MPa is recorded in Alloy 19. Since during forming, strengthening occurs to a lesser or greater extent in lower or more highly deformed localized area of the deformed part respectively, this will determine the magnitude of localized yield strength measured. As the incremental test data shows the initial undeformed strength levels and additionally the final strength until failure, sets the expected range of strengthening for a formed part for each alloy. The result of the incremental testing shown in Tables 6 through 39, clearly show a range of yield strengths are possible with the alloys here-in including the three identified distributions from the baseline value for each alloy;  $\pm 100$  MPa,  $>100$  to  $<600$  MPa, and  $\geq 600$  MPa.

TABLE 6

Incremental Test Data For Alloy 1					
Cycle Number	Cumulative Applied Strain [%]	0.2% Proof Stress [MPa]	0.5% Proof Stress [MPa]	1.0% Proof Stress [MPa]	Magnetic Phases Volume Percent [Fe %]
0	0.0	—	—	—	0.7
1	4.3	476	517	548	1.6
2	8.6	571	674	686	4.9
3	12.9	668	764	770	12.2
4	17.4	807	871	889	22.4
5	22.0	1012	1062	1067	32.8
6	26.8	1223	1267	1279	43.3
7	31.6	1443	1449	1458	45.4
8	35.6	1555	1592	1611	56.1
9	41.2	1788	1760	1762	67.5
Change (Last Cycle - First Cycle)		1312	1243	1204	66.8

TABLE 7

Incremental Test Data For Alloy 2					
Cycle Number	Cumulative Applied Strain [%]	0.2% Proof Stress [MPa]	0.5% Proof Stress [MPa]	1.0% Proof Stress [MPa]	Magnetic Phases Volume Percent [Fe %]
0	0.0	—	—	—	22.0
1	4.4	298	345	418	41.1
2	8.5	827	841	876	51.4
3	12.4	1255	1252	1290	59.1
4	16.3	1608	1616	1611	62.6
5	20.3	1868	1860	1890	64.4
6	21.0	2029	2043	—	67.1
Change (Last Cycle - First Cycle)		1731	1698	1472	45.7

TABLE 8

Incremental Test Data For Alloy 3					
Cycle Number	Cumulative Applied Strain [%]	0.2% Proof Stress [MPa]	0.5% Proof Stress [MPa]	1.0% Proof Stress [MPa]	Magnetic Phases Volume Percent [Fe %]
0	0.0	—	—	—	0.9
1	4.5	491	506	525	1.1
2	8.9	677	686	700	1.1
3	13.2	818	840	849	1.1
4	17.5	880	975	982	1.1
5	22.1	996	1100	1107	1.3
6	26.6	1074	1211	1212	1.4
7	31.3	1150	1310	1307	1.5
8	36.4	1230	1388	1402	1.9
9	40.2	1335	1502	1497	2.0
10	46.3	1404	1570	1565	2.3
11	50.0	1496	1662	1662	2.3
12	52.2	1601	1767	1797	2.5
Change (Last Cycle - First Cycle)		1110	1261	1272	1.6

TABLE 9

Incremental Test Data For Alloy 4					
Cycle Number	Cumulative Applied Strain [%]	0.2% Proof Stress [MPa]	0.5% Proof Stress [MPa]	1.0% Proof Stress [MPa]	Magnetic Phases Volume Percent [Fe %]
0	0.0	—	—	—	9.6
1	4.5	416	442	475	29.7
2	8.7	665	676	691	40.2
3	13.0	939	941	964	49.6
4	17.2	1194	1213	1214	54.8
5	21.5	1456	1497	1512	59.5
6	22.3	1691	—	—	62.6
Change (Last Cycle - First Cycle)		1275	1055	1037	53.0

TABLE 10

Incremental Test Data For Alloy 5					
Cycle Number	Cumulative Applied Strain [%]	0.2% Proof Stress [MPa]	0.5% Proof Stress [MPa]	1.0% Proof Stress [MPa]	Magnetic Phases Volume Percent [Fe %]
0	0.0	—	—	—	0.9
1	4.3	393	428	458	1.6
2	8.5	483	571	583	3.4
3	12.8	540	655	664	8.2
4	17.2	638	749	755	16.5
5	21.7	770	883	889	26.9
6	26.3	941	1060	1064	35.3
7	35.6	1120	1243	1249	45.3
8	37.5	1356	1470	1469	51.1
9	41.6	1518	1578	1575	54.5
10	46.9	1759	1782	1774	55.1
11	53.8	1843	1839	1830	58.1
Change (Last Cycle - First Cycle)		1450	1411	1372	57.2



TABLE 11

Incremental Test Data For Alloy 6					
Cycle Number	Cumulative Applied Strain [%]	0.2% Proof Stress [MPa]	0.5% Proof Stress [MPa]	1.0% Proof Stress [MPa]	Magnetic Phases Volume Percent [Fe %]
0	0.0				40.7
1	2.2	379	543	798	63.4
2	4.2	1272	1298	1351	68.1
3	6.2	1542	1546	1553	70.6
4	8.1	1670	1656	1656	71.6
5	10.4	1801	1750	1699	73.0
Change (Last Cycle - First Cycle)		1422	1207	901	32.3

TABLE 12

Incremental Test Data For Alloy 7					
Cycle Number	Cumulative Applied Strain [%]	0.2% Proof Stress [MPa]	0.5% Proof Stress [MPa]	1.0% Proof Stress [MPa]	Magnetic Phases Volume Percent [Fe %]
0	0.0	—	—	—	1.1
1	4.2	414	440	469	2.5
2	8.5	484	591	605	7.6
3	12.6	599	711	719	16.2
4	16.6	743	869	873	27.4
5	20.5	935	1067	1075	36.4
6	24.4	1131	1293	1289	46.0
7	28.1	1330	1466	1478	51.1
8	31.7	1541	1576	1638	56.5
9	35.3	1773	1735	1755	59.6
10	38.9	1944	1904	1848	59.6
11	40.2	1898	1729	—	63.0
Change (Last Cycle - First Cycle)		1484	1289	1379	61.9

TABLE 13

Incremental Test Data For Alloy 8					
Cycle Number	Cumulative Applied Strain [%]	0.2% Proof Stress [MPa]	0.5% Proof Stress [MPa]	1.0% Proof Stress [MPa]	Magnetic Phases Volume Percent [Fe %]
0	0.0	—	—	—	1.2
1	4.2	393	418	447	2.4
2	8.4	481	599	619	5.5
3	12.5	570	715	728	11.9
4	16.4	678	863	872	20.0
5	20.3	804	1030	1031	28.0
6	24.1	947	1181	1190	35.5
7	27.8	1092	1341	1339	41.3
8	31.5	1248	1473	1462	47.4
9	35.1	1426	1596	1580	51.6
10	38.8	1614	1709	1694	57.4
11	40.1	1827	—	—	62.7
Change (Last Cycle - First Cycle)		1434	1291	1247	61.5

TABLE 14

Incremental Test Data For Alloy 9					
Cycle Number	Cumulative Applied Strain [%]	0.2% Proof Stress [MPa]	0.5% Proof Stress [MPa]	1.0% Proof Stress [MPa]	Magnetic Phases Volume Percent [Fe %]
0	0.0	—	—	—	0.9
1	4.4	497	517	536	1.2
2	8.7	660	679	691	1.2
3	12.9	754	811	819	1.2
4	16.9	829	923	930	1.2
5	21.0	902	1029	1035	1.2
6	24.9	978	1125	1130	1.4
7	28.8	1048	1215	1220	1.6
8	32.7	1128	1308	1315	1.8
9	36.5	1221	1411	1397	2.0
10	40.3	1320	1492	1498	2.2
11	44.0	1374	1540	1536	2.3
12	48.9	1472	1649	1637	2.8
Change (Last Cycle - First Cycle)		975	1132	1101	1.9

TABLE 15

Incremental Test Data For Alloy 10					
Cycle Number	Cumulative Applied Strain [%]	0.2% Proof Stress [MPa]	0.5% Proof Stress [MPa]	1.0% Proof Stress [MPa]	Magnetic Phases Volume Percent [Fe %]
0	0.0	—	—	—	1.2
1	4.2	418	444	471	1.6
2	8.2	466	591	622	3.1
3	12.3	537	703	731	6.1
4	16.5	628	833	857	10.3
5	20.8	723	968	987	15.8
6	25.2	819	1096	1114	23.6
7	29.8	933	1240	1232	28.3
8	34.1	1043	1360	1337	34.7
9	38.9	1185	1448	1452	41.2
10	44.1	1342	1585	1575	42.2
11	50.5	1482	1664	1650	47.2
12	54.5	1660	1770	1795	52.3
Change (Last Cycle - First Cycle)		1242	1326	1324	51.1

TABLE 16

Incremental Test Data For Alloy 11					
Cycle Number	Cumulative Applied Strain [%]	0.2% Proof Stress [MPa]	0.5% Proof Stress [MPa]	1.0% Proof Stress [MPa]	Magnetic Phases Volume Percent [Fe %]
0	0.0	—	—	—	1.2
1	4.7	318	323	334	1.6
2	9.3	450	453	465	1.6
3	13.8	568	572	579	1.7
4	18.2	675	679	686	1.8
5	22.5	783	793	799	2.1
6	26.8	888	887	902	2.5
7	31.0	985	994	997	2.8
8	35.0	1087	1087	1104	3.4
9	39.1	1181	1192	1190	3.7
10	43.0	1234	1248	1245	3.7
11	46.3	1329	1342	1342	3.7

TABLE 16-continued

Incremental Test Data For Alloy 11					
Cycle Number	Cumulative Applied Strain [%]	0.2% Proof Stress [MPa]	0.5% Proof Stress [MPa]	1.0% Proof Stress [MPa]	Magnetic Phases Volume Percent [Fe %]
Change (Last Cycle - First Cycle)		1011	1019	1008	2.5

TABLE 17

Incremental Test Data For Alloy 12					
Cycle Number	Cumulative Applied Strain [%]	0.2% Proof Stress [MPa]	0.5% Proof Stress [MPa]	1.0% Proof Stress [MPa]	Magnetic Phases Volume Percent [Fe %]
0	0.0	—	—	—	1.5
1	4.2	402	430	460	2.1
2	8.3	467	579	597	4.6
3	12.6	542	682	695	9.9
4	16.9	651	807	816	17.7
5	21.3	824	962	970	27.3
6	26.1	990	1129	1142	36.5
7	30.8	1113	1300	1313	42.4
8	35.2	1267	1439	1463	48.3
9	40.5	1483	1555	1569	52.2
10	47.7	1701	1747	1736	59.7
Change (Last Cycle - First Cycle)		1299	1317	1276	58.2

TABLE 18

Incremental Test Data For Alloy 13					
Cycle Number	Cumulative Applied Strain [%]	0.2% Proof Stress [MPa]	0.5% Proof Stress [MPa]	1.0% Proof Stress [MPa]	Magnetic Phases Volume Percent [Fe %]
0	0.0	—	—	—	1.7
1	4.4	341	368	402	9.5
2	8.7	498	540	547	21.6
3	13.0	655	697	704	35.8
4	17.1	833	863	875	47.5
5	21.2	1009	1022	1030	54.8
6	25.2	1172	1169	1173	62.0
7	29.2	1289	1268	1276	69.2
8	32.5	1487	1443	1452	70.5
Change (Last Cycle - First Cycle)		1146	1075	1050	68.8

TABLE 19

Incremental Test Data For Alloy 14					
Cycle Number	Cumulative Applied Strain [%]	0.2% Proof Stress [MPa]	0.5% Proof Stress [MPa]	1.0% Proof Stress [MPa]	Magnetic Phases Volume Percent [Fe %]
0	0.0	—	—	—	2.0
1	4.4	400	431	459	2.0
2	8.5	538	589	600	2.3

TABLE 19-continued

Incremental Test Data For Alloy 14					
Cycle Number	Cumulative Applied Strain [%]	0.2% Proof Stress [MPa]	0.5% Proof Stress [MPa]	1.0% Proof Stress [MPa]	Magnetic Phases Volume Percent [Fe %]
3	12.8	589	701	712	3.1
4	17.2	652	805	817	4.6
5	21.6	726	911	923	6.9
6	26.2	812	1022	1033	9.7
7	30.8	891	1132	1146	13.4
8	35.7	980	1243	1246	16.1
9	40.0	1067	1330	1343	19.1
10	44.4	1162	1429	1430	20.4
11	50.3	1268	1568	1548	23.3
12	53.0	1341	1644	1622	27.6
Change (Last Cycle - First Cycle)		941	1213	1163	25.7

TABLE 20

Incremental Test Data For Alloy 15					
Cycle Number	Cumulative Applied Strain [%]	0.2% Proof Stress [MPa]	0.5% Proof Stress [MPa]	1.0% Proof Stress [MPa]	Magnetic Phases Volume Percent [Fe %]
0	0.0	—	—	—	2.4
1	4.5	304	321	357	14.0
2	8.9	492	511	517	31.9
3	13.2	721	728	752	47.9
4	17.3	984	1003	1008	58.0
5	21.4	1245	1249	1241	64.7
6	25.3	1439	1429	1420	69.5
7	30.2	1550	1571	1545	71.7
Change (Last Cycle - First Cycle)		1246	1250	1188	69.4

TABLE 21

Incremental Test Data For Alloy 16					
Cycle Number	Cumulative Applied Strain [%]	0.2% Proof Stress [MPa]	0.5% Proof Stress [MPa]	1.0% Proof Stress [MPa]	Magnetic Phases Volume Percent [Fe %]
0	0.0	—	—	—	1.6
1	4.5	349	373	392	16.0
2	8.8	430	448	462	38.2
3	13.2	648	674	696	56.6
4	17.5	998	1015	1028	67.2
5	22.0	1305	1306	1312	75.2
6	26.7	1490	1510	1505	79.1
7	31.7	1647	1626	1622	83.3
Change (Last Cycle - First Cycle)		1298	1253	1230	81.7

TABLE 22

Incremental Test Data For Alloy 17					
Cycle Number	Cumulative Applied Strain [%]	0.2% Proof Stress [MPa]	0.5% Proof Stress [MPa]	1.0% Proof Stress [MPa]	Magnetic Phases Volume Percent [Fe %]
0	0.0	—	—	—	1.9
1	4.2	390	425	470	6.2
2	8.3	555	653	664	13.0
3	12.5	645	797	806	22.2
4	17.0	769	949	954	31.9
5	21.5	889	1079	1082	39.5
6	26.2	1034	1191	1224	46.4
7	31.3	1195	1309	1320	54.4
8	38.1	1500	1487	1484	55.9
9	41.7	1569	1592	1587	61.3
10	45.5	1745	1705	1671	65.1
Change (Last Cycle – First Cycle)		1355	1280	1201	63.2

TABLE 23

Incremental Test Data For Alloy 18					
Cycle Number	Cumulative Applied Strain [%]	0.2% Proof Stress [MPa]	0.5% Proof Stress [MPa]	1.0% Proof Stress [MPa]	Magnetic Phases Volume Percent [Fe %]
0	0.0	—	—	—	3.6
1	4.6	310	312	320	26.8
2	9.0	532	535	561	38.6
3	13.5	783	784	793	45.5
4	18.1	962	965	978	51.3
5	22.9	1124	1119	1132	54.7
6	27.6	1258	1244	1246	58.3
7	32.8	1394	1379	1373	61.2
8	37.9	1498	1507	1517	62.8
9	43.7	1578	1574	1548	67.1
Change (Last Cycle – First Cycle)		1268	1262	1228	63.5

TABLE 24

Incremental Test Data For Alloy 19					
Cycle Number	Cumulative Applied Strain [%]	0.2% Proof Stress [MPa]	0.5% Proof Stress [MPa]	1.0% Proof Stress [MPa]	Magnetic Phases Volume Percent [Fe %]
0					16.3
1	4.5	340	358	392	31.0
2	8.8	642	655	677	38.7
3	13.2	879	889	918	45.7
4	17.6	1138	1146	1160	51.6
5	21.9	1420	1405	1443	56.0
6	26.2	1649	1628	1644	58.1
7	30.8	1864	1848	1847	61.3
8	35.1	2034	1983	2037	61.7
9	38.8	2107	2108	2082	64.5
Change (Last Cycle – First Cycle)		1767	1750	1690	48.2

TABLE 25

Incremental Test Data For Alloy 20					
Cycle Number	Cumulative Applied Strain [%]	0.2% Proof Stress [MPa]	0.5% Proof Stress [MPa]	1.0% Proof Stress [MPa]	Magnetic Phases Volume Percent [Fe %]
0	0.0	—	—	—	1.4
1	4.4	458	478	499	1.9
2	8.6	556	609	620	1.9
3	12.9	613	705	714	2.0
4	17.3	676	788	797	2.3
5	21.9	727	866	875	3.1
6	26.6	791	944	951	4.5
7	31.4	883	1018	1025	6.4
8	36.4	1012	1098	1103	8.7
9	41.6	1011	1170	1179	12.4
10	47.1	1084	1265	1258	15.2
11	51.8	1145	1318	1312	20.2
12	58.4	1290	1485	1492	23.8
13	65.2	1361	1518	1511	23.6
14	69.0	1502	1538	1530	27.9
15	72.5	1571	1694	1676	30.5
Change (Last Cycle – First Cycle)		1113	1216	1177	29.1

TABLE 26

Incremental Test Data For Alloy 21					
Cycle Number	Cumulative Applied Strain [%]	0.2% Proof Stress [MPa]	0.5% Proof Stress [MPa]	1.0% Proof Stress [MPa]	Magnetic Phases Volume Percent [Fe %]
0	0.0	—	—	—	1.4
1	4.2	452	484	510	1.8
2	8.3	509	619	633	2.1
3	12.6	556	703	721	3.3
4	17.0	617	783	797	6.3
5	21.7	700	870	882	11.1
6	26.4	802	968	978	16.9
7	31.1	922	1088	1097	24.9
8	36.1	1040	1212	1209	30.5
9	41.2	1204	1323	1327	36.1
10	45.1	1311	1456	1435	36.1
11	51.1	1462	1572	1587	43.4
12	56.9	1629	1679	1671	48.1
13	59.5	1713	1734	1732	48.1
Change (Last Cycle – First Cycle)		1261	1250	1222	46.7

TABLE 27

Incremental Test Data For Alloy 22					
Cycle Number	Cumulative Applied Strain [%]	0.2% Proof Stress [MPa]	0.5% Proof Stress [MPa]	1.0% Proof Stress [MPa]	Magnetic Phases Volume Percent [Fe %]
0	0.0	—	—	—	1.4
1	4.1	446	482	511	1.8
2	8.2	495	617	634	2.4
3	12.4	572	707	720	5.1
4	17.0	631	794	802	10.6
5	21.7	742	902	907	18.3
6	26.4	866	1040	1043	27.1
7	31.2	1041	1181	1201	35.2

TABLE 27-continued

Incremental Test Data For Alloy 22					
Cycle Number	Cumulative Applied Strain [%]	0.2% Proof Stress [MPa]	0.5% Proof Stress [MPa]	1.0% Proof Stress [MPa]	Magnetic Phases Volume Percent [Fe %]
8	36.1	1224	1343	1359	39.7
9	40.4	1323	1435	1493	45.8
10	46.6	1500	1586	1582	50.0
11	48.0	1769	—	—	54.6
Change (Last Cycle - First Cycle)		1323	1104	1071	53.2

TABLE 28

Incremental Test Data For Alloy 23					
Cycle Number	Cumulative Applied Strain (%)	0.2% Proof Stress (MPa)	0.5% Proof Stress (MPa)	1.0% Proof Stress (MPa)	Magnetic Phases Volume Percent (Fe %)
0	0.0	—	—	—	1.0
1	4.7	344	347	362	1.4
2	9.3	465	469	478	1.4
3	13.9	577	579	585	1.3
4	18.4	674	675	679	1.3
5	22.8	761	760	762	1.2
6	27.2	828	827	828	1.1
7	31.5	860	858	860	1.1
8	35.8	998	995	996	1.1
9	40.0	1037	1032	1034	1.1
10	44.2	1103	1098	1100	1.1
11	48.7	1158	1149	1148	1.5
Change (Last Cycle - First Cycle)		814	802	786	0.5

TABLE 29

Incremental Test Data For Alloy 24					
Cycle Number	Cumulative Applied Strain (%)	0.2% Proof Stress (MPa)	0.5% Proof Stress (MPa)	1.0% Proof Stress (MPa)	Magnetic Phases Volume Percent (Fe %)
0	0.0	—	—	—	1.3
1	4.7	333	337	347	1.5
2	9.3	458	462	472	1.4
3	13.9	574	576	583	1.4
4	18.4	676	678	682	1.4
5	22.7	772	776	777	1.3
6	27.0	866	866	871	1.3
7	31.3	955	957	957	1.4
8	35.4	1014	1031	1032	1.4
9	39.6	1121	1124	1127	1.6
10	43.6	1183	1184	1204	1.7
11	47.2	1222	1230	1224	1.8
Change (Last Cycle - First Cycle)		889	893	877	0.5

TABLE 30

Incremental Test Data For Alloy 25					
Cycle Number	Cumulative Applied Strain (%)	0.2% Proof Stress (MPa)	0.5% Proof Stress (MPa)	1.0% Proof Stress (MPa)	Magnetic Phases Volume Percent (Fe %)
0	0.0	—	—	—	1.0
1	4.7	301	309	323	1.3
2	9.3	437	444	454	1.4
3	13.7	555	563	571	1.4
4	18.1	652	666	672	1.7
5	22.4	739	763	767	2.1
6	26.6	814	851	854	2.8
7	30.8	894	941	944	3.6
8	34.9	970	1032	1031	4.5
9	39.0	1040	1110	1106	5.6
10	43.0	1098	1175	1167	5.5
11	45.4	1176	1231	1228	8.3
Change (Last Cycle - First Cycle)		875	922	905	7.3

TABLE 31

Incremental Test Data For Alloy 26					
Cycle Number	Cumulative Applied Strain (%)	0.2% Proof Stress (MPa)	0.5% Proof Stress (MPa)	1.0% Proof Stress (MPa)	Magnetic Phases Volume Percent (Fe %)
0	0.0	—	—	—	13.2
1	4.2	603	639	659	16.6
2	8.3	604	749	762	18
3	12.5	669	815	818	23.8
4	16.6	784	870	876	33.4
5	20.6	941	1014	1016	41.55
6	24.5	1153	1215	1228	49.45
7	28.3	1377	1444	1453	54.4
8	32.0	1574	1622	1630	54.1
9	35.7	1772	1770	1760	61.2
10	37.5	1874	—	—	63.3
Change (Last Cycle - First Cycle)		1271	1131	1101	50.1

TABLE 32

Incremental Test Data For Alloy 27					
Cycle Number	Cumulative Applied Strain (%)	0.2% Proof Stress (MPa)	0.5% Proof Stress (MPa)	1.0% Proof Stress (MPa)	Magnetic Phases Volume Percent (Fe %)
0	0.0	—	—	—	1.2
1	4.6	313	326	343	1.7
2	9.1	449	459	469	1.9
3	13.6	552	568	576	2.2
4	17.9	638	664	670	2.7
5	22.2	719	753	758	3.9
6	26.4	809	840	843	5.1
7	30.6	872	920	922	6.3
8	34.7	942	996	997	7.7
9	38.9	1001	1055	1059	10.1
10	43.0	1100	1148	1143	12.0
11	44.2	1200	1229	—	14.6
Change (Last Cycle - First Cycle)		887	903	800	13.4

TABLE 33

Incremental Test Data For Alloy 28					
Cycle Number	Cumulative Applied Strain (%)	0.2% Proof Stress (MPa)	0.5% Proof Stress (MPa)	1.0% Proof Stress (MPa)	Magnetic Phases
					Volume Percent (Fe %)
0	0.0	—	—	—	17.4
1	4.3	631	657	669	22.5
2	8.7	660	720	727	37.6
3	13.0	730	732	741	48.2
4	17.1	927	960	973	58.5
5	21.1	1263	1293	1297	66.1
6	25.0	1517	1539	1532	72.2
7	28.7	1691	1679	1665	72.0
Change (Last Cycle – First Cycle)		1060	1022	996	54.6

TABLE 34

Incremental Test Data For Alloy 29					
Cycle Number	Cumulative Applied Strain (%)	0.2% Proof Stress (MPa)	0.5% Proof Stress (MPa)	1.0% Proof Stress (MPa)	Magnetic Phases
					Volume Percent (Fe %)
0	0.0	—	—	—	2.0
1	4.2	573	598	621	2.6
2	8.3	625	741	756	3.1
3	12.4	667	833	850	4.9
4	16.3	725	917	932	8.6
5	20.3	811	1009	1022	13.6
6	24.2	903	1115	1128	21.1
7	28.6	1029	1248	1255	30.1
Change (Last Cycle – First Cycle)		456	650	634	27.5

TABLE 35

Incremental Test Data For Alloy 30					
Cycle Number	Cumulative Applied Strain (%)	0.2% Proof Stress (MPa)	0.5% Proof Stress (MPa)	1.0% Proof Stress (MPa)	Magnetic Phases
					Volume Percent (Fe %)
0	0.0	—	—	—	2.3
1	4.3	456	491	517	3.4
2	8.6	494	598	605	8.4
3	12.9	571	644	648	20.8
4	17.1	716	767	774	35.5
5	21.0	966	1014	1024	46.6
6	24.9	1258	1317	1322	55.6
7	27.7	1509	1523	1524	59.9
Change (Last Cycle – First Cycle)		1053	1032	1007	57.6

TABLE 36

Incremental Test Data For Alloy 31					
Cycle Number	Cumulative Applied Strain (%)	0.2% Proof Stress (MPa)	0.5% Proof Stress (MPa)	1.0% Proof Stress (MPa)	Magnetic Phases
					Volume Percent (Fe %)
0	0.0	—	—	—	2.9
1	4.4	435	469	495	5.8
2	8.8	495	566	567	17.4
3	13.1	583	622	625	32.8
4	17.2	783	819	835	47.3
5	19.7	1099	1145	1156	55.3
Change (Last Cycle – First Cycle)		664	676	661	52.4

TABLE 37

Incremental Test Data For Alloy 32					
Cycle Number	Cumulative Applied Strain (%)	0.2% Proof Stress (MPa)	0.5% Proof Stress (MPa)	1.0% Proof Stress (MPa)	Magnetic Phases
					Volume Percent (Fe %)
0	0.0	—	—	—	1.0
1	4.4	563	578	596	1.9
2	8.6	692	728	739	1.9
3	12.7	751	841	849	1.8
4	16.8	809	937	945	2.1
5	20.8	871	1025	1032	2.6
6	24.7	939	1113	1120	3.5
7	28.6	1005	1195	1202	4.8
8	33.4	1071	1280	1287	10.8
Change (Last Cycle – First Cycle)		508	702	691	9.8

TABLE 38

Incremental Test Data For Alloy 33					
Cycle Number	Cumulative Applied Strain (%)	0.2% Proof Stress (MPa)	0.5% Proof Stress (MPa)	1.0% Proof Stress (MPa)	Magnetic Phases
					Volume Percent (Fe %)
0	0.0	—	—	—	0.7
1	4.6	378	383	393	0.8
2	9.2	509	515	527	0.9
3	13.6	631	639	648	0.9
4	17.9	736	751	757	0.9
5	22.2	823	848	852	0.9
6	26.4	903	938	940	0.9
7	30.6	973	1017	1018	0.9
8	34.7	1042	1092	1093	1.0
9	38.8	1099	1153	1155	1.0
10	42.8	1175	1246	1241	1.0
11	46.9	1259	1324	1317	1.4
12	49.8	1404	1464	1445	1.5
Change (Last Cycle – First Cycle)		1026	1081	1052	0.8

TABLE 39

Incremental Test Data For Alloy 34					
Cycle Number	Cumulative Applied Strain (%)	0.2% Proof Stress (MPa)	0.5% Proof Stress (MPa)	1.0% Proof Stress (MPa)	Magnetic Phases Volume Percent (Fe %)
0	0.0	—	—	—	0.4
1	4.5	459	481	501	0.5
2	8.9	649	659	671	0.6
3	13.3	777	797	804	0.6
4	17.5	881	913	918	0.6
5	21.7	973	1016	1019	0.6
6	25.8	1053	1109	1110	0.6
7	29.9	1134	1197	1196	0.5
8	33.3	1292	1363	1351	0.7
Change (Last Cycle – First Cycle)		833	882	850	0.3

**[0102]** As can be seen from the above, the magnetic phases volume of the sheet is increased when exposed to one or a plurality of strains above the yield strength of the sheet. That is, for a given sheet material, having a magnetic phases volume that falls in the range of 0.2 Fe % to 45.0 Fe %, such value is observed to increase and the metal part that is formed indicates a magnetic phases volume that falls in the range of 0.5 Fe % to 85.0 Fe %. For example, for Alloy 1 that indicates in the sheet an initial magnetic phase volume of 0.7 Fe %, after nine (9) strains above the yield strength of the sheet indicates a magnetic phases volume of 67.5 Fe %. Alloy 2 sheet is initially 22.0 Fe % and after six (6) strains above the yield strength of the sheet indicates a magnetic phases volume of 67.1 Fe %. For each alloy provided herein, the properties including yield change as a function of applied strain in sheet form. In stamping operations, a wide range of strains rather than a singular strain is applied over the stamped part. This results in a wide range of localized strain and resulting properties in the stamped part which may include the entire range of properties found for example by the separately applied strains in the sequential cycles for each alloy.

#### Case Examples

##### Case Example #1 Structural Changes During Cold Deformation

**[0103]** These results show the key structural changes which lead to strengthening during cold deformation with commensurate increases in both yield and tensile strength during the deformation process.

**[0104]** Laboratory slabs with thickness of 50 mm were cast from Alloy 7 and Alloy 8 according to the atomic ratios in Table 1 that were then laboratory processed by hot rolling, cold rolling and annealing at 850° C. for 10 min as described in the Main Body section of the current application. Microstructure of the alloys in a form of processed sheet with 1.2 mm thickness after annealing corresponding to a condition of the sheet in annealed coils at commercial production was examined by SEM and TEM.

**[0105]** To prepare TEM specimens for a structural analysis of the annealed sheet from the alloys before deformation, the samples were first cut with EDM, and then thinned by grinding with pads of reduced grit size every time. Further thinning to make foils of 60 to 70  $\mu\text{m}$  thickness was done by

polishing with 9  $\mu\text{m}$ , 3  $\mu\text{m}$ , and 1  $\mu\text{m}$  diamond suspension solution, respectively. Discs of 3 mm in diameter were punched from the foils and the final polishing was fulfilled with electropolishing using a twin-jet polisher. The chemical solution used was a 30% nitric acid mixed in methanol base. In case of insufficient thin area for TEM observation, the TEM specimens may be ion-milled using a Gatan Precision Ion Polishing System (PIPS). The ion-milling usually is done at 4.5 keV, and the inclination angle is reduced from 4° to 2° to open up the thin area. To analyze structure in the alloys after deformation, TEM samples were cut from the gauge section of the tensile specimens close to the fracture and prepared in the similar manner. The TEM studies were done using a JEOL 2100 high-resolution microscope operated at 200 kV. The TEM specimens were studied by SEM. Microstructures were examined by SEM using an EVO-MA10 scanning electron microscope manufactured by Carl Zeiss SMT Inc.

**[0106]** The microstructure in the Alloy 7 sheet before deformation is shown by SEM and TEM micrographs in FIGS. 38a and b, respectively. The microstructure consists primarily of recrystallized micron-sized austenite grains, 1 to 10  $\mu\text{m}$  in size, containing annealing twins and stacking faults. Annealing twins are generally understood as a highly symmetrical interface within one crystal or grain and form during annealing. Stacking faults are a more general term to describing an interruption of the normal stacking sequence of atomic planes in a crystal or grain. Detailed analysis of the structure also reveals a small fraction of ferrite (<1%) and the presence of isolated nanoprecipitates typically in the 5 to 100 nm size range (FIG. 38c). Similar structure was observed in the Alloy 8 sheet before deformation shown in FIG. 39. Detailed analysis of the structure also reveals a small fraction of ferrite (<1%) and the presence of isolated nanoprecipitates typically in the 5 to 100 nm size range (FIG. 38c). Similar structure was observed in the Alloy 8 sheet before deformation shown in FIG. 39.

**[0107]** During tensile testing to failure, the initial structure undergoes NR&S leading to formation of the final structure, which is demonstrated for Alloy 7 and Alloy 8 by SEM and TEM micrographs in FIG. 40 and FIG. 41, respectively. As can be seen, the structure after deformation is much different than the starting structure and consists of two distinct microstructural regions of Microconstituent 1 and Microconstituent 2 as shown in FIG. 40b and FIG. 41b.

**[0108]** Further details of the microstructure after deformation highlighting microstructural features of each microconstituent were obtained from structural analysis of the gauge section of the tensile specimen from Alloy 8 sheet after testing to failure. A TEM bright-field micrograph corresponding to Microconstituent 1 in the sheet material is shown in FIG. 42a. Microconstituent 1 is a result of phase transformation during cold deformation and characterized by refined ferrite, with grain sizes from 20 to 750 nm, and nanoprecipitates. Its formation can be quantified by measurement of magnetic phases volume percent (Fe %) using Feriscope as demonstrated for alloys herein during incremental testing (see Main Body). In the case of Alloy 8 sheet, before deformation it has less than 1 Fe % of magnetic phases volume percent as measured by the Feriscope. After tensile testing to failure, measured value near the fracture is about 62.7 Fe %. Microconstituent 1 is found to contain significant volume fractions (~4 vol %) of nanoprecipitates typically from 2 to 20 nm in diameter although larger

nanoprecipitates can be occasionally found up to 100 nm in size. In FIG. 42b, a TEM dark-field micrograph of the Microconstituent 1 area illustrates the nanoscale ferrite grains that are typically from 150 to 300 nm in size and formed as a result of transformation from austenite during the deformation process. After transformation, the nanoscale ferrite is also found to participate in the deformation process through dislocation mechanisms. In FIG. 42c, a TEM dark-field micrograph shows a selected nanoscale ferrite grain at higher resolution. As shown, this grain contains a high density of dislocations, which form with a tangled morphology indicating that after formation, this grain continued to deform and contribute to the measured total elongation. Thus, the NR&S mechanism leading to structural evolution during cold deformation described above involves complex interaction of dislocation dominated deformation mechanisms along with phase transformation (e.g. austenite to ferrite), nanoscale phase formation (e.g. creation of nano-ferrite from 20 nm to 750 nm), nanoprecipitation and results in material strengthening confirmed by the yield strength distributions identified in FIG. 2. HREM image of the nanoprecipitate examples are shown in FIG. 42d.

**[0109]** A TEM bright-field micrograph corresponding to Microconstituent 2 in the sheet material is shown in FIG. 43a. Microconstituent 2 is represented by micron-sized un-transformed austenite and nanoprecipitates with high dislocation density and dislocation cell formation after deformation (FIG. 43b). Microconstituent 1 is also found to contain nanoprecipitates that are highlighted by circles in FIG. 43c and are typically from 2 to 20 nm in diameter although larger nanoprecipitates can be occasionally found up to 100 nm in size. In FIG. 43d, a HREM image of the nanoprecipitate example is shown.

**[0110]** This Case Example demonstrates that the microstructure of the alloys herein undergo transformation during cold deformation through the NR&S mechanism leading to formation of the microstructure with distinct microconstituents resulting in material strengthening.

#### Case Example #2 Nondestructive Analysis of Stamped Part

**[0111]** Sheet blanks from Alloy 8 with a thickness of 1.4 mm were used for stamping trial of a B-pillar at a commercial stamping facility with stamping speed estimated at 290 mm/s. Using an existing die, Alloy 8 sheet blanks were stamped into B-pillars. Non-destructive analysis of the B-pillar was done by Feritscope measurements of the local magnetic phases volume percent in different areas.

**[0112]** Feritscope measurements provide an indication of the structural changes occurring during deformation from stamping. As shown previously, in the Alloy 8 sheet, the initial sheet microstructure changes from non-magnetic (i.e. paramagnetic) to magnetic (i.e. ferromagnetic) microstructure during cold deformation through the NR&S mechanism. The baseline for the sheet in Feritscope measurements before stamping was <1 Fe %. Increase in the volume fraction of Microconstituent 1 results in higher Fe % measured. Feritscope measurements with ~20 mm grid pattern were taken from two stamped B-pillars including one which underwent 4 out of 5 stamping hits and one which underwent 5 out of 5 stamping hits. The 5<sup>th</sup> hit is mainly a flanging operation so little structural or property change was expected in the B-pillar. The examples of the grid pattern on the different areas of the B-pillars are shown in FIG. 44.

**[0113]** The summary of Fe % measurements of the B-pillar which underwent a total of 4 stamping hits is shown in FIG. 45. Note that out of the 1426 total measurements taken, 487 of these measurements remained at <1 Fe % and are not shown in FIG. 45 as in these areas, little or no strain was imposed on the sheet during stamping so it remained at its baseline value. In FIG. 46, a histogram of the Feritscope measurements on the B-pillar which underwent all 5 stamping operations is shown. In a similar fashion, out of the 1438 total measurements taken, 510 of these were still at the baseline sheet value and are not shown. Analysis of the data shows that in approximately ~65% of the areas measured, increase in Fe % corresponding to nano-ferrite formation and indicating strengthening through the NR&S mechanism was observed. The fraction of the stamping which undergoes strengthening will depend on the amount of material deformed during the stamping operation, which is highly dependent on the localized strain (i.e. amount of deformation which occurs in a particular area of a deformed part). Additionally, for both stamped B-pillars, the highest magnetic phases volume percent measured was 31 Fe % measured in the most deformed areas. Thus, the 1438 measurements show a wide range of Fe % numbers at each localized area from <1% to 31 Fe %. This clearly shows localized structural changes and this is then expected to be concurrent with localized yield strength changes leading to three distinct yield strength distributions.

**[0114]** This Case Example demonstrates significant changes in magnetic phases volume percent in the stamping as compared to initial sheet. These changes correspond to microstructural transformation the unique NR&S mechanisms leading to sheet material strengthening as it deforms.

#### Case Example #3 Destructive Analysis of Stamped Part

**[0115]** A sheet blank from Alloy 8 with a thickness of 1.4 mm were used for a stamping trial of a B-pillar at a commercial stamping facility with stamping speed estimated at 290 mm/s. Alloy sheet properties before stamping are shown in Table 40. Using an existing die, Alloy 8 sheet blanks were stamped into B-pillars.

TABLE 40

Average Tensile Properties Of 1.4 mm Thick Alloy 8 Sheet					
Ultimate Tensile Strength [MPa]	0.2% Proof Stress [MPa]	0.5% Proof Stress [MPa]	Total Elongation [%]	Rockwell C Hardness [HRC]	Magnetic Phases Volume Percent [Fe %]
1173	460	525	57.3	22.1	0.2

**[0116]** For destructive analysis, tensile specimens were cut along the entire length of the B-pillar. The view of the B-pillar before and after specimen cutting is shown in FIG. 47. Tensile specimens with reduced size (i.e. 12.5 mm gauge) were used to evaluate material properties in the stamped part. Property values measured for reduced size specimens were shown to be in good correlation with that measured during testing of ASTM E8 standard specimens. Such property correlation for Alloy 8 is shown in FIG. 48.

**[0117]** In total, 213 tensile specimens cut from the B-pillar were tested. Rockwell C hardness and Feritscope measure-

ments were taken from each tensile specimen. Tensile property data for selected specimens are listed in Table 41. Examples of the stress—strain curves for specimens cut from the B-pillar with various levels of magnetic phases volume percent (Fe %) are presented in FIG. 49. Corresponding true stress—true strain curves in FIG. 50 show extensive strain hardening in the material indicating the effect of NR&S on the sheet structure and properties during stamping.

TABLE 41

Tensile Properties of Selected Specimens Cut From The Stamping						
Magnetic Phases Volume Percent [Fe %]	0.2% Proof Stress [MPa]	0.5% Proof Stress [MPa]	1.0% Proof Stress [MPa]	Ultimate Tensile Strength [MPa]	Total Elongation [%]	Rockwell C hardness [HRC]
0.2	450	521	564	1182	61.7	27
2.1	545	634	685	1222	57.3	32
4.6	503	652	733	1212	54.2	32
9.0	621	774	869	1231	46.7	38
13.9	716	896	992	1326	39.1	39
20.2	787	1007	1147	1320	37.0	46
24.5	954	1229	1327	1410	27.0	46

**[0118]** The measured tensile properties were correlated to structural changes during stamping evaluated from direct Feritscope measurements on the grip sections of the tensile specimens after cutting from the B-pillar prior to testing. Correlation between the measured Fe % and tensile properties is shown in FIG. 51a for strength characteristics and in FIG. 51b for total elongation demonstrating linear relationships.

**[0119]** Non-destructive analysis showed the maximum value of 31 Fe % in highly bent areas of the B-pillar that cannot be used for tensile specimen cutting. However, the current correlations based on 213 data points and shown in FIGS. 51a and b allows estimation of the strength characteristics and retained ductility in these areas by extrapolation of the linear relationships to 31 Fe % as shown in FIGS. 52a and b. At the maximum value of 31 Fe %, the 0.2% proof stress is estimated at 1085 MPa, 0.5% proof stress at 1400 MPa, and ultimate tensile strength at 1490 MPa. The amount of increase in 0.5% proof stress and ultimate tensile strength in most deformed areas of the stamped B-pillar over the baseline in Table 40 is estimated to be 875 MPa and 317 MPa, respectively. The retained ductility is estimated by the total elongation at about 15% in the most deformed areas of the B-pillar after stamping. These results indicate that the material has a potential for applications requiring stamping of even more complex geometries and the resulting stamped parts retain capability for high energy absorption.

**[0120]** This Case Example demonstrates a dramatic increase in both yield and tensile strength in the stamped part as a result of material cold deformation during stamping operation. Cold deformation activates NR&S mechanism in the alloys herein leading to material strengthening. The 213 tensile specimens measured over the surface of the stamped part illustrate the resulting change in properties resulting from the localized changes found in the stamped part. While the stamped part was not deformed until failure, the range of properties found in the stamped part, are similar to the range

of tensile properties (prior to failure) found for the same alloy from incremental tensile testing as previously provided in Table 13.

#### Case Example #4 Microstructural Analysis of the Stamped Part

**[0121]** A sheet blank from Alloy 8 with a thickness of 1.4 mm was used for stamping trial of a B-pillar at a commercial

stamping facility. Detailed TEM analysis was done on the samples cut from different locations of the stamped part to demonstrate the structural response to the deformation during stamping.

**[0122]** To prepare TEM specimens for a structural analysis, the samples were first cut with EDM from the areas of interest, and then thinned by grinding with pads of reduced grit size every time. Further thinning to make foils of 60 to 70 nm thickness was done by polishing with 9 am, 3 am, and 1 am diamond suspension solution, respectively. Discs of 3 mm in diameter were punched from the foils and the final polishing was fulfilled with electropolishing using a twin-jet polisher. The chemical solution used was a 30% nitric acid mixed in methanol base. In case of insufficient thin area for TEM observation, the TEM specimens may be ion-milled using a Gatan Precision Ion Polishing System (PIPS). The ion-milling usually is done at 4.5 keV, and the inclination angle is reduced from 4° to 2° to open up the thin area. To analyze structure in the alloys after deformation, TEM samples were cut from the gauge section of the tensile specimens close to the fracture and prepared in the similar manner. The TEM studies were done using a JEOL 2100 high-resolution microscope operated at 200 kV. The TEM specimens were studied by SEM. Microstructures were examined by SEM using an EVO-MA10 scanning electron microscope manufactured by Carl Zeiss SMT Inc.

**[0123]** FIG. 53 shows the bright-field TEM images of the microstructure in the selected samples cut from the stamped B-pillar before and after tensile testing. Analyzed samples were selected with 4.6 Fe %, 13.9 Fe %, and 24.5 Fe % of magnetic phases volume percent. Corresponding tensile properties and stress-strain curves for the selected specimens were shown earlier in Case Example #3 (Table 41, FIG. 49 and FIG. 50).

**[0124]** In FIG. 53a, c, and e, the microstructure corresponding to that in the as stamped part is shown at the three levels of deformation. In FIG. 53a, the microstructure of the sample (with 4.6% Fe) is slightly deformed where grain boundaries are still clearly visible since the material trans-



formation is limited and only moderate amount of dislocations are generated in the grains. In FIGS. 53c and e, TEM images show an increase in the volume percent of Microconstituent 1 with higher dislocation density and some twins observed in both microconstituents. Through studying multiple locations, a clear correlation is found with the amount of activated NR&S occurring during stamping with increases of Fe % in the samples.

[0125] TEM analysis of the microstructure was also done for the gauge section of the corresponding samples tested in tension from the same three locations. Bright-field TEM images of the microstructure after tensile testing are provided in FIG. 53b, d, and f. It can be seen that after testing to failure, the structures in all three samples are similar with formation of distinct Microconstituent 1 and 2 regions as a result of further structural transformation through the NR&S mechanism during tensile testing. Structural evolution during tensile testing is also confirmed by Feritscope measurements showing 38 to 43 Fe % in the gauge of all tested samples.

[0126] This Case Example demonstrates microstructural changes of the alloy herein during stamping operations corresponding to localized increases in magnetic phases volume percent consistent with the localized Feritscope measurements. These specific microstructural changes are consistent with the activation of the identified NR&S mechanism and conclusively show the material strengthening occurring in the stamping.

Case Example #5 Correlation Between Incremental Tensile Testing and Destructive Analysis of Stamped Part

[0127] Nine specimens with reduced size were cut from the same Alloy 8 sheet that used for stamping trial of the B-pillar and used for incremental testing. Alloy sheet properties are shown in Table 40. Incremental tensile testing was done on an Instron mechanical testing frame (Model 3369), utilizing Instron's Bluehill control and analysis software. All tests were run at ambient temperature in displacement control. The specimen dimensions were measured as well as the magnetic phases volume percent (Fe %) prior to next increment of testing. Magnetic phases volume percent (Fe %) was measured by Fisher Feritscope.

[0128] Yield strength data collected from incremental testing of Alloy 8 sheet as well as that from tensile testing of specimens cut from the B-pillar during destructive analysis were correlated with magnetic phases volume percent (Fe %). 0.2 and 0.5% proof stress as a function of the Fe % is presented in FIG. 54. Both characteristics are shown to increase with increasing Fe % in a linear manner.

[0129] This Case Example shows good correlation between the changes in yield strength in incremental tensile specimens and that in specimens tested during destructive analysis of the B-pillar as a function of magnetic phases volume percent. Cold deformation results in structural transformation detected by an increase in Fe % leading to strengthening of alloys herein and to an increase in strength characteristic values.

Case Example #6 Properties of Alloys 8 at Variable Thickness

[0130] Laboratory slabs with thickness of 50 mm were cast from Alloy 8 according to the atomic ratios in Table 1.

The slabs were then processed by a mixture of hot and cold rolling to achieve the targeted sheet thickness of 0.5, 1.3, 3.0 and 7.1 mm. The thickest material was hot rolled only, while all other conditions were cold rolled to achieve the targeted thickness. After cold rolling the samples were wrapped in stainless steel foil to minimize oxidation and placed into an 850° C. furnace for 10 minutes then removed and allowed to cool in air. The details of each sheet processing are listed in Table 42.

TABLE 42

Details Of Processing Towards Targeted Alloy 8 Sheet Thicknesses					
Sheet Thickness [mm]	First Hot Rolling [%]	Second Hot Rolling [%]	First Cold Rolling [%]	Second Cold Rolling [%]	Third Cold Rolling [%]
0.5	80.5	84.9	25.2	31.1	30.5
1.3	80.6	77.6	40	—	—
3.0	80.7	55.5	28.3	—	—
7.1	78.6	32.3	—	—	—

[0131] Incremental tensile testing was done on an Instron mechanical testing frame (Model 5984), utilizing Instron's Bluehill control and analysis software. All tests were run at ambient temperature in displacement control. Samples were tested at a displacement rate of 0.025 mm/s during initial loading to 2% strain and 0.125 mm/s for the remaining duration of the test.

[0132] Each specimen was strained approximately 5%, and then unloaded. The specimen dimensions were measured as well as the magnetic phases volume percent (Fe %) prior to the next increment of testing. Magnetic phases volume percent (Fe %) was measured by Fisher Feritscope. Control specimen from the same sheet from each alloy was tested up to failure to evaluate initial sheet properties that are listed in Table 43 for sheet samples at each thickness.

TABLE 43

Tensile Properties Of Alloy 8 Sheet With Different Thicknesses					
Sheet Thickness [mm]	Total elongation [%]	Ultimate Tensile Strength [MPa]	0.5% Proof Stress [MPa]	True Strain [%]	True Stress [MPa]
0.5	54.1	1177	483	43.1	1799
1.3	57.9	1190	440	45.7	1862
3.0	60.2	1156	470	47.1	1823
7.1	47.8	1130	309	39.2	1662

[0133] Incremental test data for samples with each thickness herein is listed in Table 44 through Table 47. Incremental stress-strain curves along with engineering stress-strain curves and true stress-true strain curves are shown for Alloy 8 sheet with each thickness in FIG. 55a, FIG. 56a, FIG. 57a, and FIG. 58a. Good agreement between calculated true stress-true strain curve and incremental test data was observed in all cases. Yield strength and magnetic phases volume percent (Fe %) as a function of accumulated strain during incremental testing are plotted in FIG. 55b, FIG. 56b, FIG. 57b, and FIG. 58b for Alloy 8 sheet with 0.5, 1.3, 3.0, and 7.1 mm thickness, respectively. Sheet materials from Alloy 8 processed by cold rolling and annealing (0.5, 1.3 and 3.0 mm thickness) before testing have magnetic

phases volume percent ranging from 1.2 to 1.6 Fe %. Alloy 8 sheet in hot rolled condition (7.1 mm thick) has magnetic phases volume percent of 3.1 Fe % before testing. After testing, there is a significant increase in Fe % in all cases resulting in final Fe % values from 43.5 to 62.7 Fe %.

**[0134]** The incremental testing results also show an extensive increase in yield strength with increasing accumulated strain. The difference in yield strength values between first and last cycle of testing varies from 1112 to 1332 MPa confirming a significant material strengthening. Note that while this example highlights individual strains applied to the sheet in specific steps, the range of properties demonstrated are deemed simultaneously possible in a stamped part made from the alloys herein.

TABLE 44

Incremental Test Data For Alloy 8 Sheet With 0.5 mm Thickness			
Cycle Number	Cumulative Applied Strain [%]	0.5% Proof Stress [MPa]	Magnetic Phases Volume Percent [Fe %]
0	0	—	1.2
1	4.2	480	1.2
2	8.2	625	1.9
3	12.8	765	4.2
4	17.3	893	8.3
5	21.6	1041	13.8
6	26.1	1178	19.9
7	30.6	1326	27.9
8	35.3	1440	34.2
9	40.8	1598	37.5
10	44.0	1704	43.5
Change (Last Cycle – First Cycle)		1224	42.3

TABLE 45

Incremental Test Data For Alloy 8 Sheet With 1.3 mm Thickness			
Cycle Number	Cumulative Applied Strain [%]	0.5% Proof Stress [MPa]	Magnetic Phases Volume Percent [Fe %]
0	0	—	1.2
1	4.2	448	2.4
2	8.8	599	5.5
3	13.0	715	11.9
4	17.3	863	20.0
5	21.6	1030	28.0
6	26.1	1181	35.5
7	30.5	1341	41.3
8	35.1	1473	47.4
9	39.5	1596	51.6
10	46.5	1709	62.7
Change (Last Cycle – First Cycle)		1291	60.3

TABLE 46

Incremental Test Data For Alloy 8 Sheet With 3.0 mm Thickness			
Cycle Number	Cumulative Applied Strain [%]	0.5% Proof Stress [MPa]	Magnetic Phases Volume Percent [Fe %]
0	0	—	1.6
1	4.2	477	2.4
2	8.2	617	5.5
3	12.4	735	11.2

TABLE 46-continued

Incremental Test Data For Alloy 8 Sheet With 3.0 mm Thickness			
Cycle Number	Cumulative Applied Strain [%]	0.5% Proof Stress [MPa]	Magnetic Phases Volume Percent [Fe %]
4	16.7	874	19.8
5	21.0	1027	28.8
6	25.4	1181	37.6
7	29.9	1321	43.9
8	34.5	1451	50.4
9	38.8	1593	52.3
10	44.4	1709	55.0
11	45.9	1799	58.4
Change (Last Cycle – First Cycle)		1332	56.0

TABLE 47

Incremental Test Data For Alloy 8 Sheet With 7.1 mm Thickness			
Cycle Number	Cumulative Applied Strain [%]	0.5% Proof Stress [MPa]	Magnetic Phases Volume Percent [Fe %]
0	0	—	3.1
1	4.35	330	10.1
2	8.54	520	18.7
3	12.8	664	28.7
4	17.14	819	35.2
5	21.5	977	41.8
6	26.02	1143	47.5
7	30.53	1287	51.6
8	35.33	1442	55.7
Change (Last Cycle – First Cycle)		1112	45.6

**[0135]** This Case Example demonstrates that the strengthening and strain hardening mechanisms occur in the sheet material with a range of thicknesses from 0.5 to 7.1 mm.

Case Example #7 Incremental Testing of Sheet from Commercial Steel Grades

**[0136]** Sheet material from commercial steel grades of TRIP 780 and DP980 was used for incremental testing. TRIP 780 has the following chemistry (at %); 97.93 Fe, 1.71 Mn, 0.15 Cr, 0.12 Si, 0.05 C, and 0.04 Cu. DP980 has the following chemistry (at %); 96.86 Fe, 2.34 Mn, 0.42 C, and 0.38 Si. Incremental tensile testing was done on an Instron mechanical testing frame (Model 5984), utilizing Instron’s Bluehill control and analysis software. All tests were run at ambient temperature in displacement control. Samples were tested at a displacement rate of 0.025 mm/s during initial loading to 2% strain and 0.125 mm/s for the remaining duration of the test.

**[0137]** Each specimen was strained approximately 5%, and then unloaded. The specimen dimensions were measured prior to the next increment of testing. Control specimen from the same sheet from each steel grade was tested up to failure to evaluate initial sheet properties that are listed in Table 48 for each grade. Magnetic phases volume percent (Fe %) in initial sheet and in the specimen gauge after testing was measured by Fisher Feritscope that is listed in Table 49. The measurement showed no changes in Fe % before and after testing the specimens from TRIP 780 and DP980.

TABLE 48

Summary Of Average Properties Of Commercial Steel Grades								
Steel Grade	Total Elongation (%)	True Strain at Fracture (%)	0.2% Proof Stress [MPa]	0.5% Proof Stress [MPa]	1.0% Proof Stress [MPa]	Ultimate Tensile Strength (MPa)	True Stress (MPa)	Difference Between UTS and True Stress (MPa)
TRIP780	25.0	22.2	449	458	480	799	998	199
DP980	11.2	10.6	763	856	922	1027	1141	114

TABLE 49

Volume Percent Magnetic Phases (Fe %) Before And After Tensile Testing			
Steel Grade	Magnetic Phases Volume Before Tensile Test (Fe %)	Magnetic Phases Volume After Tensile Test (Fe %)	Difference Between Magnetic Phases Volume Before and After Tensile Test (Fe %)
TRIP780	69.5	69.5	0.0
DP980	87.5	87.6	0.1

[0138] Incremental test data for each steel grade is listed in Table 50 and Table 51 and illustrated in FIG. 59 and FIG. 60.

TABLE 50

Incremental Test Data For TRIP 780 Steel					
Cycle Number	Cumulative Applied Strain (%)	0.2% Proof Stress [MPa]	0.5% Proof Stress [MPa]	1.0% Proof Stress [MPa]	Magnetic Phases Volume Percent (Fe %)
1	4.53	444	451	473	69.5
2	8.92	718	725	736	—
3	13.28	818	829	837	—
4	17.6	876	890	896	—
5	21.88	914	931	937	—
6	26.56	988	1007	1009	69.5
Change (Last Cycle - First Cycle)		544	556	536	0.0

TABLE 51

Incremental Test Data For DP980 Steel					
Cycle Number	Cumulative Applied Strain (%)	0.2% Proof Stress [MPa]	0.5% Proof Stress [MPa]	1.0% Proof Stress [MPa]	Magnetic Phases Volume Percent (Fe %)
1	4.32	749	844	911	87.5
2	8.65	1047	1067	1069	—
3	12.02	1115	1124	1110	87.6
Change (Last Cycle - First Cycle)		366	280	199	0.1

[0139] This Case Example demonstrates less degree of strain hardening in commercial steel grades during deformation with no changes in magnetic phases volume percent (0 to 0.1 Fe % difference before and after deformation).

What is claimed is:

1. A method to develop yield strength distributions in a formed metal part comprising:

- (a) supplying a metal alloy comprising at least 70 atomic % iron and at least four or more elements selected from Cr, Ni, Mn, Si, Cu, Al, or C, melting said alloy, cooling at a rate of <250 K/s, and solidifying to a thickness of 25.0 mm up to 500 mm;
- (b) processing said alloy into sheet form with thickness from 0.5 to 10 mm wherein said sheet exhibits a yield strength of A1 (MPa), an ultimate tensile strength of B1 (MPa), a true ultimate tensile strength C1 (MPa), and a total elongation D1;
- (c) straining said sheet one or a plurality of times above said yield strength A1 at an ambient temperature of 1° C. to 50° C. and at a strain rate of 10<sup>0</sup>/s to 10<sup>2</sup>/sec and forming a metal part having a distribution of yield strengths A2, A3, and A4, wherein:

$A2=A1\pm 100;$  (i)

$A3>A1+100$  and  $A3<A1+600;$  and (ii)

$A4\geq A1+600.$  (iii)

2. The method of claim 1 wherein the said alloy in (a) contains at least 70 atomic percent iron is combined with four or more elements that are selected from Cr, Ni, Mn, Al, Si, Cu, or C.

3. The method of claim 1 wherein the said alloy in (a) contains at least 70 atomic percent iron is combined with five or more elements that are selected from Cr, Ni, Mn, Al, Si, Cu, or C.

4. The method of claim 1 wherein the said alloy in (a) contains at least 70 atomic percent iron is combined with six or more elements that are selected from Cr, Ni, Mn, Al, Si, Cu, or C.

5. The method of claim 1 wherein the said alloy in (a) contains at least 70 atomic percent iron up to and including a maximum of 85 atomic percent iron.

- 6. The method of claim 1 wherein;
  - Cr when selected is present at 0.2 atomic percent to 8.7 atomic percent;
  - Ni when selected is present at 0.3 atomic percent to 12.5 atomic percent;
  - Mn when selected is present at 0.6 atomic percent to 16.9 atomic percent;
  - Al when selected is present at 0.4 atomic percent to 5.2 atomic percent;
  - Si when selected is present at 0.7 atomic percent to 6.3 atomic percent;
  - Cu when selected is present at 0.2 atomic percent to 2.7 atomic percent; and
  - C when selected is present at 0.3 atomic percent to 3.7 atomic percent.

7. The method of claim 1 wherein said alloy formed in step (b) indicates

- a yield strength A1 of 250 MPa to 750 MPa;
- an ultimate tensile strength of B1 of 700 MPa to 1750 MPa;
- a true ultimate tensile strength C1 of 1100 MPa to 2300 MPa; and
- a total elongation D1 of 10% to 80%.

8. The method of claim 1 wherein said alloy formed in step (b) exhibits a magnetic phase volume percent of 0.2 Fe % to 45.0 Fe %.

9. The method of claim 1 wherein said metal part in step (c) exhibits a magnetic phase volume percent that is greater than the magnetic phase volume percent present in said sheet in step (b).

10. The method of claim 9 wherein said metal part in step (c) exhibits a magnetic phase volume of 0.5 Fe % to 85.0 Fe %.

11. The method of claim 1 wherein said alloy formed in step (c) exhibits a yield strength A4 of 850 to 2300 MPa.

12. The method of claim 1 wherein said metal part formed in step (c) contains 0.5 volume percent to 85 volume % of ferrite having a particle size of 20 nm to 750 nm.

13. The method of claim 12 wherein said metal part formed in step (c) contains nanoprecipitates having a size of 2 to 100 nm.

14. The method of claim 1 wherein A4 is further characterized as follows:  $A4 \leq C1$ .

15. The method of claim 1 wherein said straining in step (c) is achieved by the process of roll forming, metal stamping, metal drawing, or hydroforming.

16. The method of claim 1 wherein said metal part formed in step (c) is positioned in a vehicular frame, vehicular chassis, or vehicular panel.

17. The method of claim 1 wherein said metal part formed in step (c) is positioned in a storage tank, freight car, or railway tank car.

18. A method to develop yield strength distributions in a formed metal part comprising:

(a) supplying a metal alloy comprising at least 70 atomic % iron and at least four or more elements selected from Cr, Ni, Mn, Si, Cu, Al, or C, melting said alloy, cooling at a rate of  $<250$  K/s, and solidifying to a thickness of 25.0 mm up to 500 mm;

(b) processing said alloy into sheet form with thickness from 0.5 to 10 mm wherein said sheet exhibits a yield strength of A1 (MPa), an ultimate tensile strength of B1 (MPa), a true ultimate tensile strength C1 (MPa), and a total elongation D1 and a magnetic phase volume of 0.2 Fe % to 45.0 Fe %;

(c) straining said sheet one or a plurality of times above said yield strength A1 at a strain rate of  $10^0/s$  to  $10^2/sec$  at an ambient temperature of  $1^\circ$  C. to  $50^\circ$  C. and forming a metal part having a distribution of yield strengths A2, A3, and A4, wherein:

$$A2 = A1 \pm 100; \quad (i)$$

$$A3 > A1 + 100 \text{ and } A3 < A1 + 600; \text{ and} \quad (ii)$$

$$A4 \geq A1 + 600. \quad (iii)$$

wherein said metal part has a magnetic phase volume that is greater than the magnetic phase volume percent present in said sheet in step (b), said greater magnetic phase volume having a value of 0.5 Fe % to 85.0 Fe %.

\* \* \* \* \*